

Plasma spectroscopy

This article has been downloaded from IOPscience. Please scroll down to see the full text article.

1966 Rep. Prog. Phys. 29 35

(<http://iopscience.iop.org/0034-4885/29/1/302>)

View [the table of contents for this issue](#), or go to the [journal homepage](#) for more

Download details:

IP Address: 153.90.101.171

The article was downloaded on 09/01/2013 at 23:12

Please note that [terms and conditions apply](#).

Plasma spectroscopy

J. COOPER†

Plasma Physics Group, Imperial College, London

Contents

	Page
1. Introduction	36
2. Types of radiation	38
3. Equilibrium and temperatures	40
4. Local thermodynamic equilibrium	43
5. The partition functions and the lowering of the ionization potential	45
6. Coronal approximation	49
7. General solution of the rate equations	50
8. Dielectronic recombination	57
9. Validity of local thermodynamic equilibrium and coronal approximations	58
10. Line radiation	60
11. Line profiles	65
11.1. Natural line broadening	66
11.2. Doppler broadening	66
11.3. Stark broadening or pressure broadening	66
11.4. 'Plasma polarization' shift of ionic lines	80
11.5. Comparison of broadening mechanisms in a high temperature plasma	81
12. Continuum radiation	83
13. Radiative transfer	90
14. Plasma parameters	97
15. Temperature measurements	99
15.1. Relative continuum intensities	99
15.2. Relative line to continuum intensities	100
15.3. Relative intensities of lines	102
15.4. Ionization times	104
15.5. Shift-to-width ratio of Stark broadened isolated lines	104
15.6. Doppler profiles	105
15.7. Miscellaneous methods	106
16. Density measurements	106
16.1. Absolute continuum intensities	106
16.2. Absolute line intensities	108
16.3. Stark broadening	108
17. Magnetic field measurements	111
18. Radiative energy losses	112
19. Conclusions	117
Acknowledgments	118
Nomenclature	118
References	124

Abstract. In this review the optical and soft x-ray radiation emitted from an ionized gas is discussed. This radiation depends, not only on the atomic properties of the isolated radiating species, but also on the properties of the plasma in the immediate environment of the radiator. This dependence on the plasma properties is almost exclusively a consequence of the fact that ions and electrons

† Now at Joint Institute for Laboratory Astrophysics, Boulder, Colorado, U.S.A.

interact with other species via the long-range Coulomb potential. The fact that an emitting atom or ion in a plasma is never isolated from the perturbing effects of neighbouring ions and electrons is reflected in the details of the radiation in many ways. The long-range interactions with the charged components of the plasma control the populations of bound states, shift and broaden bound energy levels, lower the ionization potentials of atomic species and are the cause of continuum radiation emission and the emission of normally forbidden lines.

The distribution of particles in the possible quantum states is considered in a plasma, for which collisional excitation and de-excitation processes are controlled by the free electrons. In local thermodynamic equilibrium (L.T.E.), which corresponds to a collision-dominated plasma, the population densities can in principle be well described, but lowering of the ionization potential and partition function cut-offs become important. Conditions for the validity of L.T.E. are given. In non-L.T.E. situations the detailed processes of population and depopulation have to be considered and a detailed knowledge of cross sections and rate coefficients is required. Calculations may be performed using the collisional-radiative decay model (or the simpler coronal model); but even then, for non-hydrogenic species, metastable levels and dielectronic recombination should be considered.

The details of the emitted radiation (line radiation and line profiles, recombination radiation and bremsstrahlung) and the possible effects of radiative transfer are considered. The theoretical assumptions are examined and stressed, and experiments are discussed only when they have a direct bearing on the theoretical predictions. In particular, a large section is devoted to line broadening theory. This is because it is in this field, especially through the generalized impact approximation for electrons, that great improvements in theory have been made in recent years.

Since it is necessary to know the properties of plasmas, both in fusion research and in experiments to measure atomic parameters of highly excited and highly ionized species, methods for measuring number densities and temperatures are described. In particular, methods are discussed which can be used in high temperature plasmas which are not in L.T.E.

Radiation losses due to impurities of high electronic charge are shown to be an extremely important energy loss mechanism for the hydrogen (deuterium) plasmas studied in controlled fusion research.

Finally, some of the outstanding problems in plasma spectroscopy are mentioned.

1. Introduction

For the purpose of this review, plasma spectroscopy can be said to be the study of electromagnetic radiation emitted from ionized media. The plasma will be considered to have a temperature and degree of ionization sufficiently high so that the radiation is due to atomic rather than molecular processes, and in general highly excited and highly ionized species are of interest. However, in contrast to conventional spectroscopy where one is mainly interested in the atomic structure of an isolated atom, the radiation from a plasma depends, not only on the properties of the isolated radiating species, *but also on the properties of the plasma in the immediate environment of the radiator*. This dependence on the plasma properties is a consequence of the fact that ions and electrons interact with other species via the long-range Coulomb potential.

The fact that an emitting atom or ion in a plasma is never isolated from the perturbing effects of other ions and electrons is reflected in the details of radiation

in many ways: the long-range interactions with the charged components of the plasma control the population densities of bound states, shift and broaden energy levels (via the Stark effect), lower the ionization potentials of atomic species and are the cause of continuum radiation emission and the emission of normally forbidden lines. For a plasma which is more than a few per cent ionized, collisional excitation and de-excitation processes are dominated by free electrons (rather than atoms or ions) because of their high mean velocity and the long-range nature of their interaction. Also, since ions and electrons do not move independently, correlation and shielding effects are very important. The effective interaction is shielded out over a distance roughly equal to the Debye radius, and under many circumstances only those ions and electrons within this distance are involved in line broadening or lowering of the ionization potential. Owing to correlations, no electromagnetic radiation is propagated below the plasma frequency, and in the region just above this frequency the spectrum of continuous radiation is considerably modified by collective effects.

In the laboratory plasmas reabsorption of radiation is usually low so that the plasma is not in complete thermodynamic equilibrium with its surroundings. Energy must be supplied to keep the kinetic energy of the plasma particles high. This, of course, does not mean that the system cannot be in a quasi-steady state, and under certain circumstances the distribution of particles in the possible quantum states can be well defined (for instance, local thermodynamic equilibrium in a collision-dominated plasma).

In the past few years a large effort has been concentrated on controlled fusion experiments and plasma spectroscopy has been considerably developed in order to investigate the high temperature plasmas produced. Many of the techniques of astrophysics have been used; although the situation is somewhat easier for laboratory plasmas because they are often optically thin and so radiative transfer is unimportant.

In this review the distribution of particles in the possible quantum states, the details of the emitted radiation (line radiation and line profiles, recombination radiation and bremsstrahlung) and the possible effects of radiative transfer are considered. Cyclotron radiation, due to charged particles gyrating in a magnetic field, will not be considered in detail.

The theoretical assumptions and predictions are examined and stressed, and experiments are discussed only when they have a direct bearing on the theoretical predictions. For details of the experiments, of the instrumentation, of intensity calibration and of light sources, reference is made to the original papers and other reviews. None the less, the importance of experiments should be emphasized. Only with good experimental evidence can theoretical predictions be adequately tested, and there are many parameters (such as energy levels and oscillator strengths) which have to be determined by experiment because of the extreme difficulty of theoretical calculations. In fact, it is wise to use theoretical predictions only when experimental results are unobtainable. One of the major problems of plasma spectroscopy is to obtain a light source whose properties are sufficiently well known to give quantitative information concerning highly excited and highly ionized atoms. For this reason, and because it is necessary to know the properties of plasmas used in fusion research, methods are indicated, based on the properties of

the radiation, for determining important plasma parameters, such as electron number density and temperature. In particular, methods are discussed which can be used with high temperature plasmas which are not necessarily in local thermodynamic equilibrium.

Radiation losses due to impurities of high electronic charge are shown to be an extremely important energy loss mechanism for the hydrogen (deuterium) plasmas studied in controlled fusion research.

Finally, some outstanding problems in plasma spectroscopy are mentioned.

For the sake of convenience, wherever possible, books and more recent publications are referred to, since these usually contain adequate reference to earlier work. In particular, the book *Plasma Spectroscopy* by Griem (1964) contains much useful information.

2. Types of radiation

An atom or ion immersed in a plasma will emit radiation when radiative transitions between various quantum states occur. Since, in plasma spectroscopy,

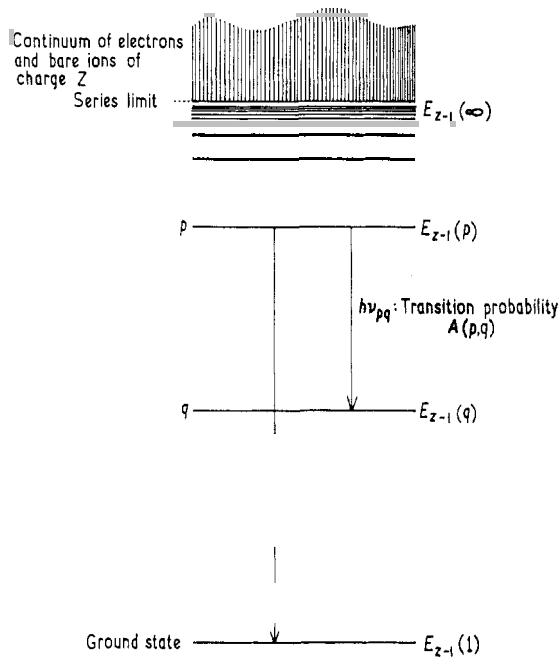


Figure 1. Schematic energy level diagram for a hydrogenic species of charge $Z-1$.

the interaction of ions and electrons with the radiating species is important, the quantum states do not necessarily correspond exactly to those of the isolated atom or ion. However, a schematic energy level diagram (figure 1) may be drawn for a hydrogenic species (this being an atom or ion having a single bound electron).

Bound, discrete, energy levels occur below the ionization limit $E(\infty)$ and a continuum of levels above.

Line radiation occurs for electron transitions between bound levels, leading to line spectra. Thus, if ν_{pq} is the frequency of radiation when a transition from a level of principal quantum number p and energy $E(p)$ to a level of energy $E(q)$ occurs, then

$$h\nu_{pq} = E(p) - E(q).$$

For allowed transitions the usual selection rules of spectroscopy have to be obeyed (White 1934).

Recombination (free-bound) radiation occurs when an electron in the continuum recombines with the ion. Since the upper level is continuous the radiation is continuous; however, there is some structure due to the discrete nature of the lower energy levels (absorption edges).

For an electron of mass m and velocity v , recombination into state p gives

$$h\nu_{vp} = E(\infty) + \frac{1}{2}mv^2 - E(p).$$

Free-free radiation occurs owing to transitions between two free energy levels. Classically this is because a moving charge radiates whenever it is accelerated or retarded.

Bremsstrahlung is caused by the acceleration of charged particles in the Coulomb field of other charged particles. The major part of the bremsstrahlung is due to electron-ion collisions and, since the initial and final states are continuous, the bremsstrahlung spectrum is also continuous.

In cyclotron (or synchrotron or betatron) radiation the acceleration is due to charged particles gyrating in a magnetic field. The major contribution is due to electrons. Although the particles are free, the spectrum of radiation is a type of line spectrum composed of frequencies that are harmonics of the cyclotron frequency (Rose and Clark 1961).

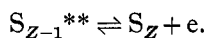
Finally, Čerenkov radiation can occur if the velocity of a particle is greater than the velocity of light in the plasma; however, this corresponds to temperatures too high to be important (Linhart 1960).

For a plasma the relative amounts of line, recombination and continuum radiation depend on the populations of the various energy levels. For instance, a fully ionized plasma emits no line radiation since an ion, fully stripped of its electrons, has no populated bound states. The degree of ionization, in general, depends on the intensive variables such as the kinetic temperatures and the number density, on the time history of the plasma, and even on its extent in space as this may decide whether reabsorption of radiation is important. Usually the degree of ionization is taken as a function of T_e and n_e .

The situation becomes much more difficult to calculate in the case of an atom or ion with more than one orbital electron. Here, two electrons may be excited simultaneously and the doubly excited states may have energy above the first ionization potential.

Figure 2 shows schematically one such doubly excited series of energy levels converging on the first excited state of the ion.

Under certain conditions, a *radiationless transition* can occur, in which the doubly excited state S_{Z-1}^{**} of the ion of charge $Z-1$ gives rise to an ion S_Z and an electron; the pair has the same energy as the original ion:



This process is known as *autoionization*. For example, if the doubly excited state of figure 2 with energy E_{d^*} above the first ionization potential of S_{Z-1} autoionizes, the resultant state is the ion S_Z in its ground state and an electron of energy E_{d^*} . The transition probability is often high ($\sim 10^{13}$ – 10^{14} sec $^{-1}$).

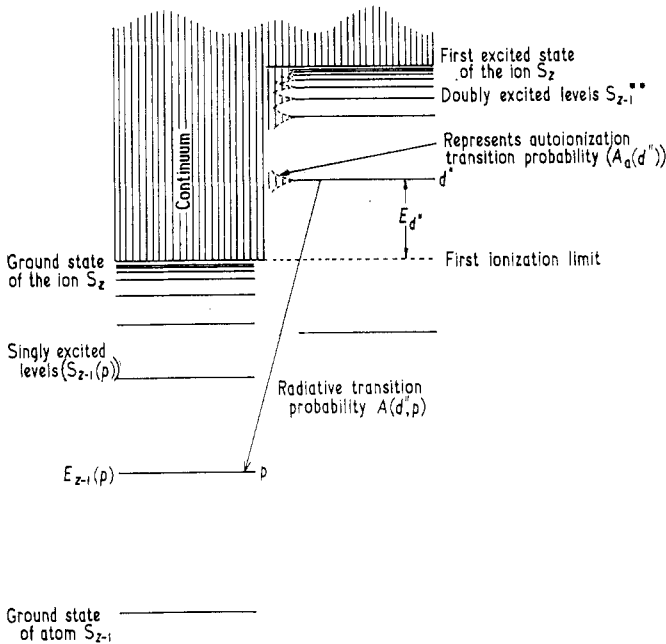


Figure 2. Schematic energy level diagram for a non-hydrogenic species of charge $Z-1$ (S_{Z-1}) showing singly and doubly excited states ($S_{Z-1}(p)$ and S_{Z-1}^{**} respectively).

The selection rules for the autoionization from a discrete doubly excited level lying above the ionization limit to a continuum level of the same energy require that the initial and final states have the same parity and total angular momentum quantum number J , and if Russell–Saunders coupling holds, then the orbital and spin quantum numbers L and S must also be conserved (Condon and Shortley 1935).

When considering the relative populations of the quantum states, these doubly excited levels should not be ignored and, in fact, dielectronic recombination (a process proceeding via the doubly excited states) may be of considerable importance (§ 8).

3. Equilibrium and temperatures

Populations of the various species existing in the plasma and of their respective energy levels, as well as many other plasma properties, are often described in terms of the electron number density n_e and electron temperature T_e . These parameters are relevant because of the dominant role of electrons in collisional processes.

Before proceeding, it is useful to ask under what conditions the term ‘*temperature*’ has any significant meaning. In the kinetic theory of gases the equilibrium

velocity distribution of particles is Maxwellian, from which the kinetic temperature is derived. In order for the statistics of this process to be valid, the mean free path for particle collisions must be far smaller than the dimensions of the containing vessel and the time between collisions must be short compared with other characteristic times, such as those for particle heating and containment.

Usually in laboratory plasmas the electron-electron mean free path and collisional relaxation times are such that the free electrons do have a Maxwellian velocity distribution to which an electron temperature T_e can be ascribed (§9). This is often not the case for ions and then the ion kinetic temperature has no meaning.

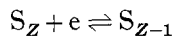
Besides the kinetic energy of the particles in a plasma there is energy in the radiation field. If the mean free path for absorption of radiation is less than the dimensions of the plasma, there is radiation equilibrium and a corresponding radiation temperature. Generally, in laboratory plasmas the optical mean free path greatly exceeds the extent of the plasma (and incidentally also the kinetic mean free path) and so complete radiation equilibrium is rarely obtained. It is usually possible to take the plasma as being optically thin, except, possibly, for the core of resonance lines (§13).

In order to ascertain the relative populations of the various quantum states, thermodynamic arguments are used if full thermodynamic equilibrium obtains. Otherwise, that is for non-thermal plasmas, it becomes necessary to consider the detailed atomic processes. These atomic processes have recently been considered by many authors (§7). Here, with minor variations, the nomenclature of Bates, Kingston and McWhirter (1962 a) is used.

The physical processes, which occur in recombination of electrons e with bare nuclei S_Z of charge Ze to form hydrogen atoms or hydrogenic ions, will now be considered in detail.

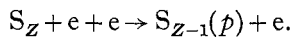
$n_{Z-1}(p), n_{Z-1}(q), \dots$ are the number densities of atoms or ions in the levels p, q, \dots (see figure 1) and n_e and n_Z the number densities of free electrons and ions of charge Ze .

For the reversible reaction represented by



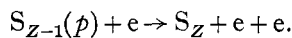
the following competing processes have to be taken into account:

(a) Three-body recombination to state p of S_{Z-1} (denoted by $S_{Z-1}(p)$)

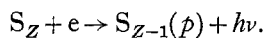


The rate coefficient $K(c', p)$, between all levels c' of the continuum and p , is such that $n_e n_Z K(c', p)$ is the number of three-body recombinations of the above type which occur per cubic centimetre per second.

(b) Collisional ionization (inverse of (a)) with rate coefficient $K(p, c')$



(c) Radiative recombination with rate coefficient $\beta(p)$



(d) Photoionization (inverse of (c))

$$S_{Z-1}(p) + h\nu \rightarrow S_Z + e.$$

(e) Collisional de-excitation with rate coefficient $K(p, q)$

$$S_{Z-1}(p) + e \rightarrow S_{Z-1}(q) + e.$$

(f) Collisional excitation with rate coefficient $K(q, p)$ (inverse of (e))

$$S_{Z-1}(q) + e \rightarrow S_{Z-1}(p) + e.$$

(g) Spontaneous and stimulated emission; $A(p, q)$ being the spontaneous transition probability

$$S_{Z-1}(p) \rightarrow S_{Z-1}(q) + h\nu.$$

(h) Photoexcitation (inverse of (g))

$$S_{Z-1}(q) + h\nu \rightarrow S_{Z-1}(p).$$

The rate coefficients of processes (a), (b), (c), (e) and (f) depend on the electron temperature T_e of the plasma.

Processes due to atom-atom, atom-ion and ion-ion collisions are not included since the relevant rates are much smaller than those for electron collisions, at least for plasmas having a degree of ionization exceeding a few per cent.

When a non-hydrogenic species is considered the problem becomes much more complicated. With more than one electron in the atom, there is more than one ionization stage possible and the pairs of processes of the above type (a) to (h) must be considered in and between the various ionization stages. In addition, these processes should be extended to include multiply excited states, and autoionization and dielectronic recombination must also be included.

In the general case, to obtain the populations of the various quantum states, rate equations are set up using the coefficients defined above; however, it is possible immediately to make some comments on these processes. In complete thermodynamic equilibrium (with both kinetic and radiative equilibrium at the same temperature T) the pairs of inverse processes (a) and (b), (c) and (d), (g) and (h), (e) and (f) occur in detailed balance, i.e. the rate of occurrence of process (a) equals the rate of process (b), etc. In this case the distribution between ionization stages is given by Saha's equation, the distribution amongst bound levels is governed by Maxwell-Boltzmann statistics, and the free electron velocity distribution is Maxwellian—all of these distributions being characterized by the same temperature T .

As already explained, in most laboratory plasmas radiative equilibrium does not obtain. However, there are two régimes for which useful approximations may be made. Firstly, for a high density plasma where collisional effects completely dominate radiative ones, there is the possibility of detailed balance between collisional processes alone. Thermodynamic arguments, which are independent of details of the rate coefficients, may then be applied in this régime, which is known as *local thermodynamic equilibrium* (L.T.E.). In plasmas this equilibrium is characterized by the electron temperature T_e , since electrons dominate the collisional processes.

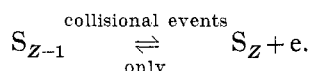
The second régime is known as the *coronal domain*. Here, the plasma is considered as optically thin so that radiation absorption and photoionization (processes *(d)* and *(h)*) are unimportant; in addition the density is sufficiently low so that three-body recombination (process *(a)*) is also unimportant. Under these conditions ionization equilibrium is a balance between collisional ionization and radiative recombination, and the actual populations depend critically on the cross sections for the processes.

In fact, the assumption of optical thinness is often made even when the rate equations are to be solved (§7). The photoexcitation (*h*) and photoionization (*d*) processes, as well as the stimulated part of the emission (*g*) depend on the local intensity of the radiation field, so that when the radiation is important, the rate equations governing the development of the above processes with time must be solved simultaneously with the equation of radiative transfer (§13). This is an extremely difficult problem. However, when the plasma is optically thin the terms in the rate equations dependent on the radiation intensity are negligible. Only in the case of local thermodynamic equilibrium, when populations of quantum states are completely determined by collisional effects, do the equation of radiative transfer and the population equations become uncoupled—at least in principle.

4. Local thermodynamic equilibrium

Thermodynamic arguments may be applied to reversible reactions in an isolated system. For a high density plasma, for which the radiative processes become negligible compared with the collisional ones, a detailed balance exists amongst the collisional processes alone.

Thus, the equilibrium of each ionization stage can be represented as



This is the equilibrium known as local thermodynamic equilibrium (L.T.E.) and “the population densities in the specific quantum states are those pertaining to a system in complete thermodynamic equilibrium, which has the same total (mass) density, temperature, and chemical composition as the actual system.” (Griem 1962 a). The temperature used is the electron temperature since this describes the distribution function of the species (electrons) dominating the reaction rates.

Thus the population of levels within a given species is described by Maxwell-Boltzmann statistics and the relative total populations of successive ionization stages are given by Saha equations, all in terms of the electron temperature T_e .

The population density of state p of (say) the species S_Z , $n_Z(p)$ is thus

$$\frac{n_Z(p)}{n_Z} = \frac{g_Z(p)}{B_Z(T_e)} \exp\left\{-\frac{E_Z(p)}{kT_e}\right\} \quad (\text{Maxwell-Boltzmann}) \quad (4.1)$$

where $g_Z(p)$ is the statistical weight of the p th state of S_Z , $E_Z(p)$ is the energy of the p th state measured from its ground state (i.e. $E_Z(1) = 0$), n_Z is the total number density of S_Z and $B_Z(T_e)$ is that part of the appropriate ionic partition function due to excitations. Thus

$$B_Z(T_e) = \sum_{\text{All } p} g_Z(p) \exp\left\{-\frac{E_Z(p)}{kT_e}\right\}. \quad (4.2)$$

There is an equation of the type (4.1) for each species of ion or atom S_Z . Saha's equation may easily be derived by calculating the extremum of the Helmholtz free energy of the system (see Ecker and Kroll 1963).

Consider a plasma consisting of neutral atoms, ions of charge 1 to Z , and electrons. Let their number densities be $n_0, n_1, \dots, n_Z, n_e$ respectively, and their total numbers be $N_0, N_1, \dots, N_Z, N_e$.

The Helmholtz free energy F is given by

$$F = -kT \ln Q \quad (4.3)$$

where Q is the partition function of the whole system and in the limit of no interactions between the particles of the plasma (when F is equal to F_0) this equals the product of the partition functions of the individual species.

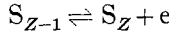
$$Q = Q_e \prod_{Z=0}^Z Q_Z \quad (4.4)$$

with

$$Q_e = \frac{(U_e)^{N_e}}{N_e!} = \frac{1}{N_e!} \left\{ 2V \left(\frac{2\pi mkT}{h^2} \right)^{3/2} \right\}^{N_e} \quad (4.5)$$

$$Q_Z = \frac{(U_Z)^{N_Z}}{N_Z!} \quad (4.6)$$

where U_e and U_Z are partition functions of an individual electron and an individual ion respectively. U_e is purely translational, while $U_Z = T_Z B_Z$ where T_Z is the translational and B_Z the internal or excitational part of the ionic partition function. For the reaction



conservation of charge gives

$$-\delta N_{Z-1} = \delta N_Z = \delta N_e \quad (4.7)$$

and for equilibrium

$$\delta F = \frac{\partial F}{\partial N_{Z-1}} \delta N_{Z-1} + \frac{\partial F}{\partial N_Z} \delta N_Z + \frac{\partial F}{\partial N_e} \delta N_e + \frac{\partial F}{\partial P} \delta P = 0. \quad (4.8)$$

As F does not contain the pressure P explicitly the condition for equilibrium becomes

$$\frac{\partial F}{\partial N_e} - \frac{\partial F}{\partial N_{Z-1}} + \frac{\partial F}{\partial N_Z} = 0. \quad (4.9)$$

Using Stirling's formula ($\log n! = n \log n - n$ for n large)

$$\frac{N_Z N_e}{N_{Z-1}} = \frac{U_e U_Z}{U_{Z-1}} \quad (4.10)$$

where the one-particle partition functions U are reckoned from the same energy zero.

$B_Z(T_e)$ and $B_{Z-1}(T_e)$ are written as the internal partition functions for the species S_Z and S_{Z-1} with their energy levels referred to the respective ground states of the individual species.

Then

$$\frac{n_Z n_e}{n_{Z-1}} = 2 \left(\frac{2\pi mkT_e}{h^2} \right)^{3/2} \frac{B_Z(T_e)}{B_{Z-1}(T_e)} \exp \left\{ -\frac{E_{Z-1}(\infty)}{kT_e} \right\} \quad (\text{Saha's equation}) \quad (4.11)$$

where, as before, $E_{Z-1}(\infty)$ is the ionization energy of the species S_{Z-1} . This equation, which gives the ratio at equilibrium of the total population densities of the ionic species S_Z to that of S_{Z-1} , is known as *Saha's equation*. Consequently, the composition of a plasma with ions up to charge Z is described by Z Saha equations and the equation of charge neutrality

$$n_e = \sum_{Z=0}^Z Zn_Z. \tag{4.12}$$

In order to write the partition function in the form given by equation (4.4) the interactions between the particles making up the plasma have been neglected, i.e. each atom is described as if it were isolated. This description immediately brings difficulties, even when the partition function $B_Z(T_e)$ (equation (4.2)) for an isolated atom is considered. Since the number of discrete levels of an isolated atom is infinite, while the energies approach the ionization limit (except for autoionizing levels), $B_Z(T_e)$ obviously diverges. This divergence is prevented when interactions between particles are included. This interaction also gives rise to a depression of the ionization potential from the value applicable to an isolated atom or ion.

Thus, although Saha's equations and Maxwell-Boltzmann statistics are valid for L.T.E., the actual evaluation of $B_Z(T_e)$ and the ionization potential is a more difficult matter.

Tabulations of Saha's equation, partition functions, continuum emission coefficients and many other properties of plasmas in L.T.E. are given by Drawin and Felenbok (1965) for many elements.

5. The partition functions and the lowering of the ionization potential

To transform an isolated atom S_{Z-1} in its ground state into an electron and an unexcited ion, both at rest, the energy $E_{Z-1}(\infty)$ is required, where $E_{Z-1}(\infty)$ is the

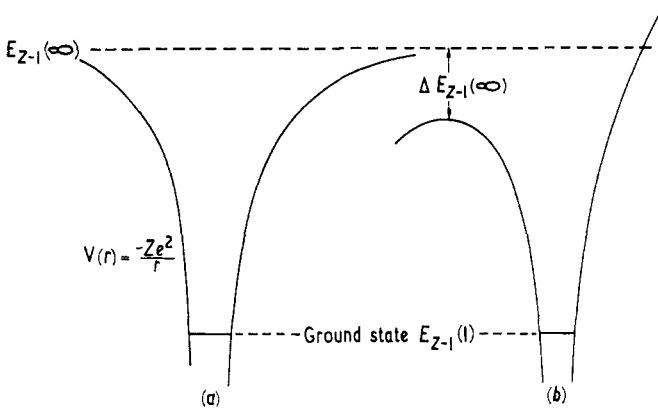


Figure 3. Representation of the potential distribution in the neighbourhood of an atomic nucleus, (a) without and (b) with a constant electric field.

ionization energy. The same transformation in an external field requires less energy. This can be interpreted as a lowering $\Delta E_{Z-1}(\infty)$ of the ionization energy, and is illustrated in figure 3 for the case of a constant electric field.

In a plasma an atom is exposed to the action of the Coulomb fields of the ions and electrons (the electric microfield). Therefore a lowering of the ionization potential is to be expected. Many attempts at the solution of this extremely complicated problem have been made recently (Unsöld 1948, Ecker and Weizel 1956, Margenau and Lewis 1959, Duclos and Cambel 1961, Griem 1962 b, Ecker and Kroll 1963, 1965, and others) and many of the results of these papers have been summarized by McChesney (1964). One approach (Griem 1962 b, Ecker and Kroll 1963) is to rederive Saha's equation, but now with an additional free-energy term F_c added to the Helmholtz free energy F_0 to represent interactions between the particles. Then, in equation (4.11) $E_{Z-1}(\infty)$ must be replaced by

$$E_{Z-1}(\infty) - \Delta E_{Z-1}(\infty)$$

where

$$\Delta E_{Z-1}(\infty) = - \left(\frac{\partial F_c}{\partial N_e} - \frac{\partial F_c}{\partial N_{Z-1}} + \frac{\partial F_c}{\partial N_Z} \right). \quad (5.1)$$

For Coulomb interactions F_c may be calculated as in the Debye-Hückel theory of electrolytes (see Fowler and Guggenheim 1952) to be

$$F_c = - \left(\frac{e^2}{3\rho_D} \right) (n_e + \sum Z^2 n_Z) \quad (5.2)$$

where ρ_D is the Debye length given by the equation

$$\frac{kT_e}{\rho_D^2} = 4\pi e^2 \left(n_e + \sum_{Z=1}^Z Z^2 n_Z \right). \quad (5.3)$$

Substitution into (5.1) gives

$$\Delta E_{Z-1}(\infty) = Ze^2/\rho_D. \quad (5.4)$$

The same result should be obtained if enthalpy is used instead of free energy, since the equilibrium cannot depend on the choice of thermodynamic function. Thus, the result of Traving (1960) of $3e^2/2\rho_D$ for the neutral atom (see Griem 1962 b and Griem 1964, p. 140) appears to be in error.

The result (5.4) is expected to be valid for densities such that the Debye theory is still valid; a condition which is written by Duclos and Cambel (1961) as

$$n_e + \sum_Z n_Z \geq (8\pi\rho_D^3)^{-1}. \quad (5.5)$$

This criterion is obeyed for most laboratory plasmas; however, in cases where it is invalid, other theories have to be used. The paper by Ecker and Kroll (1963) contains a critical review of earlier work, as well as careful consideration of the limits of validity of the above approach. Harris (1964) attempts, in calculating the free energy, to take into account perturbations of the bound electronic states by the plasma, as well as the Debye-Hückel free energy F_c . However, it has been suggested several times that the final result obtained by her is erroneous, possibly due to an incorrect choice of zero of energy (e.g. D. D. Burgess 1965, Ph.D. Thesis, University of London).

When determining the partition function $B_Z(T_e)$, in order not to count a state twice, namely, once as a bound and once as a free state, the sum should be truncated to include only levels whose energies are below the reduced ionization limit, i.e.

$$E_Z(p) \leq E_Z(\infty) - \Delta E_Z(\infty). \quad (5.6)$$

The usual procedure is to take unperturbed values of the energy levels, and Griem (1962 b) indicates that this should not be a bad approximation. A more consistent approach appears to be that of Ecker and Weizel (1956) and Smith (1964), who attempted to calculate the actual energy levels using Schrödinger's equation with a screened (Debye-Hückel) potential of the form (for species S_{Z-1} of charge $Z-1$)

$$V(r) = eZ \left\{ \frac{\exp(-r/\rho_D)}{r} \right\}. \quad (5.7)$$

After various approximations the results are essentially the same as those obtained by using the straight cut-off procedure discussed above. They do, however, emphasize that the Debye potential has only a finite number of eigenstates. Recently a quantum-statistical-mechanical paper was published by DeWitt and Nakayama (1964) who use a fluctuating screened potential rather than the Debye potential (equation (5.7)) which is essentially time averaged. These authors obtain results which are very different from Ecker and Weizel (1956), although they can recover Ecker and Weizel's values for the static limit. Their theory is difficult to understand, but, since a fluctuating microfield seems to be a better description of the actual plasma, their results cast some doubt on the previous treatments.

Even with a straight cut-off, there exist certain inconsistencies in the calculation of the partition function. At low temperatures, owing to the smallness of the exponential terms in the summation for $B_Z(T_e)$, it is usual only to consider the contribution of the ground state. However, once terms other than the ground state become important *all* levels up to the cut-off should be included. The atomic energy level tables of Moore (1949-58) usually only list those energy levels with low orbital angular momentum. Various extrapolation procedures (Ritz formulae) have been used (Drellishak *et al.* 1963, Drawin and Felenbok 1965). Yet, in view of the other errors involved, it should be sufficient to treat the missing levels of higher orbital quantum number as 'hydrogenic', in the sense that the excited electron will be moving in a virtually Coulombic ($\propto 1/r$) field. Comparison with hydrogen gives the maximum principal quantum number in the partition function sum (equation (5.6)), for species of charge $Z-1$, as

$$p_{\max} \leq \left\{ \frac{Z^2 E_H}{\Delta E_Z(\infty)} \right\}^{1/2}$$

where E_H is the ionization energy of hydrogen.

Then, Griem (1964) gives the following formula from which the contribution of the 'missing' levels can easily be estimated:

$$\begin{aligned} B_{Z-1}(T_e) &\simeq \sum_{p=1}^{p'} g_{Z-1}(p) \exp \left\{ -\frac{E_{Z-1}(p)}{kT_e} \right\} + (2S_1 + 1)(2L_1 + 1) \\ &\quad \times \sum_{p'+1}^{p_{\max}} 2p^2 \exp \left[-\frac{\{E_{Z-1}(\infty) - Z^2 E_H/p^2\}}{kT_e} \right] \\ &\simeq \sum_{p=1}^{p'} g_{Z-1}(p) \exp \left(-\frac{E_{Z-1}(p)}{kT_e} \right) + \frac{2}{3}(2S_1 + 1)(2L_1 + 1) \\ &\quad \times \left(\frac{Z^2 E_H}{\Delta E_{Z-1}(\infty)} \right)^{3/2} \exp \left(\frac{-E_{Z-1}(\infty) - \Delta E_{Z-1}(\infty)}{kT_e} \right) \end{aligned} \quad (5.8)$$

where p' is the highest principal quantum number for which all the levels of the configuration whose outer electron has angular momentum $l = p' - 1$ are included in the energy level tables, and S_1 and L_1 are the spin and orbital angular momentum quantum numbers of the parent configuration (i.e. the ground state of the next highest ionization stage). To obtain the second formula in equation (5.8), the second summation has been replaced by an integral, with all energies in the sum placed equal to the reduced ionization energy and the lower limit of the integral neglected.

In general, the possible existence of doubly excited and autoionizing levels has been overlooked in the partition function summation.

McChesney and Jones (1964) choose to neglect them; yet, these are perfectly possible energy states of an atom, each series converging on its own (depressed) series limit which is an excited state of the ion. In obtaining the equilibrium from quantum statistics all possible energy states should be included. Since these doubly and multiply excited states represent no extra mode of energy loss from the system, they too should be included in principle at least (D. D. Burgess 1965, Ph.D. Thesis, University of London). In complete L.T.E. even the autoionizing states must obey Maxwell-Boltzmann statistics with respect to the ground state of the atom, with all possible levels of the atom included in the partition function; Saha's equation is not completely valid until these levels do reach their Maxwell-Boltzmann populations with respect to the ground state.

While considering partition functions, it should be stressed that the Inglis-Teller (1939) limit (the point in a spectral series where, owing to line-broadening effects, the lines appear to merge—see § 11.3.4) should *not* be used for cutting off the summation, because bound states of the atom can exist above this limit.

Finally, it should be noted that when doing composition calculations for L.T.E. (i.e. solving Saha's equations (4.11) and the equation of charge neutrality (4.12)) it is most convenient to use as variables electron number density n_e and temperature T_e since these are independent of high density corrections, whereas the pressure P is a derived quantity. Thus

$$P = -\frac{\partial}{\partial V}(FV) = -\frac{\partial}{\partial V}\{(F_0 + F_c)V\}$$

which gives in the Debye approximation

$$P = \left(n_e + \sum_Z n_Z\right) kT_e - \frac{1}{3}e^3 \left(\frac{\pi}{kT_e}\right)^{3/2} (n_e + \sum Z^2 n_Z)^{3/2}$$

rather than just the kinetic pressure $P = (n_e + \sum_Z n_Z) kT_e$. Numerically, however, for most laboratory plasmas, this correction to the kinetic pressure does not amount to more than a few per cent.

For performing L.T.E. calculations the tables of Drawin and Felenbok (1965) are possibly the most complete and the simplest to use.

To a large extent the plasma composition (as a function of n_e and T_e) is very insensitive to the actual value of the depression of the ionization potential which is used. Slight experimental errors in n_e and T_e make it extremely difficult to distinguish between the various theories (Olsen 1961). Ecker and Kroll (1963) mention other experiments, but at present there is no satisfactory experimental verification of the Debye or any other approach.

6. Coronal approximation

For a low density optically thin plasma, the photoexcitation processes are unimportant, and radiative decay rates predominate over collisional decay rates for both line radiation and free-bound radiation. This is the situation occurring in the solar corona (see Woolley and Allen 1948, Elwert 1952). The population of the p th level in equilibrium will, to a close approximation, be a balance between collisional excitation (process (f) , §3) and spontaneous emission (process (g)). Since the total transition probability $A(p) (= \sum_{q < p} A(p, q))$ from an excited level p is large, the populations of the excited states will be small, so that only collisional excitation from the ground state ($p = 1$) need be considered. Then, at equilibrium

$$n(p) A(p) = n(1) n_e K(1, p)$$

and therefore

$$\frac{n(p)}{n(1)} = \frac{n_e K(1, p)}{A(p)}. \quad (6.1)$$

The $K(1, p)$ are in general strongly dependent on the electron temperature. Since for this coronal approximation it is necessary that $n(p)$ be much less than $n(1)$, this must be checked by substituting typical values. Similarly, neglecting the population of the upper bound levels, the state of ionization can essentially be determined from the balance between collisional ionization (process (b)) from the ground state and radiative recombination (process (c)). Recombination to all levels p is included, since recombination to an excited state is followed immediately by spontaneous emission (although in practice $\beta(p)$ decreases rapidly with increasing p).

Then, at equilibrium

$$n_Z n_e \sum_p \beta(p) = n_{Z-1} n_e K(1, c')$$

where $\sum_p \beta(p)$ is the total radiative recombination coefficient for transition from species S_Z (not necessarily hydrogenic) to S_{Z-1} , and $K(1, c')$ is the total collisional ionization coefficient for the transition from the ground state of S_{Z-1} to species S_Z and an electron (with energies corresponding to all possible levels c' of the continuum). Thus

$$\frac{n_Z}{n_{Z-1}} = \frac{K(1, c')}{\sum_p \beta(p)} = \text{function of } T_e \text{ only.} \quad (6.2)$$

This ratio is independent of the electron number density n_e , in contrast to Saha's equation (equation (4.11)) which gives an n_e^{-1} dependence. This is because both radiative recombination and collisional ionization are two-body processes with the same functional dependence on n_e . The ratio n_Z/n_{Z-1} depends critically on the cross sections for the processes.

The results of Post (1961) can be used as an instructive, qualitative example. He uses approximate cross sections for one-electron (hydrogenic) and three-electron (lithium-like) ions to calculate the relative abundances of some common impurity ions in a plasma. The results indicate that in the coronal régime the predictions of Saha's equation are a long way out, and that heavy ions can exist at extremely high temperatures without being fully stripped of electrons (see figure 4).

A. Burgess (1964) has pointed out that, under certain circumstances, for non-hydrogenic ions, dielectronic recombination (a process via the autoionizing levels) can compete with radiative recombination $\sum_p \beta(p)$. Further discussion of the solution of the rate equations and dielectronic recombination is included in §§7 and 8.

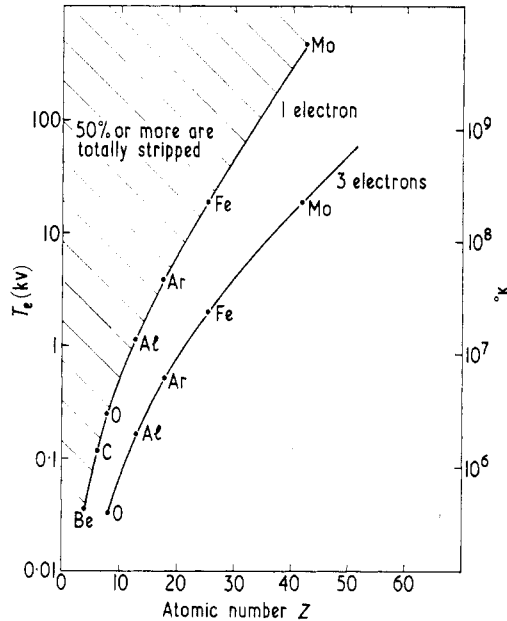


Figure 4. Equilibrium ionization: the curves indicate the temperature at which the abundance of a given ion is 50%. (After Post 1961.)

The coronal type of argument has been applied with considerable success to problems of the solar corona (see Seaton 1964 for a review).

7. General solution of the rate equations

In régimes where neither the L.T.E. nor the coronal approximations are valid, the problem is essentially to solve the differential equations describing the population and depopulation of levels by the processes described in §3. Considerable advances have been made in the last few years owing, partially, to the increasing knowledge of cross sections necessary for the rate coefficients and, partially, to the use of high-speed computers for the calculations. A considerable number of papers have been published dealing with this problem to a greater or lesser degree of sophistication. It is impossible to describe all these papers in detail but the principles involved are illustrated with reference to the article by Bates, Kingston and McWhirter (1962 a), which followed earlier work by Bates and Kingston (1961) and McWhirter (1961).

An optically thin hydrogenic plasma is assumed. The authors consider the process $S_{Z-1} \rightleftharpoons S_Z + e$, where S_Z is a bare nucleus. Then the rate of increase of

$n_{Z-1}(p)$ with time is given by

$$\begin{aligned} \frac{d}{dt}n_{Z-1}(p) = & -n_{Z-1}(p) \left\{ n_e K(p, c') + n_e \sum_{q \neq p} K(p, q) \right\} - n_{Z-1}(p) \left\{ \sum_{q < p} A(p, q) \right\} \\ & + n_e \sum_{q \neq p} n_{Z-1}(q) K(q, p) + \sum_{q > p} n_{Z-1}(q) A(q, p) + n_Z n_e \{ K(c', p) + \beta(p) \} \end{aligned} \quad (7.1)$$

where the first term is the rate for collisional processes from p to the continuum c' and to all other levels q . The second term represents spontaneous emission from p to levels q with energy below that of p . The third term represents collisional population of p from all other bound levels q . The fourth term is the population by spontaneous transitions from levels q above p , and, finally the last term represents collisional and radiative recombination from the continuum to level p . There are no processes involving absorption since the plasma is assumed optically thin.

For the purpose of computation, it was found convenient to normalize the population densities to the equilibrium population densities $n_E(p)$, as given by Maxwell-Boltzmann statistics and Saha's equation. Thus

$$\begin{aligned} n_E(p) &= \frac{g_{Z-1}(p)}{B_{Z-1}(T_e)} n_{Z-1} \exp \left\{ \frac{-E_{Z-1}(p)}{kT_e} \right\} \quad (\text{from equation (4.1)}) \\ &= \frac{g_{Z-1}(p)}{2B_Z(T_e)} \left(\frac{h^2}{2\pi m k T_e} \right)^{3/2} \exp \left\{ \frac{E_{Z-1}(\infty) - E_{Z-1}(p)}{kT_e} \right\} n_e n_Z \quad (\text{from equation (4.11)}) \\ &= p^2 n_e n_Z \left(\frac{h^2}{2\pi m k T_e} \right)^{3/2} \exp \left\{ \frac{I(p)}{kT_e} \right\} \end{aligned} \quad (7.2)$$

where $I(p) = E_{Z-1}(\infty) - E_{Z-1}(p)$ is the ionization potential of level p . In deriving this equation use has been made of the facts that $B_Z(T_e) = 1$ for a bare ion and that $g_{Z-1}(p) = 2p^2$ for a hydrogenic ion. Ionization depression has been neglected in Saha's equation.

The principle of detailed balancing then allows the coefficients for collisional events to be related; thus

$$n_E(p) K(p, q) = n_E(q) K(q, p)$$

and

$$n_E(p) K(p, c') = n_E n_Z K(c', p).$$

Equation (7.1) is then rewritten as

$$\begin{aligned} \frac{dn_{Z-1}(p)/dt}{n_E(p)} = & -\rho(p) \{ n_e K(p) + A(p) \} + \sum_{q \neq p} \rho(q) n_e K(p, q) \\ & + \sum_{q > p} \rho(q) \frac{n_E(q)}{n_E(p)} A(p, q) + n_e K(p, c') + \frac{n_e^2}{X n_E(p)} \beta(p) \end{aligned} \quad (7.3)$$

where

$$\rho(p) = \frac{n_{Z-1}(p)}{n_E(p)}; \quad K(p) = K(p, c') + \sum_{q \neq p} K(p, q); \quad A(p) = \sum_{q < p} A(p, q)$$

and $X = n_e/n_Z$.

This infinite set of coupled differential equations describes the course of recombination with time. Examination of equation (7.2) shows that for a wide

range of plasmas the Saha equilibrium number densities of excited states $\{n_E(p)\}$ are much less than the number densities of free electrons and bare nuclei. It follows for a still wider range that

$$n_{Z-1}(p) \ll n_e \quad (p \neq 1). \quad (7.4)$$

Bates, Kingston and McWhirter (1962 a) then show that if this condition (equation (7.4)) is satisfied and, in addition, if the mean thermal energy is much less than the first excitation energy (i.e. if $n_{Z-1}(p) \ll n_{Z-1}(1)$, $p \neq 1$) once a steady state is reached, considerable simplifications can be made. In such a plasma a quasi-equilibrium of number densities of excited states is established almost instantaneously without the number densities of free electrons and bare nuclei being appreciably altered (since the $n_{Z-1}(p)$ are very small). This is because the relaxation times for the excited levels are very much shorter than the relaxation times for the ground level or the free electrons. The collisional rate coefficients between excited levels are much greater than the rate coefficients to the ground level and, in addition, the ground state cannot decay by spontaneous transitions, so that the quasi-equilibrium is one in which the excited levels can be referred to a particular set of number densities of ions in the ground state, free electrons and bare nuclei. (An exception to the above occurs when metastable levels are possible, for, owing to their small spontaneous radiative decay rates, they are not necessarily in a quasi-equilibrium with the ground state.) In consequence $dn_{Z-1}(p)/dt$ can be put equal to zero, except for the ground state ($p = 1$), without causing significant error.

The condition for $n_{Z-1}(p) \ll n_e$ is summarized by Bates *et al.* (1962 b) for the hydrogenic case as

$$n_e \gg 10^{14+Z'} \text{ cm}^{-3} \quad \text{where} \quad 2Z' = T_e/1000 \quad \text{for} \quad T_e \text{ in } ^\circ\text{K}.$$

It is interesting to note that the above condition also happens to ensure that the lifetime of an electron in any level of importance in recombination exceeds the time the electron takes to describe its orbit. If this were not true a collision could not be regarded as a distinct event.

In solving the equations (7.3) (now with $dn_{Z-1}(p)/dt = 0$, $p \neq 1$) an infinite matrix was avoided by taking advantage of the fact that, when p is large enough, collisional processes are much more important than radiative processes, so that for values of p greater than some value (p' , say) $n_{Z-1}(p)$ satisfies Saha's equation

$$\text{(i.e. } n_{Z-1}(p) = n_E(p) \text{ for } p > p').$$

Bates *et al.* (1962 a), using various approximations for the rate coefficients and cross sections, have carried out these computations to determine $dn_{Z-1}(1)/dt$ (which is also the rate of disappearance of free charges), for a wide range of electron number density and temperature. Their results have been expressed by tabulating the quantities α^{CR} and S^{CR} where

$$dn_{Z-1}(1)/dt = -dn_Z/dt = \alpha^{\text{CR}} n_Z n_e - S^{\text{CR}} n_{Z-1}(1) n_e. \quad (7.5)$$

The quantity α^{CR} was given the name *collisional-radiative recombination coefficient* and S^{CR} the name *collisional-radiative ionization coefficient*; these coefficients depend only on T_e , n_e and various atomic parameters.

Bates *et al.* (1962 a) give the appropriate scaling laws with Z . Plots of α^{CR} and S^{CR} are given in figures 5 and 6 against n_e for various values of T_e .

Figure 7 shows the steady state ionization ratio n_Z/n_{Z-1} for hydrogen (n_{Z-1} being taken equal to $n_{Z-1}(1)$). This figure shows clearly the high density limit, where L.T.E. is valid (n_Z/n_{Z-1} proportional to n_e^{-1}) and the low density limit where the coronal approximation is valid (n_Z/n_{Z-1} independent of n_e).

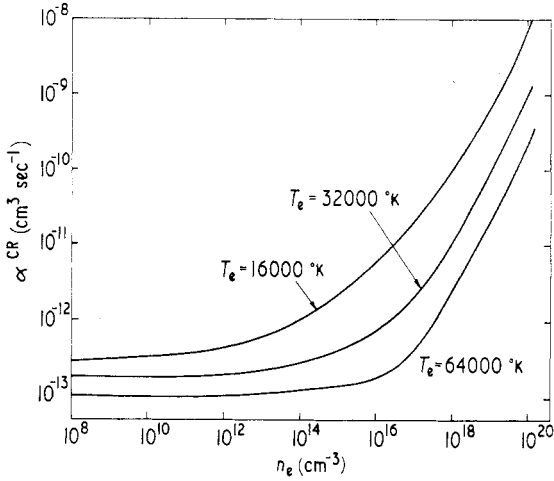


Figure 5. Optically thin hydrogen ion plasma: collisional-radiative recombination coefficient α^{CR} . (After Bates *et al.* 1962 a.)

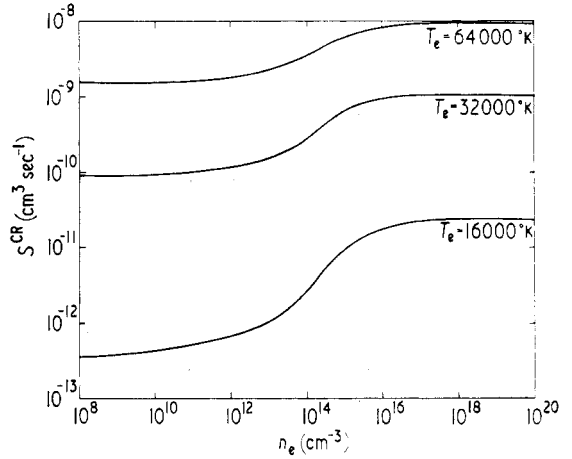


Figure 6. Optically thin hydrogen ion plasma: collisional-radiative ionization coefficient S^{CR} . (After Bates *et al.* 1962 a.)

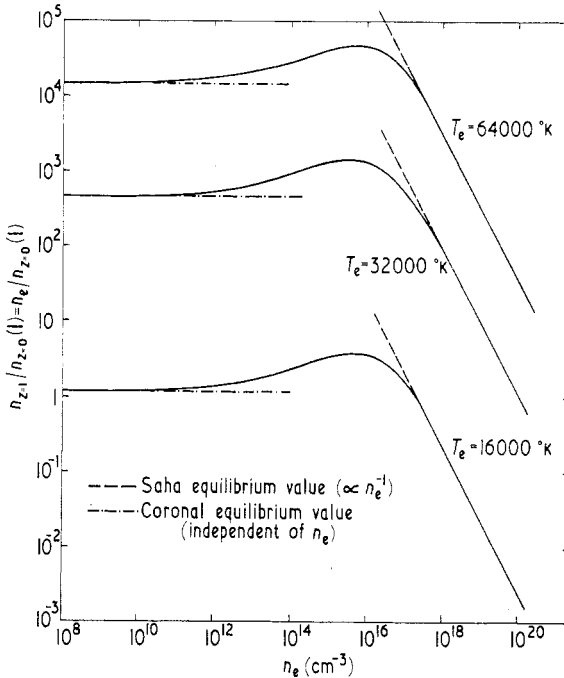


Figure 7. Optically thin hydrogen ion plasma: ionization ratio of number density in ground state ($n_{Z+0}(1)$) to number of ions ($n_{Z+1} = n_e$). (After Bates *et al.* 1962 a.)

In fact in steady state

$$\frac{\alpha^{\text{CR}}}{S^{\text{CR}} n_e} = \left(\frac{n_{Z-1}}{n_e n_Z} \right) \geq \left(\frac{h^2}{2\pi m k T_e} \right)^{3/2} \exp \left(\frac{I(1)}{k T_e} \right) \quad (7.6)$$

the equality occurring in a high density plasma for which L.T.E. is valid

$$(I(1) = E_{Z-1}(\infty) \quad \text{since} \quad E_{Z-1}(1) = 0).$$

Investigations by Byron, Stabler and Bortz (1962), Hinnov and Hirschberg (1962) and Makin and Keck (1963) have resulted in relatively simple analytic expressions for the collisional-radiative rate coefficients which are valid over certain ranges of conditions. An alternative approach is that of D'Angelo (1961). He considered the complicated reaction paths followed by individual electrons, but his final results are essentially in agreement with those of Bates *et al.* (1962 a).

Calculations using two simple physical models, one due to Wilson (1962) and the other to Griem (1964), are able to reproduce closely the results of Bates *et al.* (1962 a) and give some insight into the processes.

It is known that the collisional cross sections between closely spaced levels increase with principal quantum number, whereas the corresponding radiative decay rates decrease.

Owing to the very short electron-electron collision time, there is in general a Maxwellian velocity distribution for the free electrons (§9). The physical picture is that this thermal equilibrium in the continuum extends down to the upper bound levels owing to the high collisional rates between the upper bound levels and the continuum. Since this is imposed on the upper levels by the free electrons, the thermal equilibrium of the bound levels is linked to the continuum and their populations are given by the modified Saha equation (equation (7.2)). There is therefore some level in the ion, known as the 'thermal limit' (Wilson 1962), above which the distributions are thermal (and consequently the levels are called thermal); below the thermal limit the distributions can be approximated by a coronal distribution linked to the ground state.

For low electron densities, for which the coronal approximation is applicable, the thermal limit is close to the ionization limit. As n_e increases, the thermal limit drops lower and lower until at sufficiently high densities it reaches the ground level and all levels have a thermal population (i.e. Maxwell-Boltzmann and Saha's equations are valid).

Wilson's (1962) simplified picture is for what he calls the 'semi-coronal' régime. He defines the thermal limit p_t as the level at which upward and downward transitions are equally probable (balancing collisional ionization and collisional excitation from that level with the total radiative decay and collisional de-excitation from that same level). He then considers this thermal limit to be close to the ionization limit (hence the term 'semi-coronal'), so that, as in the coronal approximation, all bound levels intermediate between the ground level and the thermal limit may be neglected. In determining the ionization ratio, the only processes which need to be considered as contributing to ionization and recombination are the processes of radiative decay from thermal levels above the thermal limit and collisional excitation into thermal levels. When a transition from a thermal level

occurs, the level is immediately filled from the continuum, so maintaining a thermal population.

Defining the coefficients α_t and S_t , such that

$$\alpha_t = \sum_{p=p_t}^{\infty} \sum_{q=1}^{p_t-1} n_{Z-1}^{-1} n_e^{-1} n_{Z-1}(p) A(p, q) \quad (7.7)$$

and

$$S_t = \sum_{p=p_t}^{\infty} K(1, p) \quad (7.8)$$

the equation, similar to (6.2) for the ionization ratio, is, for the semi-coronal régime,

$$\frac{n_Z}{n_{Z-1}} = \frac{K(1, c') + S_t}{\sum_{p=1}^{p_t-1} \beta(p) + \alpha_t} \quad (7.9)$$

Griem (1964) in his model considers p' to be the lowest principal quantum number for which collisional excitation is still as probable as radiative decay. He then says that the effective ionization rate is approximately equal to the sum of the collisional rates for all levels less than p' into all levels greater than p' , because, once an electron gets into such states greater than p' , it most likely becomes a free electron before cascading down again. This is because for almost all levels the cross sections for excitation from a given level are much larger than those for de-excitation from the same level.

Similarly, the effective recombination rate is estimated by the sum of collisional and radiative rates from all levels greater than p' to all levels less than p' . Using approximations for the required cross sections in hydrogen, Griem obtains analytic expressions for α^{CR} and S^{CR} which are remarkably close to those of Bates *et al.* (1962 a).

Recently many further calculations have been made using collisional-radiative decay models similar to that of Bates *et al.* (1962 a).

The instantaneous population densities of the excited levels of hydrogen-like ions in a plasma are calculated by McWhirter and Hearn (1963) and Bates and Kingston (1963), and results are obtained for the power lost by line radiation, radiative recombination and bremsstrahlung.

Bates *et al.* (1962 b) discussed a relatively simple extension to optically thick plasmas. Detailed calculations were carried out on hydrogen-like plasmas, for the following cases: (i) plasmas optically thick towards lines of the Lyman series, (ii) plasmas thick towards lines of all series, and (iib) and (iic), plasmas as in cases (i) and (ii) but also optically thick towards the Lyman continuum. For instance, if the Lyman lines are completely absorbed the downward radiative transitions from level p to level 1 are balanced by reverse upward transitions. It is therefore necessary to remove all terms involving the spontaneous transition probabilities $A(p, 1)$ from the set of equations (7.3) governing the equilibrium. This effectively makes level 2 stable with respect to radiative transitions, so that when the equations are solved the term in $dn_{Z-1}(2)/dt$ is retained. The authors find that self-absorption may reduce the recombination coefficient α^{CR} considerably even in the low density limit.

The experimental results of Irons and Millar (1964) and Cooper and Kunkel (1965) are in agreement with the calculations of Bates *et al.* (1962 b) for a plasma opaque to Lyman radiation.

In two further papers by Bates and Kingston (1964 a, b) recombination and energy balance in a decaying magnetically confined plasma were considered: firstly for an $H-H^+-e$ plasma and then for a $He-He^+-e$ plasma. These take into account not only the possible differences between electron, ion and atom temperatures but also losses to the walls. The quasi-equilibrium T_e and T_i and corresponding collisional-radiative recombination coefficient α^{CR} are calculated for a wide range of optically thin and optically thick plasmas. Comparison with the experimental data of Hinnov and Hirschberg (1962) and Motley and Kuckes (1962) shows quite good agreement.

Drawin, in a series of papers, by solving the rate equations, has computed population densities and in some cases the relaxation times necessary to obtain a steady state. An optically thin hydrogen plasma is considered in Drawin (1964 a) and an optically thin helium-I plasma in Drawin (1964 b). For helium I, collisional processes taking into account the metastable 2^3S state are included.

Drawin (1965, Euratom-CEA Rep. FC 290) computes the populations of optically thin He II, using older cross sections which are zero at threshold and new values which are finite at threshold. He finds that the populations of excited states do not depend so strongly on the analytical form of the excitation cross section as the pure coronal conditions suggest, owing to strong mutual coupling of excited states. Drawin (1965) considers modifications of the optically thin hydrogen results when a superposed diffusion current of neutral hydrogen atoms is included. Drawin (1965, Euratom-CEA Rep. FC 302) takes into account, for hydrogen, He I (including metastables) and He II, the possibility of various amounts of resonance absorption by an appropriate multiplication coefficient for the spontaneous transition probability $A(2, 1)$. Good agreement has been found between these calculations and experiments carried out in a Penning discharge (Drawin *et al.* 1965).

There are many more examples of the collisional-radiative or simpler coronal type models being applied to the analysis of radiation from high temperature plasmas, taking into account the transient nature of the plasma by solving the time-dependent equations.

Perhaps the most detailed example is that of Kolb and McWhirter (1964), who carried out an analysis for theta-pinch discharges by coupling the coronal equations to the two-fluid hydromagnetic equations and took into account radiation losses from carbon, nitrogen, oxygen and neon impurities in a deuterium plasma. They showed in fact that a few per cent impurities have a drastic effect on the electron temperature (which is significant for the interpretation of many proposed thermonuclear discharges—see §18). Results of Bogen *et al.* (1964) show only qualitative agreement with the predicted time variation of T_e , but quite good agreement for the maximum values.

Other examples of calculations of the radiation from high temperature gas discharges and experimental comparisons are listed below, space being insufficient to comment on them in detail.

Hobbs *et al.* (1962) and Burton and Wilson (1961) study ZETA, the latter paper taking into account both a loss rate and injection of neutral atoms.

Jahoda *et al.* (1963) analyse the O VIII spectrum from the SCYLLA I theta-pinch and obtain qualitative, although not quantitative, agreement.

Hinnov (1964) interprets the observed impurity radiation in a discharge of the C-stellerator.

Goldman and Kilb (1964) use the rate equations to determine the time of appearance of various impurity lines in a deuterium theta-pinch plasma, and from this infer an electron temperature.

Oertel and Griem (1965) discuss the effects of spatial gradients and transient behaviour on spectral line radiation from impurities in a low energy theta-pinch plasma.

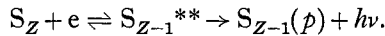
Eckerle and McWhirter (1966) consider departures from L.T.E. in the plasma produced by a magnetically driven shock wave, and show that, under certain circumstances, L.T.E. relations cannot be used, but the plasma has to be described through α^{CR} and S^{CR} coefficients of Bates *et al.* (1962 a, b).

Although quantitative comparison is often difficult, owing to uncertainties both in cross sections and in actual conditions of the discharges, most of these calculations predict at least the gross behaviour of the discharge. None of the above treatments takes into account the phenomenon of dielectronic recombination (in fact, most of the analyses apply to hydrogenic systems only). Owing to the possible importance of this process, especially in the coronal régime, it will be considered in the next section. Also the above treatments include absorption only in the crudest possible way; the far more difficult problem of solving the rate equations coupled to the radiative transfer equation is briefly discussed in § 13.

8. Dielectronic recombination

In dielectronic recombination a radiationless, reversible transition (inverse autoionization) takes place between an ion S_Z and an electron to give a doubly excited bound level of S_{Z-1} , denoted by S_{Z-1}^{**} , followed subsequently by a radiative transition to a singly-excited state of S_{Z-1} , denoted by $S_{Z-1}(p)$, below the ionization limit.

Thus



For this process to occur S_{Z-1} must have at least two electrons, so that it is not possible in hydrogenic systems.

The corresponding recombination coefficient α^{D} , via a particular state d'' (see figure 2), is given by Bates and Dalgarno (1962) as

$$\alpha^{\text{D}} = \frac{A(d'', p) A_a(d'') g_{Z-1}(d'')}{\{A(d'', p) + A_a(d'')\} 2g_Z(1)} \left(\frac{h^2}{2\pi m k T_e} \right)^{3/2} \exp\left(-\frac{E_{d''}}{k T_e}\right)$$

where $A(d'', p)$ is the probability of the radiative transition between doubly excited level $d''(S_{Z-1}^{**})$ and level p , $A_a(d'')$ is the probability of the autoionizing transition to level d'' , $g_{Z-1}(d'')$ is the statistical weight of S_{Z-1}^{**} , $g_Z(1)$ is the statistical weight of S_Z (assumed to be in its ground state) and $E_{d''}$ is the amount by which the energy of S_{Z-1}^{**} exceeds the ground state energy of S_Z .

At low temperatures, owing to the exponential factor, only a few states contribute (Bates 1962). Recently, however, A. Burgess (1964, 1965) has shown that at high temperatures a very large number of doubly excited states contribute, and the summation over states d'' (and p) to obtain α^D (total) must take these into account. Calculations for $\text{He}^+ + e$ are shown in figure 8. Results of Burgess and Seaton (1964) for dielectronic recombination of Fe^{+15} go a long way towards explaining discrepancies between temperatures of the solar corona obtained from Doppler profiles and ionization equilibria.

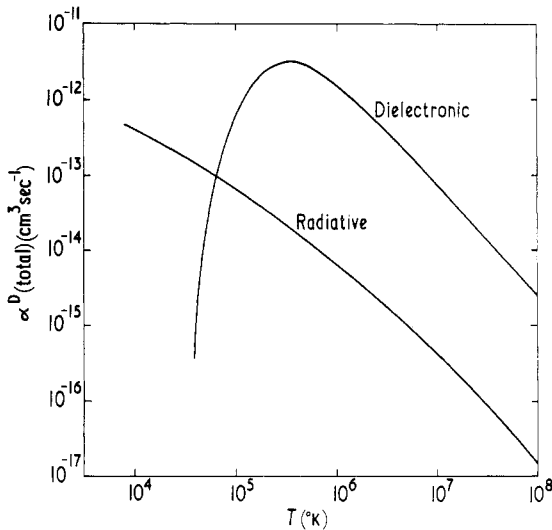


Figure 8. Dielectronic recombination coefficient α^D (total), for $\text{He}^+ + e$. (After Burgess 1964.)

These results indicate that, in dealing with ions more complex than hydrogen, the effects of dielectronic recombination should be considered.

The importance of the overall effect for laboratory plasmas is still uncertain. Collisional processes involving the doubly excited states will have to be included in collisional-radiative decay models; collisions will reduce the contribution of higher states, in the doubly excited series, to the summation involved in calculating α^D (total), since close to the series limit collisional ionization becomes more probable than radiative decay or autoionization.

9. Validity of local thermodynamic equilibrium and coronal approximations

This topic has been investigated by Griem (1963, 1964) and by Wilson (1962), who have obtained various criteria.

For the L.T.E. approximation the following conditions must be satisfied:

(a) The electron velocity distribution at any place in the plasma is Maxwellian (with corresponding temperature T_e).

(b) Collisional rates are so high compared with radiative rates in any population or depopulation process that a pseudo-detailed balance holds for collisional events only.

(c) The ions in the plasma do not move to regions of significantly different electron temperature in the relaxation time required for their level populations to come into equilibrium resulting from collisions with free electrons.

(d) In transient plasmas the equilibrium times are sufficiently short compared with the times for a significant change in the electron temperature, so that at any time a quasi-stationary near-L.T.E. state may be established.

Normally the electron Maxwellization time is quite short, but the time required for bound levels to equilibrate is much longer. Spitzer (1956) gives the electron-electron relaxation time as

$$t_{ee} = \frac{0.266 T_e^{3/2}}{n_e \ln \Lambda} \quad (9.1)$$

where T_e is in $^{\circ}\text{K}$ and $\ln \Lambda$ is a slowly varying function of n_e and T_e , usually of the order of 10.

For condition (a) to be satisfied for a plasma, it is necessary that t_{ee} be much shorter than both the heating time and the containment time. Applying condition (b) to free electrons, it is necessary that t_{ee} must be much less than radiative decay rates for free-free radiation (bremsstrahlung). Wilson (1962) showed that this particular criterion gives $T_e \lesssim 5 \times 10^{11} \ln \Lambda \text{ } ^{\circ}\text{K}$, a condition which is completely satisfied at all feasible temperatures.

Because, for almost all levels, cross sections for collisional excitation are much larger than those for de-excitation, near L.T.E., the population of a given level is mostly determined by a balance between collision-induced transitions from higher levels with collisional excitation into these higher levels. The condition (b) for a level to be in L.T.E. with respect to all higher levels is equivalent to saying that the total radiative decay rate should be much smaller ($< 1/10$, say) than the total rate of excitation from this level to all higher levels, for in equilibrium this collisional excitation rate must equal the collisional population rate from higher levels.

Griem (1963, 1964), using estimates for the cross sections involved in a hydrogenic system, showed that a level of principal quantum number p of S_{Z-1} is in equilibrium with higher levels provided that

$$n_e \geq 7 \times 10^{18} \frac{Z^7}{p^{17/2}} \left(\frac{kT_e}{Z^2 E_H} \right)^{1/2} \text{ cm}^{-3} \quad (9.2)$$

where $Z^2 E_H = E_{Z-1}(\infty)$ is the ionization energy of a hydrogenic ion of charge $Z-1$. This result is in agreement with the more detailed calculations of McWhirter and Hearn (1963) and Bates and Kingston (1963).

For complete L.T.E., Griem considers that the collisional population rate of the ground state should be ten times greater than the radiative population rate via the resonance transition from the first excited state, and obtains the criterion that

$$n_e \geq 9 \times 10^{17} Z^7 \left(\frac{kT_e}{Z^2 E_H} \right)^{1/2} \left(\frac{E_{Z-1}(2)}{Z^2 E_H} \right)^3 \text{ cm}^{-3} \quad (9.3)$$

where $E_{Z-1}(2)$ is the energy of the first excited state with respect to the ground state ($E_{Z-1}(1) = 0$). This derivation was for a hydrogen-like species where

$$E_{Z-1}(\infty) = Z^2 E_H$$

but it was pointed out that the oscillator strength of the resonance transition cancels out, and that the approximation should be reasonable for other species. However, it should be applied with care to systems with low-lying resonance levels (e.g. lithium-like) where there is the possibility of ground and first excited states being in equilibrium without complete L.T.E. Wilson (1962) considers the position of the thermal limit (§ 6) and then derives a condition for the electron density to be so large that this limit reaches to the ground state.

This condition can be written as

$$n_e \geq 5.6 \times 10^{17} Z^7 \left(\frac{kT_e}{Z^2 E_H} \right)^{1/2} \left\{ \frac{E_{Z-1}(\infty)}{Z^2 E_H} \right\}^3 \text{ cm}^{-3}. \quad (9.4)$$

Apart from the difference in the numerical constant, Griem's condition uses the energy of the first excited state whereas Wilson uses the ionization energy. Wilson's condition is more stringent and should be used when low excited states exist. These conditions for complete L.T.E. may be relaxed if the resonance transitions are self-absorbed and become optically thick, because this effectively reduces the radiative population rate of the ground state.

The relaxation distances and times of conditions (c) and (d) for which the electron temperature should not change appreciably are also given by Griem. These criteria are very important. Eckerle and McWhirter (1966) have shown that, for a T tube, under certain conditions, the state of the plasma lags behind the rapidly varying electron temperature owing to the slow ionization and recombination rates, although the electron density is quite high enough to satisfy equations (9.2) or (9.3).

For the coronal domain Wilson (1962) gives the condition that his coefficients α_t and S_t (equations (7.8) and (7.7)) should be less than 10% of the corresponding coefficients $\sum_p \beta(p)$ and $K(1, c')$ used in the coronal equations.

This can be written for species S_{Z-1} as

$$n_e \lesssim 1.4 \times 10^{14} Z^7 \left(\frac{kT_e}{Z^2 E_H} \right)^4 \left(\frac{Z^2 E_H}{E_{Z-1}(\infty)} \right)^{1/2} \text{ cm}^{-3}. \quad (9.5)$$

Calculations show that many high temperature laboratory plasmas fall into the coronal (or at least semi-coronal) régime.

In order to apply the coronal equations and the results of Bates *et al.* (1962 a) it is also necessary that the plasma be optically thin—this is discussed in § 13.

10. Line radiation

In the preceding sections, especially §§ 4 and 7, it has been indicated how the population densities may be found in principle.

In this and the following sections the details of the radiation are considered, that is, the intensity and wavelength distribution of line radiation and of continuum and recombination radiation.

Before accurate predictions concerning line radiation can be made it is usually necessary to classify the transitions involved (see, for example, Edlén 1964), i.e. if Russell-Saunders coupling is applicable, it is necessary to know the quantum numbers L , S and J of both states involved in the transition.

Moore's tables (1949–58) are quite complete for neutral atoms and for species of low stages of ionization; however, for transitions involving the highly ionized species often encountered in high temperature gas discharges, the classification of even the strong lines is not always complete. Various authors have in fact used high temperature discharges specifically for classification purposes. These discharges have distinct advantages for the excitation of gaseous elements, such as the rare gases (see, for example, Fawcett *et al.* 1961, Bochasten *et al.* 1963, Fawcett *et al.* 1964, Peacock 1964, House and Sawyer 1964, Fawcett and Gabriel 1965).

There is a most interesting example of how high temperature gas discharges can reproduce the conditions of the solar corona. An intense set of emission lines in the vacuum ultra-violet between 167 Å and 220 Å has been observed in the spectrum of the solar corona (Tousey 1964, Hinteregger *et al.* 1964). These emission lines were first produced in the laboratory by the toroidal discharge ZETA (Fawcett *et al.* 1963), and later in theta-pinch discharges (Elton *et al.* 1964, House 1964, House *et al.* 1964). The transitions were ascribed to the element iron, and in further work Fawcett and Gabriel (1965) found similar systems of lines for the elements calcium to nickel inclusive. Several attempts at classification were made (Alexander *et al.* 1965, Zirin 1964) and recently Gabriel *et al.* (1965) assigned them to various 3p–3d transitions in Fe VIII to XII.

The radiation is described in terms of the Einstein A and B coefficients. Consider an atom or ion which has quantum states p of higher and q of lower energy. The probability per unit time that an atom in state p emits a photon $h\nu$ ($= h\nu_{pq} = h\nu_{qp}$) is written as $A(p, q)$. The induced emission and absorption depend on the intensity of radiation $I(\nu)$, and coefficients $B(p, q)$ and $B(q, p)$ are defined such that $B(p, q)I(\nu)$ is the probability per unit time that an atom in state p is induced to emit a photon $h\nu$. Similarly, $B(q, p)I(\nu)$ is the probability per unit time that an atom in state q absorbs a photon $h\nu$. The total emission probability is $\{A(p, q) + B(p, q)I(\nu)\}$. In equilibrium, the total rates in the two directions $p \rightarrow q$ and $q \rightarrow p$ must balance. Thus, if $n(p)$ and $n(q)$ are the population densities of atoms in states p and q respectively, then the principle of detailed balancing yields

$$n(q) B(q, p) I(\nu) = \{A(p, q) + B(p, q) I(\nu)\} n(p).$$

But, in complete thermodynamic equilibrium at temperature T , Maxwell-Boltzmann statistics must apply, i.e.

$$\frac{n(p)}{n(q)} = \left\{ \frac{g(p)}{g(q)} \right\} \exp\left(-\frac{h\nu}{kT}\right)$$

and $I(\nu)$ is given by Planck's radiation law as

$$I(\nu) = \left(\frac{2h\nu^3}{c^2}\right) \left\{ \exp\left(\frac{h\nu}{kT}\right) - 1 \right\}^{-1}.$$

This leads immediately to

$$g(p) B(p, q) = g(q) B(q, p) \quad (10.1)$$

and

$$A(p, q) = \left(\frac{2h\nu^3}{c^2}\right) B(p, q). \quad (10.2)$$

These coefficients, defined in terms of the intensity, are sometimes known as the Milne coefficients.

Quantum mechanics (Dirac 1958) gives the total rate of emission of energy between states $|p'\rangle$ and $|q'\rangle$, in the electric dipole approximation, as

$$\frac{4}{3} \frac{(2\pi\nu)^4}{c^3} |\langle p' | e\mathbf{x} | q' \rangle|^2 \quad (10.3)$$

and the absorption cross section $\sigma_{q'p'}(\nu)$ (the probability per unit time of absorption of a photon taking place with an incident photon crossing unit area per unit time per unit frequency range) as

$$\sigma_{q'p'}(\nu) = \frac{8\pi^3}{3hc} |\langle p' | e\mathbf{x} | q' \rangle|^2 \quad (10.4)$$

where the factor $\frac{1}{3}$ is introduced by averaging over all orientations of the atom.

In the case considered here, the upper and lower states are degenerate with statistical weights $g(p)$ and $g(q)$, so that, dividing (10.3) by $h\nu$ and summing over states,

$$g(p) A(p, q) = \frac{64\pi^4 \nu^3}{3hc^3} \sum_{p'q'} |\langle p' | e\mathbf{x} | q' \rangle|^2. \quad (10.5)$$

$\sum_{p'q'} |\langle p' | e\mathbf{x} | q' \rangle|^2$, with summation over all components of the upper and lower states, is known as the line strength (Condon and Shortley 1935, p. 98).

The spontaneous transition probability is often written in terms of the absorption oscillator strength f_{qp} , such that

$$g(q) f_{qp} = g(p) A(p, q) \frac{mc^3}{8\pi^2 e^2 \nu^2}. \quad (10.6)$$

These f values may be computed exactly for hydrogen by quantum mechanics. They are given by the formula

$$f_{qp} = \frac{2^6}{3\sqrt{(3)\pi}} \frac{1}{g(q)} \left| \frac{1}{q^3} \frac{1}{p^3} \right| \left(\frac{1}{q^2} - \frac{1}{p^2} \right)^{-3} g_{bb} \quad (10.7)$$

where $g(q) = 2q^2$ is the statistical weight of the lower level, and g_{bb} is the Gaunt (1929) factor tabulated by Menzel and Pekeris (1936). The individual oscillator strengths are tabulated for the most important transitions in hydrogen by Green *et al.* (1957).

Owing to the finite lifetime of the atomic states the transition will not be infinitely sharp. Also the plasma will perturb the eigenstates of emitting atoms and ions so that the transitions will be both broadened and shifted from their unperturbed values (ν_{pq}). This gives rise to the line profile $\phi(\nu)$ defined so that the probability of emission in the interval $\nu, \nu + d\nu$ is $\phi(\nu) d\nu$. For this to be meaningful the width of the profile should be much less than ν_{pq} , and $\phi(\nu)$ is normalized such that

$$\int_{\text{line}} \phi(\nu) d\nu = 1.$$

The line profile should not be confused with the actual observed intensity distribution since this may be distorted by radiative transfer effects (§ 13).

The power radiated per unit volume per unit solid angle and per unit frequency interval is

$$\epsilon(\nu) = \frac{h\nu}{4\pi} \phi(\nu) A(p, q) n(p) \quad (10.8)$$

and the total power radiated in the line per unit solid angle is

$$\epsilon_t = \frac{h\nu}{4\pi} A(p, q) n(p). \quad (10.9)$$

In the optically thin case there is no interaction of the radiation with the plasma ($B(p, q)$ terms unimportant) and all the radiation escapes, so that, for a homogeneous layer of thickness D , the total emitted intensity is

$$I_t = \int I(\nu) d\nu = \frac{h\nu}{4\pi} A(p, q) n(p) D. \quad (10.10)$$

The total number of photons absorbed per unit volume per second is

$$n(q) B(q, p) I(\nu).$$

But, for an isotropic intensity distribution, the photon flux per unit frequency range is $4\pi I(\nu)/h\nu$, so that multiplying $\sigma_{p'q'}(\nu)$ of equation (10.4) by this value gives the probability of absorption for an atom in sub-level q' . The total number of absorptions per unit volume is found by multiplying by the number density of the sub-level ($= n(q)/g(q)$) and summing over all the components of the initial and final states. Therefore

$$n(q) B(q, p) I(\nu) = \frac{4\pi I(\nu)}{h\nu} \frac{n(q)}{g(q)} \frac{8\pi^3 \nu}{3hc} \sum_{p'q'} |\langle p' | e\mathbf{x} | q' \rangle|^2$$

and

$$g(q) B(q, p) = \frac{32\pi^4}{3h^2 c} \sum_{p'q'} |\langle p' | e\mathbf{x} | q' \rangle|^2. \quad (10.11)$$

Equations (10.11) and (10.5) are, of course, consistent with (10.1) and (10.2).

In terms of the absorption coefficient $\sigma_{qp}(\nu)$ for all components, the total energy of line radiation absorbed is

$$4\pi n(q) \int_{\text{line profile}} \sigma_{qp}(\nu) I(\nu) d\nu.$$

Thus, assuming the intensity remains constant over the line profile, comparison with the above gives

$$\int_{\text{line}} \sigma_{qp}(\nu) d\nu = \frac{8\pi^3 \nu}{3hcg(q)} \sum_{p'q'} |\langle p' | e\mathbf{x} | q' \rangle|^2 = \frac{\pi e^2}{mc} f_{qp} \quad (10.12)$$

and

$$\sigma_{qp}(\nu) = \frac{h\nu}{4\pi} B(q, p) \phi(\nu) \quad (10.13)$$

where now $\phi(\nu)$ refers to the profile for absorption.

In order to be able to measure the oscillator strength (or $A(p, q)$) by emission measurements, not only must the total intensity be measured (equation (10.10)), but also the population density $n(p)$ of the upper state must be known. This means

the use of a light source whose properties are accurately known. In general this must be a plasma in local thermodynamic equilibrium, since only then do the population densities of the quantum states become independent of detailed rate coefficients. Arcs and shock tubes may often be used for neutral and singly ionized species, but it is extremely difficult to obtain highly ionized species in L.T.E.

A detailed review of oscillator strength measurements has been given by Foster (1964) and of measurements and calculations by Nicholls and Stewart (1962). A bibliography of available results has been compiled by Glennon and Wiese (1962, 1963)†. Although much experimental work on neutral elements is available, in plasma spectroscopy ionized species are important and here, owing mainly to difficulties of obtaining L.T.E. plasmas, the available experimental measurements are very sparse.

Mastrup and Wiese (1958) have made measurements on O II and N II, Olsen (1963) on Ar II, Koopman (1964) on Ne II and Berg *et al.* (1964) on O II and O III; the first two sets of authors used stabilized arcs and the last two shock tubes. Although relative oscillator strengths for a given species may be fairly accurate, the absolute values of oscillator strengths for ionized species are not much better than about 20 to 30%.

Often, therefore, experimental results for a particular transition are not available, and one has to resort to calculation. The electronic wave functions ($|p\rangle$ and $|q\rangle$) are written in terms of sums of products of single-particle wave functions which are themselves products of angular and radial parts. The angular part of the wave function can be handled by methods due to Racah (1942, 1943, 1949) (see Edmonds 1957), and the resulting formulae for transition probabilities in *LS* coupling are given by Rohrlich (1959) and Kelly (1964 a).

These results are expressed in terms of the square of the radial matrix element, which for a transition $p'l' \rightarrow p''l''$ (p and l are principal and orbital quantum numbers of the 'jumping' electron) is

$$\sigma^2 = \frac{1}{4l_{>}^2 - 1} \left\{ \int R_{p'l'}(r) R_{p''l''}(r) r dr \right\}^2 \quad (10.14)$$

where $l_{>}$ is the larger of l' and l'' and $R_{pl}(r)$ are normalized radial wave functions of the jumping electron multiplied by r . The problem is to calculate the $R_{pl}(r)$, because exact solutions only exist for hydrogen and other one-electron systems. Since it is necessary to integrate over the product of two different wave functions, it is easy to show that the determination of σ^2 is much less accurate than the determination of energy eigenvalues, which involve only the square of one wave function.

Various methods for obtaining the $R_{pl}(r)$ exist. Probably the most accurate method to obtain these wave functions is via the Hartree-Fock self-consistent field (Hartree 1957) and in certain cases the results obtained by this method may be accurate to better than 10% (i.e. see Trefftz *et al.* 1957, Kelly 1964 b, and Pfennig *et al.* 1965). Also used are variational calculations, in which wave functions are found by minimizing the energy matrix elements (see Salpeter and Zaidi 1962) and numerical solutions of Schrödinger's equation with a potential chosen to give

† For further reference see W. L. Wiese, M. W. Smith and B. M. Glennon, *A Critical Data Compilation of Atomic Transition Probabilities for Hydrogen through Neon*, NSRDS-NBS 4, Vol. 1.

correct energy values (see Stone 1962), but these, as with the Hartree–Fock method, involve a considerable amount of computation.

Much simpler, and in many cases equally accurate, is the Coulomb approximation of Bates and Damgaard (1949) (see also Seaton 1958). This makes use of the fact that often the major contribution to the integral for σ^2 (equation (10.14)) is from a region of large r where the potential is closely Coulombic (i.e. $\sim Ze/r$). Hydrogenic wave functions with an effective principal quantum number are then used. The Coulomb approximation is not valid for transitions whose wave functions strongly overlap with the core (mainly s electrons and to some extent p electrons), but for outer electrons the accuracy can be taken as about 20%. A tabulation of oscillator strengths in the Coulombic approximation with *LS* coupling is given by Griem (1964). For simple atoms, i.e. those with one electron outside a closed shell, agreement between this theory and experiment is usually better than 10%. This method is particularly useful for transitions between highly excited states.

In the screening approximation of Layzer (1959) and Varsavsky (1961), screened hydrogenic radial wave functions are obtained from an expansion of the wave function in inverse powers of the nuclear charge. This method should be suitable for highly ionized systems but, as yet, there is not always good agreement with results obtained by other methods.

When *LS* coupling cannot be applied, other methods, such as the intermediate coupling approximation of Garstang (1954), have to be used. Quite good agreement between Garstang's results and measurements by Olsen (1963) for Ar II have been found.

Only allowed transitions have been considered here; for a review of forbidden transitions see Garstang (1962). However, in a plasma the perturbation due to surrounding particles often mixes the wave functions of an atom sufficiently to allow transitions which are forbidden if the atom is isolated.

11. Line profiles

The shape of a spectral line is important since it contains information concerning the environment of the emitting atom or ion in the plasma. The profile of the actual line observed is modified by radiative transfer (§ 13), and there can be saturation at or below the black-body intensity (self-absorption) or absorption in colder boundary layers (self-reversal). However, when the plasma is optically thin the profile of the observed radiation will be the same as the emission line profile $\phi(\omega)$ (which is, for a given atom, such that $\phi(\omega) d\omega$ is the probability of emission between ω and $\omega + d\omega$).

The broadening mechanisms which may be important in a plasma are Doppler broadening, natural broadening and Stark (sometimes called pressure) broadening. Estimates for resonance broadening and van der Waals broadening (Griem 1964) show that these mechanisms can usually be neglected. In the past few years, following the work of Baranger, Griem and their co-workers, the Stark broadening theory has been considerably improved. (Detailed reviews of this modern theory are given by Baranger (1962) and Griem (1964).)

In this section the broadening mechanisms are reviewed and the results of the modern theory are discussed at some length.

11.1. Natural line broadening

This broadening is due to the finite lifetime of the excited states and yields a dispersion profile (Lorentz profile) (see Heitler 1954):

$$\phi(\omega) = \frac{1}{\pi w_N} \left\{ 1 + \frac{(\omega - \omega_0)^2}{w_N^2} \right\}^{-1} \quad (11.1)$$

where

$$\int \phi(\omega) d\omega = 1$$

and ω_0 is the frequency at the line centre. The half half-width w_N depends on the Einstein transition probabilities of all transitions originating from the upper and lower levels (principal quantum numbers u and l)

$$w_N = \frac{1}{2} \left\{ \sum_{p'} A(u, p') + \sum_{q'} A(l, q') \right\}. \quad (11.2)$$

In laboratory plasmas this is almost always negligible (except for autoionization broadening of doubly excited states).

11.2. Doppler broadening

Owing to the motion of the emitting atom the frequency of the emitted radiation (as seen by an observer at rest) is altered by the Doppler effect such that

$$\frac{\Delta\omega}{\omega} = \frac{v}{c} \quad (11.3)$$

where the line of sight is parallel to the velocity v of the atom.

If the emitting atoms have a Maxwellian velocity distribution, the broadened line profile will have a Gaussian shape

$$\phi(\omega) = \frac{1}{\beta\sqrt{\pi}} \exp \left\{ -\frac{(\omega - \omega_0)^2}{\beta^2} \right\} \quad (11.4)$$

where $\beta^2 = 2kT_i\omega_0^2/Mc^2$, M is the ion mass and T_i the ion temperature. The half half-width w_D is given by

$$w_D = (\ln 2)^{1/2} \omega_0 \left(\frac{2kT_i}{Mc^2} \right)^{1/2}. \quad (11.5)$$

Apart from full kinetic equilibrium the ion temperature is not necessarily the same as T_e . The electrons and ions may have quite different kinetic temperatures, even though they both have very nearly Maxwellian distributions. This is because momentum transfer cross sections are small for particles of very different masses. In the general case the Doppler profile has to be related to the velocity distribution of the emitting species (see § 15.6).

11.3. Stark broadening or pressure broadening

When the phenomenon responsible for line broadening consists of interactions between the radiating atoms or ions, the broadening is density dependent, in

contrast to that in the above mechanisms. Since the radiator is much more strongly perturbed by charged particles than by neutral ones, only electrons and ions need be considered as perturbers in a highly ionized plasma. The interaction between the radiator and the perturber can usually be described by the first term in a multipole expansion of the interaction, i.e. as

$$V(t) = -\mathbf{d} \cdot \mathbf{E} \quad (11.6)$$

where \mathbf{d} is the dipole moment of the radiator and \mathbf{E} is the electric field produced by the perturber at the centre of the radiator.

In line-broadening calculations it is generally a valid approximation to consider the perturber as a classical particle describing a classical path. (For a brief discussion, see §11.3.3.) One can then consider the radiating atom to be perturbed during the duration of a collision defined as $\tau_c \simeq \rho/\bar{v}$ where ρ is the impact parameter and \bar{v} the mean velocity of the perturber. Because of the usually large difference in electron and ion velocities, the two collision times are very different. Often for electrons, the duration of the collision τ_c can be regarded as short compared with the time between collisions. This enables the electron broadening to be calculated on the basis of the *impact approximation*, for which the emitting system is virtually unperturbed most of the time and the broadening is described in terms of impacts which are well separated in time. For the long-range Coulomb interactions the collisions can never be separated in time; however, if the average interaction is weak (in so far as the interactions cause only small perturbations of the radiator) the collisions may be considered to act separately. (This point is further discussed in §11.3.3.) To make this impact approximation the duration of the collision must obviously be less than the unperturbed lifetime of a state.

For the slowly moving ions the perturbation is practically constant over the times of interest (which are, at most, of the order of the inverse of the linewidth in frequency units), so that their motion may be neglected completely. Their effect is calculated via the static Stark effect, taking into account the statistical distribution of the electric fields at the emitting atom or ion. This is known as the *quasi-static approximation*.

A general procedure is firstly to determine the shifts and intensities of the various components of a given line (the Stark pattern) of the radiator for an arbitrary electric field \mathbf{E} (see, for instance, Bethe and Salpeter 1957). The impact approximation is then used to calculate the electron-broadened profiles of the components, and finally the whole broadened pattern is averaged over the statistical distribution of the ion field.

In order to illustrate the principles of the quasi-static and impact approximations, very simple examples are considered.

11.3.1. *Quasi-static broadening.* The simple theory of quasi-static (or statistical) broadening (Holtsmark 1919) has been well described by Margenau and Lewis (1959).

In the simplest form of this theory the emitter is assumed to be perturbed by the nearest ion only. (This form of binary interaction describes the line wings adequately, but breaks down at the line centre when the description should be in terms of many weak perturbations by distant ions.)

The probability of finding the nearest ion at a distance r (and no ion any nearer) is, if interactions between the charged perturbers are neglected,

$$dP(r) = \exp \left\{ - \left(\frac{r}{\rho_m} \right)^3 \right\} d \left(\frac{r}{\rho_m} \right)^3 \quad (11.7)$$

where ρ_m is the average distance between perturbers given by

$$\frac{4}{3}\pi n = \rho_m^{-3}$$

where n is the density of perturbers. Since the field at the emitter due to the nearest ion is $E = Ze/r^2$, the probability $dP(E)$ of the emitter being subjected to an electric field E (normalized, such that

$$\int_0^{E=\infty} dP(E) = 1)$$

is in this nearest-neighbour approximation

$$dP(E) = \left(\frac{3}{2E} \right) \left(\frac{E_0}{E} \right)^{3/2} \exp \left\{ - \left(\frac{E_0}{E} \right)^{3/2} \right\} dE \quad (11.8)$$

where E_0 is the value of E at ρ_m . More generally, for no interaction between the perturbers

$$dP(\beta) = W_H(\beta) d\beta$$

where $W_H(\beta)$ is the Holtsmark ion field strength distribution function, and $\beta = E/E_0$.

The shift of the energy levels in this static field is then calculated by the usual methods of quantum mechanics (see Bethe and Salpeter 1957).

The shift of one Stark component may be written as

$$\Delta\nu = \frac{C_\mu}{2\pi r^\mu} \propto E^{\mu/2} \quad (11.9)$$

where r is the distance between the perturber and emitting atom and the coefficients C_μ are constant. $\mu = 2$ for atoms subject to the linear Stark effect and $\mu = 4$ for quadratic Stark effect. Substitution in the distribution function gives the line profile.

In general

$$\phi(\Delta\nu) d(\Delta\nu) = W_H(\beta) d\beta$$

giving (i) for linear Stark effect ($\mu = 2$)

$$\beta = \frac{E}{E_0} = \frac{\Delta\nu}{\Delta\nu_0}$$

$$\phi(\Delta\nu) = W_H \left(\frac{\Delta\nu}{\Delta\nu_0} \right) \frac{1}{\Delta\nu_0}$$

and (ii) for quadratic Stark effect ($\mu = 4$)

$$\beta = \frac{E}{E_0} = \left(\frac{\Delta\nu}{\Delta\nu_0} \right)^{1/2}$$

$$\phi(\Delta\nu) = W_H \left\{ \left(\frac{\Delta\nu}{\Delta\nu_0} \right)^{1/2} \right\} \frac{1}{2} (\Delta\nu_0 \Delta\nu)^{-1/2}$$

where (for (i) and (ii))

$$\Delta\nu_0 = \frac{C_\mu}{2\pi\rho_m^\mu} = \frac{C_\mu}{2\pi} \left(\frac{4\pi n}{3} \right)^{\mu/3}$$

In more detailed quasi-static theory the interactions between the perturbers have to be taken into account in the calculations of the ion field strength distribution function (similar to $W_H(\beta)$). Mozer and Baranger (1960) have evaluated the distributions of the field at neutral atoms and singly charged ions, taking into account Debye shielding by electrons and pair interactions (ion-ion correlation) between the ions. Their results are likely to be accurate if $R = \rho_m/\rho_D \leq 1$.

The $\Delta\nu$ in equation (11.9) is calculated quantum-mechanically on the assumption that the field at the emitter is uniform. However, for close perturbers there is a large field gradient, i.e. the quadrupole interaction has to be considered. Müller (1965) argues that for atoms having only a quadratic Stark effect (with frequency perturbation proportional to $1/r^4$) the quadrupole interaction (proportional to $1/r^3$) can be important for low densities. He in fact indicates that, within the quasi-static approximation for ions, this quadrupole term should dominate the quadratic Stark effect in neutral helium at densities less than about 10^{16} – 10^{17} particles per cubic centimetre. To explain asymmetries in the profile of $L\alpha$ observed by Boldt and Cooper (1964), Nguyen-Hoe, Drawin and Herman (1964) have calculated the quasi-static ion broadening taking into account both linear and quadratic Stark effect for an intermolecular ion field having both a dipole and a quadrupole component. More recent work by Griem (1965) is qualitatively in agreement with results of these calculations, but in detail there is strong disagreement.

11.3.2. *Impact approximation.* The features of the impact approximation are discussed with reference to the theory of Lindholm (1941) using a quasi-classical approach (see Traving 1960 and Sobel'man 1957).

In the quasi-classical approximation the calculation of the intensity distribution $I(\omega)$ in a line amounts to the Fourier analysis of the oscillations of the equivalent atomic oscillator. In the general case the function $f(t)$ describing the dipole moment of a perturbed oscillator has the form

$$\begin{aligned} f(t) &= A(t) \exp \left\{ j \int_0^t \omega(t') dt' \right\} \\ &= A(t) \exp \{ j\omega_0 t + j\eta(t) \} \end{aligned} \tag{11.10}$$

where ω_0 is the unperturbed frequency and $\eta(t)$ is the sum of the phase changes in the interval 0 to t .

The mean intensity radiated by the oscillator in a given frequency interval is proportional to the power spectrum of $f(t)$ (see, for instance, Freeman 1958). This can be shown to be equal to the time average of the square of the modulus of the Fourier component $|F(\omega)|$ of the varying dipole moment of the oscillator $f(t)$. Thus

$$\begin{aligned} I(\omega) &= \lim_{T \rightarrow \infty} \left\{ \frac{1}{T} \left| \int_{-T/2}^{T/2} f(t) \exp(-j\omega t) dt \right|^2 \right\} \\ &\equiv \langle |F(\omega)| \rangle_{av}^2 \end{aligned} \tag{11.11}$$

where $\langle \rangle_{av}$ denotes a time average.

By means of the Wiener-Khintchine theorem (Wiener 1930, Khintchine 1934), this is expressed in terms of the more convenient autocorrelation function $\Phi(s)$.

Thus

$$I(\omega) = \int_{-\infty}^{\infty} \Phi(s) \exp(-j\omega s) ds \quad (11.12)$$

where

$$\begin{aligned} \Phi(s) &= \lim_{T \rightarrow \infty} \left\{ \frac{1}{T} \int_{-T/2}^{T/2} f^*(t) f(t+s) dt \right\} \\ &\equiv \langle f^*(t) f(t+s) \rangle_{\text{av}} \end{aligned} \quad (11.13)$$

($f^*(t)$ is the complex conjugate of $f(t)$).

This autocorrelation function, or its quantum-mechanical equivalent, has been the starting point for many line-broadening calculations (see Margenau and Lewis 1959, Traving 1960, Baranger 1962, Griem 1964).

In the Lindholm theory $A(t)$ is put equal to 1 in equation (11.10) and $f(t)$ is represented by

$$f(t) = \exp\{j\omega_0 t + j\eta(t)\}. \quad (11.14)$$

The amplitude of the oscillation stays constant, i.e. it is assumed that no transfer of energy from the perturber to the oscillator occurs. There is thus no mechanism in this particular theory for the perturbation to induce transitions to neighbouring levels, and the perturbation is said to be *adiabatic*.

To calculate $I(\omega)$, and hence the line profile, it is necessary to calculate $\Phi(s)$. Put

$$\begin{aligned} \phi(s) &= \Phi(s) \exp(-j\omega_0 s) \\ &= \lim_{T \rightarrow \infty} \left\{ \frac{1}{T} \int_{-T/2}^{T/2} \exp[j\{\eta(t+s) - \eta(t)\}] dt \right\}. \end{aligned} \quad (11.15)$$

Now, to calculate the differential of $\phi(s)$ note that

$$\begin{aligned} \exp[j\{\eta(t+s+\Delta s) - \eta(t)\}] - \exp[j\{\eta(t+s) - \eta(t)\}] \\ = \exp[j\{\eta(t+s) - \eta(t)\}] \{\exp(j\eta') - 1\} \end{aligned} \quad (11.16)$$

where η' denotes the additional phase shift in time Δs ($= (\partial\eta/\partial s)\Delta s$). Thus

$$\Delta\phi(s) = \phi(s+\Delta s) - \phi(s) = \langle \exp[j\{\eta(t+s) - \eta(t)\}] \{\exp(j\eta') - 1\} \rangle_{\text{av}} \quad (11.17)$$

where the time average has been taken.

This expression for $\Delta\phi(s)$ can be simplified further if a time interval Δs can be found such that:

(i) Δs is sufficiently large so that the phase changes during Δs are statistically independent of the instantaneous phase $\eta(s)$. The mean value of the product may then be replaced by the product of the mean values of the factors.

(ii) Δs is sufficiently small so that $\Delta\phi(s)$ can be replaced by a differential. Thus

$$d\phi(s) = \phi(s) \langle \exp(j\eta') - 1 \rangle_{\text{av}}. \quad (11.18)$$

Averaging these factors separately is the essential step in the impact approximation, since (i) above will be true if an impact occurs during Δs . (The validity of this approximation will be discussed later in this section, and in § 11.3.3.)

By the ergodic hypothesis the time average of a quantity is the same as the statistical average of this quantity over the ensemble. In this case the average has to be taken over all possible collisions which cause a phase change in the interval

Δs ($= ds$ in differential form). If n is the perturber number density and \bar{v} is the mean perturber velocity, the number of impacts with the oscillator with impact parameter between ρ and $\rho + d\rho$ is

$$n\bar{v}ds2\pi\rho d\rho. \tag{11.19}$$

Since the phase shift $\eta'(\rho)$ due to a collision is a function of the impact parameter, summing over all possible collisions in Δs gives

$$\begin{aligned} \langle \exp(j\eta') - 1 \rangle_{av} &= n\bar{v}ds \int_0^\infty 2\pi[\exp\{j\eta'(\rho)\} - 1] \rho d\rho \\ &= n\bar{v}ds(\sigma_r - j\sigma_i) \end{aligned} \tag{11.20}$$

where σ_r and σ_i (the optical cross sections) stand for -2π times the real and imaginary parts of the integral.

In order to write the above integral (equation (11.20)) it has been assumed that the phase shift due to each impact may be considered separately and that they are completed in time Δs . Thus

$$d\phi(s) = -n\bar{v}ds(\sigma_r - j\sigma_i)\phi(s)$$

or

$$\phi(s) = \exp\{-n\bar{v}(\sigma_r - j\sigma_i)s\}. \tag{11.21}$$

Converting to $\Phi(s)$ and performing the Fourier transformation gives finally that

$$I(\omega) d\omega = \frac{n\bar{v}\sigma_r}{\pi} \frac{d\omega}{(\omega - \omega_0 - n\bar{v}\sigma_i)^2 + (n\bar{v}\sigma_r)^2}. \tag{11.22}$$

This is a dispersion or Lorentz profile of half half-width $w = n\bar{v}\sigma_r$ and shift $d = n\bar{v}\sigma_i$ from the unperturbed central frequency ω_0 .

The phase shift $\eta'(\rho)$ is easy to calculate in this adiabatic approximation, for, since no transitions between levels are caused by the perturbers, the state of the emitter is described at all times as if the perturbers were at rest, i.e. by the ordinary quantum mechanics of the Stark effect.

The frequency shift of the line due to a perturber at distance r from the emitter is

$$\Delta\omega = \frac{C_\mu}{r^\mu} \tag{11.23}$$

where $\mu = 2$ for linear Stark effect and $\mu = 4$ for quadratic Stark effect (as in § 11.3.1). For a neutral emitter the classical path is a straight line and

$$r = \{\rho^2 + \bar{v}^2(t - t_0)^2\}^{1/2} \quad \text{for impact at time } t_0.$$

Therefore

$$\begin{aligned} \eta'(\rho) &= \int_{-\infty}^\infty \Delta\omega dt = \int_{-\infty}^\infty \frac{C_\mu dt}{\{\rho^2 + \bar{v}^2(t - t_0)^2\}^{\mu/2}} \\ &= \sqrt{\pi} \frac{\Gamma\{\frac{1}{2}(\mu - 1)\} C_\mu}{\Gamma(\frac{1}{2}\mu) \bar{v}\rho^{\mu-1}}. \end{aligned} \tag{11.24}$$

The integral should be over the time that the perturber interacts with the emitter, but a sufficient approximation results when it is performed from $-\infty$ to $+\infty$.

This expression for the phase shift $\eta'(\rho)$ can then be put into the integral of equation (11.20) and σ_i and σ_r determined (see Traving 1960).

In the case of the quadratic Stark effect ($\mu = 4$) the integration is performed numerically with the result that

$$2w = 11.37 C_4^{2/3} \bar{v}^{1/3} n \quad \text{and} \quad d/w = \sqrt{3} \quad (\text{exact}). \quad (11.25)$$

For the linear Stark effect ($\mu = 2$) the integral can be evaluated analytically but it diverges at large impact parameters, and has to be cut off at some impact parameter ρ_{\max} . Thus

$$w = \frac{n\pi^3 C_2^2}{\bar{v}} \left\{ 0.923 - \ln \left(\frac{\pi C_2}{\rho_{\max} \bar{v}} \right) + \frac{\pi^2 C_2^2}{24 \bar{v}^2 \rho_{\max}^2} + \dots \right\}. \quad (11.26)$$

This does not depend critically on ρ_{\max} , but it is reasonable to take ρ_{\max} about equal to the Debye radius ρ_D , since the fields of the perturbers are screened out over this distance. However, the impact approximation is never valid for too large ρ (see below).

These results should be compared with the earlier theories of Lorentz (1906) and Weisskopf (1932). In the Lorentz picture (see White 1934) collisions completely interrupt the emission and the half half-width w is equal to the collision frequency. According to Weisskopf, collisions are effective if the phase shift exceeds some value of the order of unity, i.e. $\eta'(\rho) > \eta_0 \sim 1$. Thus collisions are effective for all impact parameters less than ρ_W (the Weisskopf radius) such that (from equation (11.24))

$$\rho_W = \left\{ \frac{\sqrt{(\pi)} \Gamma\{\frac{1}{2}(\mu-1)\} C_\mu}{\Gamma(\frac{1}{2}\mu) \bar{v} \eta_0} \right\}^{1/(\mu-1)} \quad (11.27)$$

The frequency of such collisions is $n\pi\bar{v}\rho_W^2$, so that the Lorentz-Weisskopf half-width is

$$w = n\bar{v}\pi\rho_W^2. \quad (11.28)$$

The result obtained above (11.25) for the width for $\mu = 4$ is obtained when $\eta_0 = 0.64$. The Lorentz-Weisskopf theory, however, predicts no shift.

The validity of the impact approximation can now be examined in more detail. From equation (11.21) significant contributions to $\phi(s)$ only occur when $n\bar{v}\sigma_r s \lesssim 1$ (otherwise $\exp(-n\bar{v}\sigma_r s)$ becomes small) so that times of interest in determining the line profile are less than about $(n\bar{v}\sigma_r)^{-1}$. This condition, $n\bar{v}\sigma_r \Delta s \ll 1$, ensures that the differential form for $\phi(s)$ can be used in equation (11.21) and equation (11.18). Δs has to be much larger than the times for which there is a non-vanishing perturbation, i.e. the duration τ_c of a typical collision, since for an incompleting collision η' would not be independent of $\eta(s)$. Thus

$$\tau_c \ll \Delta s \lesssim (n\bar{v}\sigma_r)^{-1} = w^{-1} \quad (11.29)$$

(w in angular frequency). But, according to Lorentz (1906), the half half-width w is equal to the collision frequency, so that the condition $\tau_c \ll w^{-1}$ is equivalent to the statement that the duration of a collision has to be much shorter than the average time between collisions.

Thus, if $\tau_c \ll w^{-1}$ is fulfilled, both conditions necessary to write equation (11.20) are satisfied (i.e. each impact may be considered separately and it is completed in times of interest).

From the properties of the Fourier transformation, for a frequency separation of $\Delta\omega$ from the line centre, times of interest s are given by $s\Delta\omega \simeq 1$. But for the

impact approximation to be valid these times must be greater than the typical collision time τ_c . Thus

$$\Delta\omega \ll \tau_c^{-1} \quad (11.30)$$

a condition which gives the frequency range over which the line profile may be calculated by the impact approximation.

Since $\tau_c \simeq \rho/\bar{v}$, it is obvious that this condition can never be satisfied for very large ρ .

11.3.3. *Modern Stark broadening theory for electrons.* There have been many simplified pictures of the broadening effects of collisions on a spectral line (Lorentz 1906, Weisskopf 1932, Lenz 1953, Lindholm 1941, Foley 1946), and most of these involve the adiabatic assumption, i.e. they replace the full interaction between the perturbing electron and the radiating atom by a potential depending only on the position of the perturber. However, electrons can, and often do, cause transitions to neighbouring states and these inelastic collisions make the adiabatic assumption invalid. A related difficulty is the degeneracy of the atomic states, i.e. a collision can be elastic and still change the state of the atom, again making the adiabatic approximation invalid (Spitzer 1940). Also the broadening of lines, already closely split by the ionic field, has to be calculated. Since electron and ion effects are of the same order of magnitude, the problem of overlapping lines arises.

The first realistic treatment of inelastic collisions was due to Anderson (1949) and that of overlapping lines to Kolb (1957, Ph.D. Thesis, University of Michigan), Kolb and Griem (1958) and Baranger (1958 a).

In this modern theory (Baranger 1962, Griem 1964) the quantum-mechanical equivalent of the autocorrelation function $\Phi(s)$ is used.

A classical path is generally taken for the perturbing electrons (i.e. a straight-line path when the radiating species is an uncharged atom, and a hyperbolic path for ionic radiators); the effect of electrons on the emitting species is represented by a time-dependent perturbation $\tilde{V}(t)$ which is added to the Hamiltonian of the atom. Usually only the dipole interaction is considered and the higher multipole interactions between the perturber and radiating atom are neglected, since it is found that relatively distant collisions (large impact parameter, ρ) are the most important.

In order for the classical path approximation to be used, the extent of the wave packet which represents the electron has to be negligible. This is valid whenever the de Broglie wavelength of the perturbing electron is considerably smaller than the impact parameters of all collisions which contribute significantly to broadening,

$$\text{i.e.} \quad \hbar/m\bar{v} \ll \rho_{\min}. \quad (11.31)$$

A ρ_{\min} occurs naturally in the impact approximation owing to breakdown of the perturbation methods used (see later in this section) and fortunately collisions at smaller impact parameters contribute very little to the broadening. The assumption is made that the perturber path is fixed and does not depend on the energy exchanged between it and the radiator (i.e. the 'back reaction' is neglected). This means that energy gained or lost in an inelastic collision by the perturber (typically equal to the energy separation between the level and the nearest

interacting levels) must be substantially less than the energy of the perturber (typically $\sim kT_e$). This is almost always the case for lines in the optical range.

It is possible to proceed without making the classical path approximation (Baranger 1958 b) but the results are analogous and the approximation almost always valid.

After making the classical path approximation, the modern theory makes the impact approximation in much the same way as in the Lindholm theory (§ 11.3.2). Thus, after a time Δs , the perturbers are considered to be statistically independent of each other, so that the term equivalent to $\langle \exp(j\eta') - 1 \rangle_{\text{av}}$ is calculated by assuming that a single perturber is present and then multiplying by the number of perturbers having impacts in time Δs (equivalent to (11.19) in § 11.3.2). At first sight this seems to be inconsistent for the long-range interaction of Stark broadening, since collisions are actually never separated in time. However, when there are many weak (large impact parameter) collisions during the time interval Δs , perturbation theory is used and the lowest non-vanishing terms are additive. Multiplying by the number of perturbers n is therefore a consistent procedure. Another possibility is that a strong collision occurs during Δs . This is a rare event and when it occurs not much error is incurred in disregarding all other weak collisions for that time interval, and considering a single perturber again. The calculation of $\exp\{j\eta'(\rho)\}$ of § 11.3.2 can be identified with a calculation of the **S** matrix for the scattering of the perturbing electron.

The resulting integrals over impact parameter are found, for hydrogen, to diverge logarithmically for both small and large impact parameters. The divergence at large impact parameters is due to the breakdown of the impact approximation from two possible causes. First, the duration of a collision ($\sim \rho/\bar{v}$) is necessarily long for weak collisions, so that not all collisions can be completed in the times of interest Δs in Fourier integral. Thus, as in equation (11.30), the cut-off should come at $\rho_L \simeq \bar{v}\Delta s \simeq \bar{v}/\Delta\omega$ (Lewis 1961) with $\Delta\omega$ the frequency separation from the line centre. Secondly, the perturbers cannot be regarded as moving independently of each other, for correlations give rise to Debye shielding of the electric field of the perturber. This divergence can be removed by applying a cut-off usually at $\rho = 1.1\rho_D$ where ρ_D is the Debye length (Griem *et al.* 1962 a); however, if ρ_L is smaller than this it should be used.

The divergence at small impact parameters is due to the inapplicability of perturbation methods to strong (i.e. close) collisions. In fact one collision must change the radiator very little if the differential form of $\Phi(s)$ is to remain valid. The usual procedure (Baranger 1962, Griem 1964, Anderson 1949) is to cut off the integral at some minimum impact parameter ρ_{min} , effectively where the phase change due to collisions becomes large, and then to represent all collisions with $\rho < \rho_{\text{min}}$ by a 'strong' impact term of the Lorentz-Weisskopf type (i.e. adding $n\bar{v}\rho_{\text{min}}^2\pi$ to the width). This procedure generally introduces only a small error in the linewidths, for which most of the broadening is due to weak collisions. Similar considerations for cutting off the integrals are applicable to other species besides hydrogen. For ionized helium lines (Griem and Shen 1961) the hyperbolic classical paths, under certain conditions, may provide an automatic cut-off for small ρ . Also for the broadening of lines from isolated levels (i.e. non-degenerate in orbital quantum number and having a quadratic Stark effect) (Griem *et al.* 1962 a) the

integrals converge at the upper limit and no cut-off is necessary if the difference in frequency between the level under consideration and the nearest interacting level is greater than the plasma frequency ω_p .

To obtain finally the correlation function $\Phi(s)$ (and hence the line shape by Fourier inversion) after integrating with respect to ρ , an integration over the velocity distribution of the perturbers has to be performed, i.e. over the electron Maxwellian distribution. Since the results depend only on the velocity distribution of the free electrons being Maxwellian and not on velocities of ions or their population densities, the theory may be used when complete L.T.E. does not hold.

Before considering details of calculations which have been performed, it is worth restating the assumptions involved in the impact approximation. It is necessary to find a time Δs , such that the distribution of perturbers around the radiator, after the time Δs has elapsed, is statistically independent of the original distribution. Since the largest impact parameter is usually determined by the Debye shielding distance, the electron correlation time $1/\omega_p$ is the most important. Thus, it is necessary to have

$$\Delta s \gtrsim \frac{\rho_D}{\bar{v}} = \frac{1}{\omega_p}. \quad (11.32)$$

Secondly, Δs must be sufficiently short for the wave functions of the emitter to remain substantially unaltered, and a differential form of $\Phi(s)$ (as in equation (11.18)) may be used. Physically Δs must be shorter than the average time between strong collisions, which is approximately $1/w$ where w is the width. Thus

$$1/w \geq \Delta s \geq 1/\omega_p.$$

The validity condition is thus

$$w \ll \omega_p = \frac{\bar{v}}{\rho_D}. \quad (11.33)$$

Therefore (as in § 11.3.2) the impact approximation is valid if strong collisions occur at intervals much longer than the duration of a typical collision (in fact, τ_c for a typical collision is less than ρ_D/\bar{v}). On the other hand, the quasi-static approximation is good when strong collisions are always going on. Briefly, the impact approximation should hold for a frequency separation from the unperturbed line ($\Delta\omega$) up to the order of the inverse of the duration of a typical collision (τ_c^{-1}). If the width and shift are small compared with this τ_c^{-1} , then the central core of the line is well represented by a dispersion shape (see Baranger 1958 a). The quasi-static approximation should be valid for $\Delta\omega \gg \tau_c^{-1}$.

For the modern theory of electron impact broadening to be accurate, the typical collision must be weak and a strong collision must be a rare event; this ensures that the typical collisions (which cannot be actually separated in time) can be treated by perturbation theory, and that the strong collision correction is relatively unimportant.

The condition for a typical collision to be weak (cf. Baranger 1962, p. 503), for a typical impact parameter ρ and for p the principal quantum number of the upper state of the line, may be written as

$$\rho > \rho_{\min} \left(\sim \frac{\hbar}{m\bar{v}} p^2 \right). \quad (11.34)$$

For electrons this is usually easily satisfied if the interparticle distance ρ_m is taken as a typical impact parameter. However, under certain circumstances, for a non-degenerate level, the typical impact parameter for broadening can become less than ρ_m and the weak collision term in the width is no longer dominant (van Regemorter 1964). Sufficiently far in the wings, the Lewis cut-off $\rho_L = \bar{v}/\Delta\omega$ is less than ρ_{min} but now the quasi-static approximation is used, since the perturbers do not move significantly during the times of interest ($\sim 1/\Delta\omega$) for the Fourier transformation which gives the line shape (Griem 1962 e) (i.e. $\Delta\omega \gg \tau_c^{-1}$ is well satisfied).

11.3.4. *Calculations of Stark broadening parameters and comparison with experiment.* The details of the calculations depend on whether the radiation is emitted by a neutral atom or an ion, and whether the energy levels are hydrogenic (i.e. degenerate in orbital quantum number l) or not.

In the hydrogenic case overlapping lines have to be considered; the l degeneracy leads to a linear, rather than a quadratic, Stark effect. To apply the degenerate scheme it is only necessary that the splitting of the states should be small compared with the inverse of the duration of a typical collision, i.e. for electronic broadening the splitting should be less than about the plasma frequency ω_p (taking $\tau_c \sim \rho_D/\bar{v}$). The classical path is hyperbolic for ions and straight for atoms.

Stark profiles for $H\alpha$, $H\beta$, $H\gamma$ and $H\delta$ and $L\alpha$ and $L\beta$ were computed by Griem *et al.* (1959, 1962 c), using the impact approximation for the electrons and the quasi-static approximation for the ions. However, since the linear Stark effect is operative, the quasi-static splitting is the dominant factor. The detailed structure of the Stark pattern yields directly the characteristic features of the broadened line profiles, i.e. pronounced central peaks in $H\alpha$ and $H\gamma$ due to the presence of unshifted Stark components, and a central trough in $H\beta$ due to the components being shifted away symmetrically.

Griem and Shen (1961) have evaluated the broadening of hydrogenic ion lines using hyperbolic classical paths, and in particular have calculated profiles for the lines He II 4686 Å and He II 3203 Å.

Results for the above lines, and also the hydrogenic neutral helium lines 3965 Å and 4471 Å, are conveniently tabulated by Griem *et al.* (U.S. Naval Res. Lab. Rep. 5805) and Griem (1964) as a function of the reduced wavelength

$$\frac{\Delta\lambda}{E_0} = \frac{\Delta\lambda}{e} \left(\frac{4}{3}\pi n_e\right)^{2/3} \quad (11.35)$$

for various temperatures T_e and number densities n_e . The widths are only a slow function of T_e (see § 16.3).

Usually only the broadening of the upper level of the line is considered, but for $H\beta$ the broadening of the lower level was also considered (Griem *et al.* 1962 c). The overall error for the width of $H\beta$ is estimated at about 5%.

Experimentally the predictions for the Balmer lines have been tested by Berg *et al.* (1962) using a T tube and Wiese *et al.* (1963) in a wall-stabilized arc. The experimental results indicated that the theory was accurate as regards widths to about 15% for $H\alpha$ and $H\gamma$, and to about 5% for $H\beta$.

Elton and Griem (1964) have verified the theoretical predictions for $L\alpha$ and $L\beta$ to within 10% over three orders of magnitude in relative intensity using a T tube,

although Boldt and Cooper (1964), using an arc, find some asymmetry between the wings of $L\alpha$.

Berg *et al.* (1962) also find satisfactory agreement (10%) for the ionized helium linewidths, but a shift, attributed to plasma polarization (§ 11.4), was also observed.

Even for the lines considered above, the impact approximation used to calculate electron broadening breaks down in the far line wings and eventually the quasi-static approximation has to be used. Griem (1962 e) gives asymptotic wing formulae. Experiments of Wiese *et al.* (1963) indicate, however, that these do not completely agree with the observed $H\beta$ wings.

For higher series members of the Balmer and other series, the quasi-static approximation should sometimes be applicable to both electrons and ions, and the Holtmark profiles of Underhill and Waddell (1959) can be used. Using low pressure radio-frequency discharges, Ferguson and Schuller (1963) (in hydrogen) and Vidal (1964) (in hydrogen and helium) measured profiles of the Balmer series up to about H_{16} . They indicate that in the region of validity of a quasi-static description of the perturbations and even in the transition region to the impact approximation for electrons, there is good agreement between the experimental results and the quasi-static calculations including correlation and shielding. But Armstrong (1964 a) argues that for large principal quantum numbers modification to the impact approximation, including the Lewis (1961) cut-off procedure, gives a better description of Ferguson and Schuller's results. This point is argued against by van Regemorter (1964) who has modified the results of Griem *et al.* (1962 c) to take into account that at low densities the sub-levels of higher series numbers cannot be considered as completely degenerate. Yet again, Griem (1965) argues that these results are invalid, because in the line wings the Lewis cut-off is smaller than the ρ_{\max} proposed by van Regemorter.

As one proceeds up a given series (to higher principal quantum numbers), the spacing between the levels decreases and the broadening, proportional to p^2 for the quasi-static width, increases. The lines overlap and eventually merge, the point at which merging occurs being the well-known Inglis–Teller (1939) limit. The complete theory of this transition region is very complicated and has not been worked out. Except at high temperatures, when Doppler broadening may dominate, most estimates give roughly the same result for the principal quantum number p_m at which merging occurs (Inglis and Teller 1939, Armstrong 1964 b); for singly charged perturbers this is $\log p_m \simeq 3.21 - 0.143 \log n_e$, where n_e is the electron density in cm^{-3} .

For isolated lines, i.e. lines from levels whose components of different orbital quantum number l are well separated, it is found that the quadratic Stark effect is operative and the broadening is caused mainly by electron impacts. The theory in this case was originally worked out for the strong lines of neutral helium by Griem *et al.* (1962 a).

In the electron impact theory the shifts d and the widths w , which, as in the Lindholm theory, are the imaginary and real parts of the same complex function, give rise to profiles of the dispersion or Lorentz type, i.e.

$$I(\omega) \sim \frac{1}{w\pi} \frac{1}{1 + \{(\omega - \omega_0 - d)/w\}^2}. \quad (11.36)$$

In the theory of Griem *et al.* (1962 a) cut-offs at small impact parameter are adjusted so that the results tend correctly to both the high velocity and low velocity limits. In the low velocity (low temperature) limit the adiabatic theory of Lindholm (§ 11.3.2) is adequate; this can be worked out exactly and for quadratic Stark effect gives $d/w = \sqrt{3}$. In the high velocity limit perturbation theory can be used throughout. Here the ratio of line shift to width depends upon the interacting states involved, and frequently becomes small when the contributions of the states to the shift cancel.

In the intermediate region, when perturbation theory breaks down for small impact parameters, the 'strong' collision term of Lorentz-Weisskopf type (see § 11.3.3) has to be included. In the expression for the width weak impacts dominate, so that the strong collision's correction is relatively unimportant. Investigations by Griem and Shen (1962), based on a dispersion equation relating the widths and shifts, and a comparison of various cut-off procedures suggest that uncertainties due to 'strong' collisions are only about 5% in the case of the widths, but may amount to 20% of the width in the case of the shifts. Other cut-off procedures are available (see e.g. Vainshtein and Sobel'man 1959) but these have not been used extensively.

To obtain the final line profile for these isolated lines, the ion broadening has to be taken into account. The ion velocities are usually small enough for broadening to be taken as adiabatic. In the adiabatic case a general procedure has been developed by Anderson (Anderson 1952, Anderson and Talman 1955) which reduces in one limit to the adiabatic impact approximation and in the other to almost the exact quasi-static result. Griem *et al.* (1962 a) use this procedure to show that the quasi-static approximation for ions does not cause serious errors if the parameter

$$\sigma \left\{ = \frac{w}{\bar{v}} \left(\frac{3}{4\pi n} \right)^{1/3} \right\} \gtrsim 1 \quad (11.37)$$

where \bar{v} is the perturber thermal velocity. Since this is usually true, it is reasonable to use the quasi-static approximation for the ions throughout the calculations; however, Mazing (1961) considers the impact approximation should be used.

Final profiles of the lines are expressed in terms of two parameters:

(i) The reduced frequency

$$x = \frac{\omega - \omega_0 - d}{w} \quad (11.38)$$

where d and w are the impact shifts and half half-widths.

(ii) The quasi-static ion broadening parameter

$$\alpha = \left\{ \frac{4\pi n_e}{3} \right\} \left\{ \frac{2\pi C_d}{w} \right\}^{3/4} \quad (11.39)$$

The profiles $j(\alpha, x)$ (for use when $\sigma \gtrsim 1$) are tabulated by Griem *et al.* (1962 a) and Griem (1964); Griem *et al.* (1962 a) also give profiles $j(x, \alpha, \sigma)$ for use when $\sigma < 1$. For α small these profiles differ little from dispersion shape.

The original calculations of Griem *et al.* (1962 a) contain quasi-static profiles of only the simple Holtsmark type, but a later paper (Griem 1962 c) uses the distribution functions of Mozer and Baranger (1960) which take into account both

ion-ion correlations and Debye shielding by electrons. Resulting profiles $j_R(x, \alpha)$ expressed in terms of the Debye-shielding parameter

$$R = \left(\frac{3}{4\pi n_e} \right)^{1/3} \frac{1}{\rho_D} \\ = \frac{\text{mean distance between ions}}{\text{Debye radius}}$$

are contained in the works of Griem (1962 c, 1964). For $\alpha \lesssim 0.5$ and $R \lesssim 0.8$, simple and reasonably accurate expressions are available for the total width and total shift. Thus, for neutral atoms

$$w_{\text{total}} = \{1 + 1.75\alpha(1 - 0.75R)\} w \quad (11.40)$$

and

$$d_{\text{total}} = \{d/w \mp 2.0\alpha(1 - 0.75R)\} w. \quad (11.41)$$

In equation (11.41), the + or - sign is taken according to whether quasi-static effects shift the line to the red or blue, respectively (i.e. depends on sign of C_4). For singly ionized emitters, $0.75R$ has to be replaced by $1.2R$.

Tables of w , d/w and α at a density of $n_e = 10^{16} \text{ cm}^{-3}$ are given by Griem (1964) as a function of T_e for many neutral and singly ionized atoms (helium through to calcium and neutral caesium).

The parameter α scales as $n_e^{1/4}$, d as n_e and d/w is independent of n_e .

In calculating most of these results (neutral helium excepted) the necessary oscillator strengths have been obtained by the Coulomb approximation (Bates and Damgaard 1949) using LS coupling. The Coulomb approximation is likely to be fairly accurate since in Stark theory only transitions between the upper state and nearby perturbing levels need to be considered. It is estimated that the overall accuracy in the widths is about 20%. No cut-off for large impact parameters was used in these calculations, since the integral converges anyway; thus the results are only accurate if the spacing of the nearest perturbing level from the upper level of the line is greater than the plasma frequency ω_p (see § 11.3.3). Violation of this condition can cause a serious overestimation of the shifts d (Griem *et al.* 1962 a).

With regard to experimental verification of the theory for isolated lines, Berg *et al.* (1962) found fair agreement for the neutral helium lines, although Lincke (1964, Ph.D. Thesis, University of Maryland) indicates that there may be a small systematic overestimation of the widths. Lincke in fact proposes that a 10% correction should be added to the electron density calculated by comparing the neutral helium lines with theoretical estimates. Even excluding this correction, the theory seems to be correct to better than 20%.

The experimental results for the neutral and singly ionized heavier elements (Stampa (1963) for neutral nitrogen, Day (1965, Ph.D. Thesis, University of Maryland) for ionized nitrogen, Jung (1963) and Wiese and Murphy (1963) for neutral oxygen, and Stone and Agnew (1962) for neutral caesium) show agreement between observed and calculated widths to about 10%. The agreement in shifts is only good when the shifts are large, because errors due to the 'strong' collision term are important for small shifts.

Further minor modifications of theory, in particular with reference to small asymmetries of the $H\beta$ profile, are discussed by Griem (1964). He argues that, when

both electrons and ions are treated by the quasi-static approximation, the correction due to the quadrupole term in the interaction (Kudrin and Sholin 1963 a) can be neglected. The leading quadrupole term, considered by Müller (1965) to be important in the quasi-static case, becomes zero in the weak collision term of the impact approximation when a simple classical average over angles is performed. Yet again, Brêchot and van Regemorter (1964 a, b) have found the quadrupole term to be important in an adiabatic impact approximation. Nguyen-Hoe *et al.* (1964) found it necessary to include the quadrupole term in quasi-static broadening to explain the asymmetries observed by Boldt and Cooper (1964) in the $L\alpha$ profile. Recently Griem (1965) has determined wing formulae for $L\alpha$ in which many corrections, including the quadrupole interaction in both quasi-static and impact broadening, are included. Here, according to the velocities and frequency separation from the line centre, electron broadening is treated by the impact approximation, which accounts either for Debye shielding or for the finite duration of collisions (Lewis cut-off), or by quasi-static theory. The results, which, including asymmetries, are expected to be accurate to better than 10%, now show reasonable agreement with experiment. However, the overall importance of quadrupole interactions is still not completely clear. The so-called 'polarization' shift is discussed in the next section.

Magnetic fields are considered to be negligible in the above theories and experiments; however, in the presence of a magnetic field the Stark broadening of the components of a line split by the Zeeman effect have to be considered. At high magnetic fields these effects cannot be compounded separately using the Stark broadening results obtained at zero magnetic field; for instance, the trajectories of the electrons in impact broadening may be considerably influenced by the field (Drawin, Herman and Nguyen-Hoe 1965, Euratom-CEA Rep. FC 321, Maschke and Voslamber 1965, Euratom-CEA Rep. FC 311).

In conclusion, the modern theory gives good predictions for the linewidths, but theoretical uncertainties are much greater for shifts and wing formulae.

11.4. 'Plasma polarization' shift of ionic lines

This effect was first postulated by Berg *et al.* (1962) to explain a blue shift of the He II 4686 Å line, and should, if true, be applicable to all ionic lines.

Essentially, in the neighbourhood of an emitting ion, on the average, there are more electrons than ions (although when only singly ionized species occur $n_e = n_i$ overall), so that there is a net local negative charge density. In fact, due to the Coulomb field, at radius r from an ion of charge Ze , the equilibrium densities (by Maxwell-Boltzmann statistics) will be

$$n_e = n_{e0} \exp\left(\frac{Ze^2}{rkT}\right) \quad (11.42)$$

and

$$n_i = n_{i0} \exp\left(-\frac{Ze^2}{rkT}\right). \quad (11.43)$$

Thus, with $n_{e0} \simeq n_{i0} \simeq n_e$, the space charge density is

$$\rho(r) \simeq -\frac{2n_e Ze^3}{rkT_e} \quad (11.44)$$

and the shift in energy of a level corresponding to an electron in an orbit of radius r in a singly charged ion, due to $\rho(r)$, is (Griem 1964)

$$\Delta E = \frac{4\pi e^4 n_e}{kT_e} \langle r \rangle \quad (11.45)$$

where $\langle r \rangle$ is the expectation value of the radius (the radial matrix element which is proportional to the square of the effective principal quantum number of the state).

If this shift were true, wavelength perturbations in highly ionized plasmas would be quite severe. Many objections have been raised to this view (D. D. Burgess 1965, Ph.D. Thesis, University of London, Burgess and Cooper 1965 a, Kudrin and Sholin 1963 b, Kudrin and Tarosov 1963). Even at high densities the number of electrons within an atomic orbit is very small, 10^{-5} or less. Further, the collision event time scale is much smaller than the period of the electron orbit, so that the applicability of a time-averaged potential is very doubtful. (De Witt and Nakayama (1964) obtained very different results for calculated energy levels in the cases of time-dependent and time-independent screened potentials—see § 5.) The collisions of the electrons involved should be analogous to those in the impact theory. On this picture the major effect of the emitting species being ionized would appear to be a slight increase in the number of electron collisions and a slight decrease in the number of ion collisions. (The Stark broadening calculations for ionized helium (Griem and Shen 1961) already contain hyperbolic classical paths, which, under certain circumstances, can provide an automatic cut-off at some minimum impact parameter (ρ_{\min}), and, consequently, make ‘strong’ corrections unnecessary. Also, in the quasi-static ion calculations, use was made of the ion field strength distributions of Mozer and Baranger (1960) which already contain ion-ion correlations.)

Experimental measurements of line shifts in singly ionized nitrogen (Day 1965, Ph.D. Thesis, University of Maryland, Day and Griem 1965) and singly ionized argon (Burgess and Cooper 1965 a) failed to detect ‘plasma polarization’ shifts of the magnitude predicted.†

11.5. Comparison of broadening mechanisms in a high temperature plasma

The mechanisms that have been considered are natural broadening, which has a dispersion (Lorentz) profile, Stark broadening, with a dispersion profile for electron impacts, and Doppler broadening with a Gaussian profile if the emitters have a Maxwellian velocity distribution. Shifts of various components of a line due to the Zeeman effect will be discussed in § 17.

In experimental situations instrumental broadening must also be considered.

If the profiles of a line due to two different broadening mechanisms are $\phi_1(\lambda)$ and $\phi_2(\lambda)$, then the resultant profile is obtained by a convolution integral

$$\phi(\lambda)_{\text{resultant}} = \int_{-\infty}^{\infty} \phi_1(\xi) \phi_2(\lambda - \xi) d\xi. \quad (11.46)$$

† A more recent estimate by Griem (private communication, 7th Int. Conf. on Ionization Phenomena on Gases, Belgrade, August 1965) is in terms of shielding which is caused by electrons that may be considered as being in doubly excited states of the preceding ion in the ionization sequence. The resulting blue shifts are typically an order of magnitude below those estimated from equation (11.45).

When only dispersion and Gaussian profiles need to be convolved together, the resultant profile is the well-known Voigt profile (see Allen 1963, Davis and Vaughan 1963). Under certain conditions one broadening mechanism may dominate the resulting profile. Yet, even if Doppler broadening dominates in the line centre, the far wings will tend to deviate from Gaussian shape owing to the inclusion of any Stark or natural broadening for which the wing intensities decay more slowly.

In L.T.E. plasmas at high density and relatively low temperatures, an inspection of Griem's (1964) tables and comparison with the Doppler widths shows that for most neutral and singly ionized emitters the Stark effect often dominates. The hydrogen lines may in fact be up to 100 Å broad, due to the Stark effect alone. However, values for the Stark coefficients are only tabulated for neutral and singly ionized species, and that only for temperatures up to 80 000 °K.

Laboratory plasmas which are not in L.T.E. and fall in the coronal domain may have electron temperatures of 100 eV† or more, so that Stark broadening parameters of highly ionized species in a high temperature plasma have to be estimated.

These estimates have again been given by Griem (1962 d) whose results are summarized here.

At sufficiently high temperature the impact approximation, which gives rise to line profiles of dispersion type, is valid for the ions as well as the electrons. One might think that in high temperature plasmas, in which radiative decay is more important than collisional de-excitation, collisional broadening will be less important than natural width. However, impact broadening is usually not characterized by cross sections similar to those for de-excitation by electrons since the broadening calculations involve interactions with energy levels near the upper level of the line. Furthermore, in high temperature plasmas most of the broadening of hydrogenic ions (linear Stark effect) is not even caused by electrons but by light ions such as hydrogen (since the width is inversely proportional to the perturber velocity; compare equation (11.26)). Thus natural broadening is not necessarily larger than the Stark broadening.

Griem's (1962 d) estimates give the following half half-width w (in frequency units):

$$\text{natural broadening } 2w_{\text{natural}} \simeq 10^9 Z^4 \text{ sec}^{-1} \quad (11.47)$$

for hydrogenic resonance lines and correspondingly smaller values for higher members of the Lyman series.

For resonance lines the contribution from collisions of light ions such as hydrogen with the emitting hydrogenic ions (charge $Z - 1$) is approximately

$$2w_{\text{impact}} \simeq 10^{-5} Z^{-2} T_i^{-1/2} n_e \quad (11.48)$$

where T_i is the ion kinetic temperature in keV and n_i is taken equal to n_e (i.e. the plasma is assumed to be composed mainly of hydrogen (or deuterium)).

The impact approximation is valid at high temperatures and relatively low densities. At high densities, even if at high temperature, one should use the quasi-static approximation as soon as it yields narrower profiles (Griem and Shen 1961) and in such cases the electron contribution is no longer negligible.

† 1 eV = 11 605 °K.

For non-hydrogenic ions the equation (11.48) is an overestimate since the ion impacts then cause only a quadratic Stark effect.

For resonance lines natural broadening usually dominates the Stark broadening; however, this is not necessarily true for highly excited states, since the Stark broadening scales roughly as $(p_u/2)^5$ where p_u is the principal quantum number of the upper state. Where impact broadening is due to light ions resonance broadening can always be neglected.

If appropriate estimates are used (Griem 1962 d) it may be shown that Doppler and Stark broadening are comparable for a number density n_e given by

$$n_e \simeq 10^{18} Z^{7/2} T_i p_l^{-2} \left(\frac{2}{p_u} \right)^5$$

where T_i is in kev and p_l is the principal quantum number of the lower state. In general, only for transitions between highly excited states will Stark broadening be important. If the impact approximation were no longer valid or if the quadratic Stark effect only were relevant, the above critical density would be an underestimate.

Similarly, Doppler and natural widths will be comparable when

$$T_i \simeq 10^{-6} Z^5 \text{ kev.}$$

For light ions ($Z < 10$) the Doppler width is in general larger than the natural width.

In conclusion, in high temperature plasmas (~ 100 ev) the Doppler effect generally dominates the profiles; however, in low temperature, high density L.T.E. plasmas Stark broadening is usually more important.

12. Continuum radiation

Bremsstrahlung and recombination radiation will be treated together. Precise quantum-mechanical calculations can only be performed for hydrogenic systems (i.e. the recombination of an electron with a bare ion). For many-electron systems only approximate treatments exist and in general the modification of the continuum caused by autoionization is ignored, although in principle this should be included (Fano 1961, Fano and Cooper 1965).

In this section the form of the hydrogenic results will be considered, and a few comments on recent results will be given (for a review see Finkelnburg and Peters 1957, Unsöld 1955).

In the recombination of a free electron with velocity v with an ion of charge Z to form a bound state of S_{Z-1} with principal quantum number q , or, conversely, for the photoionization from level q , the relationship between the frequency of emission or absorption is given by

$$h\nu = \frac{1}{2}mv^2 + E_{Z-1}(\infty) - E_{Z-1}(q). \quad (12.1)$$

The continuum emission is generally derived from the recombination cross section σ_{vq} . The relation between this and the absorption cross section (cf. equation (10.4)) may be evaluated by the principle of detailed balancing in thermodynamic equilibrium. Then the number of photoionizations in the frequency interval $d\nu$ from a level q must equal the number of recombinations to this same level from the

corresponding interval dv . If it is assumed that photoionization from level q leaves the ion in its ground state (i.e. doubly excited states not included), then σ_{vq} is defined so that the number of recombinations between ground-state ions and electrons per unit volume from the velocity range v and $v + dv$ is given by

$$n_Z(1) n_e f(v) \sigma_{vq} v dv \quad (12.2)$$

where $f(v)$ is the electron velocity distribution and $n_Z(1)$ is the density of ions in the ground state. For an isotropic intensity distribution, the photon flux per unit frequency range is $4\pi I(\nu)/h\nu$; therefore the total number of absorptions per unit volume for the frequency range $d\nu$ is

$$n_{Z-1}(q) \frac{4\pi I(\nu)}{h\nu} \sigma_{qv}(\nu) d\nu \quad (12.3)$$

($\sigma_{qv}(\nu)$ is written as $\sigma_{qv}(\nu)$ to emphasize that the final state is free).

In equilibrium the stimulated recombination (negative absorption) to level q is obtained, as in § 10, by multiplying (12.3) by $\exp(-h\nu/kT)$. Detailed balance then gives

$$n_{Z-1}(q) \frac{4\pi}{h\nu} I(\nu) \sigma_{qv}(\nu) \left\{ 1 - \exp\left(-\frac{h\nu}{kT}\right) \right\} = n_Z(1) n_e f(v) \sigma_{vq} v dv. \quad (12.4)$$

In thermodynamic equilibrium at temperature T

$$\frac{n_{Z-1}(q)}{n_e n_Z(1)} = \frac{g_{Z-1}(q)}{2g_Z(1)} \left(\frac{h^2}{2\pi mkT} \right)^{3/2} \exp\left\{ \frac{E_{Z-1}(\infty) - E_{Z-1}(q)}{kT} \right\} \quad (\text{Saha})$$

$$f(v) dv = 4\pi \left(\frac{m}{2\pi kT} \right)^{3/2} \exp\left(-\frac{1}{2} \frac{mv^2}{kT}\right) v^2 dv \quad (\text{Maxwellian distribution})$$

and

$$I(\nu) = \frac{2h\nu^3}{c^2} \left\{ \exp\left(\frac{h\nu}{kT}\right) - 1 \right\}^{-1} \quad (\text{Planck's radiation law}).$$

Then, using (12.1) with $h\nu = m v dv$ the Milne (1921) formula is obtained, i.e.

$$\frac{\sigma_{qv}(\nu)}{\sigma_{vq}} = \frac{m^2 c^2 v^2}{\nu^2 h^2} \frac{g_Z(1)}{g_{Z-1}(q)}. \quad (12.5)$$

In photoionization, the final states p' are continuous, and the wave functions are in general normalized such that

$$\langle p'' | p' \rangle = \delta\{E(p'') - E(p')\}. \quad (12.6)$$

Equation (10.4) can then be used directly to give the total photoionization (absorption) cross section per unit frequency range as (cf. equation (10.12))

$$\sigma_{qv}(\nu) = \frac{8\pi^3 \nu}{3hc g_{Z-1}(q)} \sum_{p'q'} |\langle p' | e\mathbf{x} | q' \rangle|^2 \quad (12.7)$$

where the summation is now over all initial and final states of fixed energy. Often the photoionization cross section for unit energy range is used, in which case the

above must be multiplied by h . Bates (1946) gives other possible normalization procedures for the continuum wave functions. A review of theoretical and experimental determinations of photoionization cross sections is given by Ditchburn and Öpik (1962).

By analogy with equation (10.12) the photoionization can be expressed as a differential absorption oscillator strength, i.e.

$$\sigma_{qv}(\nu) = \frac{\pi e^2}{mc} \frac{df}{d\nu}. \quad (12.8)$$

Menzel and Pekeris (1936) give the photoionization cross section for a hydrogenic species of charge $Z-1$ as

$$\sigma_{qv}(\nu) = \frac{2^6 \pi^4 e^{10} m Z^4}{3 \sqrt{(3)} ch^6} \frac{g_{fb}}{q^5 \nu^3} \quad (12.9)$$

where g_{fb} is the free-bound Gaunt factor. Apart from the Gaunt factor, this is identical with the Kramers (1923) result. For frequencies in the optical region g_{fb} is generally about unity; however, in the radio-frequency region it may become considerably larger than unity (see Elwert 1948, Oster 1961). These Gaunt factors, both free-bound and free-free, have been tabulated by Karzas and Latter (1961).

Using the Milne relation (12.5) with (for a hydrogenic species) $g_Z(1) = 1$ and $g_{Z-1}(q) = 2q^2$, (12.9) becomes

$$\sigma_{vq} = \frac{2^7 \pi^4 e^{10} Z^4}{3 \sqrt{(3)} mc^3 h^4} \frac{g_{fb}}{\nu q^3 v^2}. \quad (12.10)$$

For hydrogenic systems, $n_Z(1) = n_Z$ and $E_{Z-1}(\infty) - E_{Z-1}(q) = Z^2 E_H / q^2$ where $E_H = 2\pi^2 e^4 m / h^2$ is the ionization energy of hydrogen.

The recombination radiation due to free electrons in L.T.E. (i.e. with a Maxwellian velocity distribution at temperature T_e) is then obtained from equation (12.2).

Thus the total power radiated in frequency interval $d\nu$ for recombination to level q is

$$\begin{aligned} P_q^R(\nu) d\nu &= h\nu n_e n_Z f(\nu) \nu \sigma_{vq} d\nu \\ &= n_e n_Z g_{fb} \frac{Z^4 K}{(kT_e)^{3/2}} \exp\left(-\frac{h\nu}{kT_e} + \frac{Z^2 E_H}{q^2 kT_e}\right) \frac{d\nu}{q^3} \end{aligned} \quad (12.11)$$

where

$$K = \frac{64\pi^{3/2} e^4 h}{3^{3/2} m^2 c^3} (E_H)^{3/2}.$$

The complete spectral distribution is obtained by summation over the permitted quantum levels. At any frequency the lowest q permissible in the summation is given by the condition

$$h\nu = \frac{1}{2} m v^2 + \frac{Z^2 E_H}{q^2} \geq \frac{Z^2 E_H}{q^2} \quad (12.12)$$

i.e. for any given ν

$$q_{\min} > \left(\frac{Z^2 E_H}{h\nu}\right)^{1/2}. \quad (12.13)$$

Thus the total recombination radiation at frequency ν is

$$P^R(\nu) d\nu = \frac{n_e n_Z g_{fb} K Z^4}{(kT_e)^{3/2}} \exp\left(-\frac{h\nu}{kT_e}\right) \sum_{q \geq (Z^2 E_H / h\nu)^{1/2}}^{\infty} \exp\left(\frac{Z^2 E_H}{q^2 kT_e}\right) \frac{d\nu}{q^3}. \quad (12.14)$$

A lower limit to the total power radiated can be obtained by integrating $P^R(\nu)$ over all frequencies resulting from capture into the ground state only ($p = 1$; $\nu \geq Z^2 E_H / h$).

This is the dominant term, and gives

$$P_1^R = 1.3 \times 10^{-32} n_Z n_e Z^4 T_e^{-1/2} \text{ w cm}^{-3} \quad (\text{for } T_e \text{ in kev}). \quad (12.15)$$

At large values of q the levels approach a continuum and the summation over q can be replaced by an integral. For $q > q^*$

$$\sum_{q=(q^*+1)}^{\infty} \frac{1}{q^3} \exp\left(\frac{Z^2 E_H}{q^2 kT_e}\right) \rightarrow -\frac{1}{2} \int_{(q^*+1)}^{\infty} \exp\left(\frac{Z^2 E_H}{q^2 kT_e}\right) d\left(\frac{1}{q^2}\right). \quad (12.16)$$

The choice of q^* is rather arbitrary. One possible choice is the principal quantum number at which Stark broadening of the level becomes comparable with the spacing between neighbouring levels (the Inglis–Teller limit—§ 11.3.4). In terms of the variable $u_q = Z^2 E_H / q^2 kT_e$, the limits in the above integral are

$$u_q = 0 \quad \text{and} \quad u_q = u^* = Z^2 E_H / (q^* + 1)^2 kT_e.$$

To include bremsstrahlung Unsöld (1955) finds that it is sufficient to extend the above range of integration. The integration limit $u_q = 0$ corresponds to ionization, $u_q > 0$ corresponds to bound states, and thus $u_q < 0$ corresponds to the free continuous states. Integration between 0 and $-\infty$ in (12.16) with respect to u_q thus gives the recombination into free states, i.e. bremsstrahlung. Thus,

$$P^B(\nu) d\nu = n_e n_Z g_{ff} \frac{Z^2 K}{2E_H} (kT_e)^{-1/2} \exp\left(-\frac{h\nu}{kT_e}\right) d\nu \quad (12.17)$$

where now the free-free Gaunt factor is used.

The relative power radiated by bremsstrahlung as a function of wavelength for various temperatures is shown in figure 9. The bremsstrahlung power (as a function of wavelength) is maximum when $h\nu = 2kT_e$, that is, at $6.2/kT_e$ (kev) Å.

Since both initial and final states are free the total bremsstrahlung is obtained by integrating over all frequencies from zero to infinity (and approximating $g_{ff} = 1$) to give

$$P^B = 5 \times 10^{-31} n_Z n_e Z^2 T_e^{1/2} \text{ w cm}^{-3} \quad (T_e \text{ in kev}). \quad (12.18)$$

The exact form of the Gaunt factors appears to be unimportant; for instance, Kogan and Migdal (1961) calculate the power radiated by bremsstrahlung using both the Born approximation (valid at high energies) and the semi-classical approximation and find only a minor difference in the total power radiated.

Bremsstrahlung and recombination radiation always exist together in proportions depending on the electron temperature, and the total is expressed by performing the integral in (12.16) from u^* to $-\infty$.

Thus the total power radiated per unit volume by bremsstrahlung and recombination in a plasma of fully stripped ions of charge Z is given by

$$\begin{aligned}
 P^{B+R}(\nu) d\nu &= \frac{32\pi^{1/2} e^4 hZ}{3^{3/2} m^2 c^3} \\
 &\times \left\{ g_{\text{ff}} \exp\left(\frac{Z^2 E_{\text{H}}}{kT_e(q^* + 1)^2}\right) + \frac{2Z^2 E_{\text{H}}}{kT_e} \sum_{q \geq (Z^2 E_{\text{H}}/h\nu)^{1/2}}^{q^*} g_{\text{fb}} \frac{1}{q^3} \exp\left(\frac{Z^2 E_{\text{H}}}{q^2 kT_e}\right) \right\} \\
 &\times n_e n_Z \left(\frac{Z^2 E_{\text{H}}}{kT_e}\right)^{1/2} \exp\left(-\frac{h\nu}{kT_e}\right) d\nu. \tag{12.19}
 \end{aligned}$$

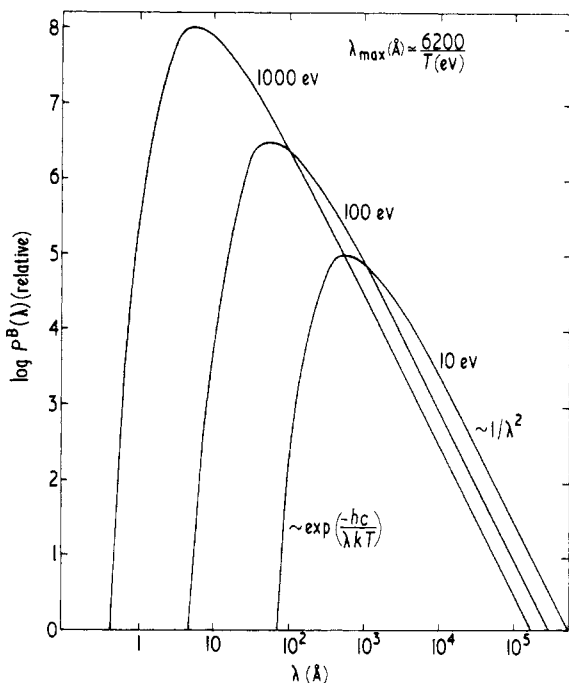


Figure 9. Relative bremsstrahlung power distribution $P^B(\lambda)$ for temperatures of 10, 100 and 1000 eV.

Then, on the assumption that the Gaunt factors are approximately equal to unity:

(i) At low frequency, $\nu < \nu^* = Z^2 E_{\text{H}}/hq^{*2}$ (i.e. $q > q^*$), the only term remaining in the curly bracket is of the form $\exp(h\nu/kT_e)$ and consequently $P^{B+R}(\nu)$ has a flat frequency response in the range 0 to ν^* .

(ii) At high frequencies, $\nu > \nu_1 = Z^2 E_{\text{H}}/h$, all terms in the summation are present and the curly bracket is frequency-independent, and thus $P^{B+R}(\nu)$ falls off as $\exp(-h\nu/kT_e)$.

(iii) At medium frequencies the spectrum has a step-like structure with exponential fall-off on the high frequency side of steps which themselves are due to terms having $1 \leq q \leq q^*$.

The spectrum of $P^{B+R}(\nu)$ is shown schematically in figure 10. Bremsstrahlung completely dominates recombination radiation for $kT_e \gtrsim 3E_H Z^2$. Even for hydrogen various corrections have to be made in equation (12.19) for $P^{B+R}(\nu)$. Close to the plasma frequency $\omega_p (= (4\pi n_e e^2/m)^{1/2})$ correlations between ions and electrons in the plasma become important, and the radiation (caused classically by the acceleration of an electron in the field of an ion) is reduced below the value expected from (12.19) with exact Gaunt factors (see Dawson and Oberman 1962, 1963, Oster 1964, Birmingham *et al.* 1965), but the appropriate correction is not likely to be important for $\omega \gtrsim 2\omega_p$.

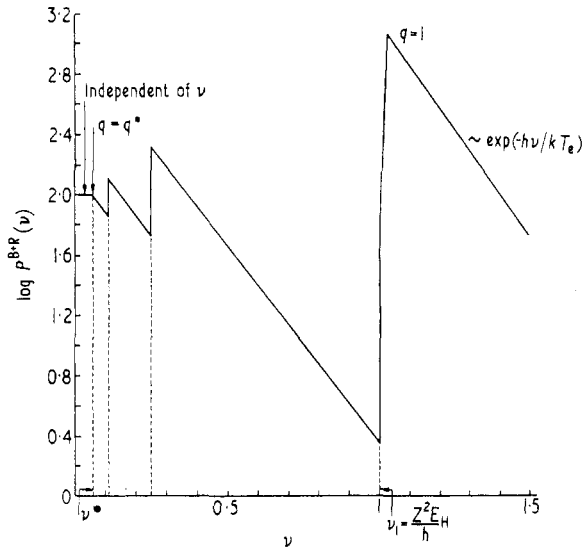


Figure 10. Schematic representation of the distribution with frequency of bremsstrahlung and recombination radiation $P^{B+R}(\nu)$.

While cyclotron radiation is not being dealt with in this review, it should be mentioned that the presence of a magnetic field modifies the continuum emission at low frequencies, and Goldman and Oster (1964) have shown that the total spectrum cannot be interpreted as a superposition of cyclotron radiation on the continuum of bremsstrahlung emission in the absence of the magnetic field. Absorption is also high close to the plasma frequency and, of course, radiation is not propagated below it (with the exception of the 'whistler' mode which can propagate in the presence of a magnetic field).

Griem (1962 b) has shown that the effect of the lowering of the ionization potential (§5) is only to multiply the formula for $P^{B+R}(\nu)$ by $\exp(-\Delta E_{Z-1}(\infty)/kT_e)$.

In hydrogen the H^- continuum should also be considered (see Geltman 1962, 1965). Griem (1964, p. 120) gives a graph of the ratio of negative and normal hydrogen continuum emission as a function of wavelength for various temperatures at $n_e = 10^{16} \text{ cm}^{-3}$ (the ratio being proportional to n_e). For wavelengths in the visible this contribution will nearly always be negligible for temperatures greater than about 15 000 °K.

In the general case for a non-hydrogenic species, the photoionization cross section of equation (12.7) has to be found. As with the calculations for oscillator strengths (§10), the angular parts of the wave function can be easily handled, but now the radial integrals are expressed as

$$\int G_{vl}(r) R_{ql}(r) r dr \quad (12.20)$$

where $G_{vl}(r)$ is the continuum radial wave function. This integral is difficult to evaluate because often the positive and negative contributions to the integral are nearly equal in magnitude. Cooper (1962) has used Hartree-Fock methods for photoionizations from the ground state, but most calculations have used the quantum defect method of Seaton (1958) and Ham (1955). This method of calculation of the continuum wave functions $G_{vl}(r)$ is similar to the Coulomb approximation of Bates and Damgaard (1949), since it makes use of the fact that the main contributions to the integral of (12.20) come from regions of relatively large r for which the potential is closely Coulombic. But now the continuum wave functions are expressed as a linear combination of two Coulombic wave functions; the coefficients of these two functions depend on a generalized quantum defect and are chosen so as to produce the correct asymptotic behaviour at large values of r . Calculations have been performed by Burgess and Seaton (1960) and Anderson and Griem (1963) (see Griem 1964). These should be reasonable for light atoms, provided the kinetic energy of the ejected electron is less than the ionization energy, which is usually true at the frequencies of interest.

As mentioned in §11.3.4, close to the limit of any series a quasi-continuum exists, due to the merging of discrete lines when their broadening becomes greater than the spacing between levels (see also §16.3).

Experimentally there are very few reliable measurements of continua from atoms and ions of interest in plasma spectroscopy. Direct methods exist for photoionization cross sections of atoms or negative ions in their ground state (Ditchburn and Öpik 1962). However, about the only practical method for highly excited states of atoms or ions is by measuring the recombination radiation from plasmas whose properties are accurately known. Work by Olsen (1961) and Maecker and Peters (1954) gave results which fitted badly to modified hydrogenic calculations, but no comparison has been made with quantum defect calculations. Comparison of the measurements of Schlüter (1962), using a stabilized argon arc, with the calculations of Biberman *et al.* (1961), who use an oversimplified approximation based on the quantum defect method, shows poor agreement both in the absolute intensity of the continuum and also its wavelength dependence. However, further quantum defect calculations have been performed for neon, argon, krypton and xenon (Schlüter 1965), and the agreement with continua from an argon arc and shock-excited argon, krypton and xenon is reported as "sufficient".

Very little is known experimentally about continuum emission from highly ionized atoms. In the SCYLLA discharge (Jahoda *et al.* 1964) it has been found that the continuum intensity is about six times larger than the predicted value, and also that, although the continuum is dominated by free-bound transitions, there is little sign of the expected discontinuity at the termination of the O VIII Lyman series.

13. Radiative transfer

When the plasma is optically thin, the emission coefficients and the observed intensities are directly proportional. However, once some radiation is absorbed, radiative transfer has to be considered.

The equation of radiative transfer (see Chandrasekhar 1950, Ambartsumyan 1958) can be written as

$$\frac{1}{\chi(\nu, x)} \frac{dI(\nu, x)}{dx} = -I(\nu, x) + \frac{J(\nu, x)}{\chi(\nu, x)} \quad (13.1)$$

where $I(\nu, x)$ is the intensity of radiation at frequency ν in direction x at point x (measured along the line of sight), $\chi(\nu, x)$ is the absorption coefficient and $J(\nu, x)$ the emission coefficient (i.e. the power radiated at point x per unit solid angle in the x direction per unit volume and frequency interval). The ratio $J(\nu, x)/\chi(\nu, x) = S_\nu(x)$ is known as the *source function*. If the optical depth τ_ν is defined by

$$d\tau_\nu = -\chi(\nu, x) dx,$$

then the equation of radiative transfer can be rewritten as

$$\frac{dI(\nu, x)}{d\tau_\nu} = I(\nu, x) - S_\nu(x). \quad (13.2)$$

In evaluating the effective emission and absorption coefficients $J(\nu, x)$ and $\chi(\nu, x)$, not only do spontaneous emission, induced emission and absorption have to be taken into account, but also scattering of radiation has to be considered. Scattering of radiation is a two-photon process since it involves both an incoming and an outgoing photon. The total amount scattered in a given direction at a certain point in the plasma depends on the radiation intensity at that point coming from all directions; however, it is usual to include scattering in the emission coefficient $J(\nu, x)$. The only scattering process likely to be important in a laboratory plasma is that of resonance fluorescence (see Heitler 1954); here a photon corresponding in energy to an allowed electron transition is absorbed and then a photon is re-emitted in a different direction. In this process, there is a correlation between the directions of the incoming and outgoing photons, which is expressed in terms of a redistribution function, giving the probability of re-emission in a given direction with respect to that of the incident photon (see Hummer 1962).

In laboratory plasmas the depth is generally quite small, so that radiative transfer is often important only for resonance lines, whereas in astrophysical plasmas radiative transfer becomes important throughout the spectrum (see Athay and Thomas 1961). Consider two atomic energy levels separated by energy $h\nu$ and designated 1 (lower) and 2 (upper), so that $n(1)$ and $n(2)$ are the number densities in the lower and upper states respectively. The corresponding line at frequency ν is assumed to be well separated from other lines, and background continuum is also assumed to be absent. ϕ_ν , ϕ'_ν and j_ν are the normalized profiles for absorption, induced emission and spontaneous emission respectively. Oxenius (1966) has shown that the profile for the stimulated emission ϕ'_ν is always identical with that for spontaneous emission j_ν , and not with the profile associated with absorption ϕ_ν , as has usually been assumed.

Close to L.T.E. the lifetimes of excited states are collision-limited and scattering (mainly resonance fluorescence) becomes unimportant because essentially there is not enough time for this two-quantum process to occur.

If resonance fluorescence is neglected

$$J(\nu, x) = \epsilon(\nu) = n(2) A(2, 1) \frac{h\nu}{4\pi} j_\nu \quad (13.3)$$

and

$$\chi(\nu, x) = \frac{h\nu}{4\pi} \left\{ B(1, 2) n(1) - B(2, 1) n(2) \frac{\phi_\nu'}{\phi_\nu} \right\} \phi_\nu \quad (13.4)$$

(= $\sigma_{12}(\nu) n(1) - \sigma_{21}(\nu) n(2)$, in comparison with equation (10.13)).

$B(1, 2)$, $B(2, 1)$ and $A(2, 1)$ are the usual Einstein coefficients defined, as in § 10, with respect to intensity (sometimes called the Milne coefficients). Thus

$$B(2, 1) g(2) = B(1, 2) g(1)$$

and

$$A(2, 1) = B(2, 1) 2h\nu^3/c^2. \quad (13.5)$$

The equation of radiative transfer (13.1) becomes

$$\frac{4\pi}{(h\nu)} \frac{dI}{dx}(\nu, x) = -B(1, 2) n(1) I(\nu, x) \left\{ 1 - \frac{B(2, 1) n(2) \phi_\nu'}{B(1, 2) n(1) \phi_\nu} \right\} \phi_\nu + A(2, 1) n(2) j_\nu. \quad (13.6)$$

The optical depth (including stimulated emission) is given by

$$d\tau_\nu = -(h\nu/4\pi) B(1, 2) n(1) \left\{ 1 - \frac{B(2, 1) n(2) \phi_\nu'}{B(1, 2) n(1) \phi_\nu} \right\} \phi_\nu dx \quad (13.6a)$$

and the source function

$$S_\nu(x) = \frac{2h\nu^3}{c^2} \left(\frac{g(2) n(1) \phi_\nu}{g(1) n(2) \phi_\nu'} - 1 \right)^{-1} \frac{j_\nu}{\phi_\nu}. \quad (13.7)$$

In L.T.E., detailed balancing arguments show that

$$j_\nu = \phi_\nu = \phi_\nu' \quad \text{and} \quad \frac{g(2) n(1)}{g(1) n(2)} = \exp\left(\frac{h\nu}{kT_e}\right)$$

by Boltzmann statistics. Thus, in L.T.E.,

$$S_\nu(x) = \frac{2h\nu^3}{c^2} \left\{ \exp\left(\frac{h\nu}{kT_e}\right) - 1 \right\}^{-1} = B_\nu(T_e) \quad (13.8)$$

i.e. the effective absorption and emission coefficients are related by Kirchhoff's law, with the Planck function $B_\nu(T_e)$ being at the *local* temperature T_e (a function of position only).

Because scattering is neglected the source function $S_\nu(x)$ is independent of direction. Close to L.T.E., when resonance fluorescence is unimportant, $j_\nu = \phi_\nu = \phi_\nu'$ is a good approximation, and it follows from equation (13.7) that (except for the slow ν^3 variation) $S_\nu(x)$ is constant over the line, i.e. independent of direction and frequency.

Resonance fluorescence was considered by Hearn (1964 a) in the low density limit when atoms, excited by absorption of radiation, can emit spontaneously before suffering a collision. He found that the assumption that $S_\nu(x)$ is independent of frequency and direction gives line profiles and total line intensities correct to better than 10% for radiation emitted normally to the plasma boundary, even in extreme non-L.T.E. situations.

In what follows it will be taken that $S_\nu(x)$ is independent of frequency and direction over the small frequency interval covered by the line, and that $j_\nu = \phi_\nu = \phi'_\nu (= \phi(\nu))$.

The solution of the equation of radiative transfer (equation (13.2)), gives that the intensity emerging (at $x = 0$) from a plasma of depth D measured along the line of sight is

$$I(\nu, 0) = - \int_0^{\tau_\nu(D)} S_\nu \exp(-\tau_\nu') d\tau_\nu' \quad (13.9)$$

provided no radiation is incident at $x = D$. The optical depth is by definition measured along the line of sight, and is given by

$$\tau_\nu(D) = - \int_0^D \chi(x, \nu) dx.$$

For small optical depth (i.e. optically thin approximation) τ_ν is small, so that $\exp(\tau_\nu) \simeq 1$.

Then

$$\begin{aligned} I(\nu, 0) &\rightarrow - \int_0^{\tau_\nu(D)} S_\nu d\tau_\nu \\ \lim_{\tau_\nu \rightarrow 0} &= \frac{h\nu}{4\pi} A(2, 1) j_\nu \int_0^D n(2) dx \end{aligned} \quad (13.10)$$

using (13.6a) and (13.7)

$$= \int_0^D \epsilon(\nu) dx \quad (\text{from 13.3}).$$

This formula (cf. (10.10)) is the usual one for emission from an optically thin plasma and depends directly on the emission profile j_ν and the number of excited atoms per unit area along the line of sight (i.e. $\int_0^D n(2) dx$).

In the case of large $\tau_\nu(D)$

$$\begin{aligned} I(\nu, 0) &\rightarrow - \int_0^\infty S_\nu \exp(-\tau_\nu') d\tau_\nu' \\ &= S_\nu(\tau_\nu = 0) + \frac{dS_\nu}{d\tau_\nu} \Big|_{\tau_\nu=0} + \frac{d^2 S_\nu}{d\tau_\nu^2} \Big|_{\tau_\nu=0} + \dots \end{aligned}$$

by integration by parts. But, by MacLaurin's theorem

$$S_\nu(\tau_\nu = 1) = S_\nu(\tau_\nu = 0) + \frac{dS_\nu}{d\tau_\nu} \Big|_{\tau_\nu=0} + \frac{1}{2} \frac{d^2 S_\nu}{d\tau_\nu^2} \Big|_{\tau_\nu=0} + \dots$$

Thus, for large optical depths, provided that the higher order terms do not contribute too much, the observed intensity is roughly equal to the source function at an optical depth of $\tau_\nu \simeq 1$.

In L.T.E. the problem of radiative transfer is relatively easy since the source function is only a function of the electron temperature ($B_\nu(T_e)$) and the populations of states are determined by collisional processes alone.

In an emission line which is strongly self-absorbed, a given optical depth corresponds to a smaller geometrical depth of plasma at the line centre than in the line wings. Since the emitted intensity is now roughly that of a black body at the temperature for the point at which the optical depth is about unity, the line centre tends to have a lower intensity than at some frequencies further into the line wings, assuming the outer layers are cooler than the interior (for L.T.E. calculations, see Cowan and Dieke 1948). In L.T.E. such a central minimum is characteristic of optically thick inhomogeneous layers, but this is not necessarily true for non-L.T.E. situations.

In the non-L.T.E. situation the problem of radiative transfer becomes extremely difficult, since the equation of radiative transfer and the rate equations determining the population densities become coupled together. This is because photoexcitation processes depend on the *local* value of $I(\nu)$, while the source function and optical depth depend on the population densities $n(1)$ and $n(2)$. $S_\nu(x)$ is now not $B_\nu(T_e)$ but a function of the geometry of the plasma as well as its density and temperature. Consider a plasma for which the coronal distribution applies; if the dimensions are increased until the optical depth becomes large (and hence photoexcitation becomes important), a thermal population will be imposed upon the system. This will develop upwards from the ground level, since resonance radiation absorption is most important, and not downwards from the continuum as happens in the case of increasing density.

A two-level atomic model, with Doppler profiles for absorption and emission, has been treated for systems not in L.T.E. by Hearn (1963) (for a plane parallel slab of plasma) and Cuperman *et al.* (1963, 1964) (for a spherical plasma). Cuperman *et al.* (1964) also consider the influence of a non-Maxwellian electron distribution.

Hearn (1963) found that a central dip is obtained in the profile of the emitted radiation even for a plasma which is homogeneous in the sense that both n_e and T_e are constant. This saturation at large optical depths is easily explained. Near the edge of the plasma photons can easily escape and there exists only an outward flux of photons. Compared with the centre of the plasma photoexcitation rates are thus less and the ratio $n(2)/n(1)$ decreases towards the edge of the plasma (i.e. the effective 'excitation temperature' increases towards the centre of the plasma). The geometrical depth at the line centre for $\tau_\nu \simeq 1$ is less than that for the wings, consequently the equivalent S_ν is less at the centre owing to its dependence on $n(2)/n(1)$. Hearn also found that as regards the total rate of loss of energy the photon diffusion model of Zanstra (1949) and Osterbrock (1962) gives quite good results.

Since in most of the non-L.T.E. calculations (§7) the plasma is assumed optically thin, the circumstances under which the optically 'thin' approximation can be used will now be considered.

Consider a homogeneous plasma of depth D measured along the line of sight, with the source function S_ν independent of τ_ν (as in L.T.E.).

Then equation (13.9) gives

$$I(\nu, 0) = S_\nu[1 - \exp\{-\tau_\nu(D)\}]. \quad (13.11)$$

Since S_ν is only slowly varying over the line profile, equation (13.11) can be integrated to give the total intensity I_t

$$I_t = S_\nu \int_0^\infty \{1 - \exp(-\tau_\nu)\} d\nu$$

which, for small optical depths, can be expanded as

$$I_t \simeq S_\nu \int_0^\infty (\tau_\nu - \frac{1}{2}\tau_\nu^2 + \dots) d\nu. \quad (13.12)$$

From equation (13.6a) τ_ν is proportional to ϕ_ν . Thus if τ_0 is the optical depth at line maximum and ϕ_0 the corresponding value of ϕ_ν , τ_ν may be written as

$$\tau_\nu = \frac{\tau_0}{\phi_0} \phi_\nu. \quad (13.13)$$

Hence

$$I_t \simeq S_\nu \frac{\tau_0}{\phi_0} - S_\nu \frac{\tau_0^2}{2\phi_0^2} \int \phi_\nu^2 d\nu. \quad (13.14)$$

Two profiles are of interest, for lines of frequency ν_0 :

(i) Doppler broadening gives a Gaussian profile, such that

$$\phi_\nu = \phi(\nu) = \phi_0 \exp\left\{-\frac{\ln 2}{w_D^2}(\nu - \nu_0)^2\right\} \quad \text{where} \quad \phi_0 = \left(\frac{\ln 2}{\pi}\right)^{1/2} \frac{1}{w_D}$$

and

$$w_D = (\ln 2)^{1/2} \nu_0 \left(\frac{2kT_1}{Mc^2}\right)^{1/2}. \quad (13.15)$$

(ii) Dispersion profile of half half-width w_S

$$\phi_\nu = \phi_0 \left\{1 + \frac{(\nu - \nu_0)^2}{w_S^2}\right\}^{-1} \quad \text{with} \quad \phi_0 = \frac{1}{\pi w_S}$$

The case of the dispersion profile is interesting, since for Stark broadening of isolated lines w_S is proportional to n_e . Under certain circumstances this can mean that the optical depth becomes independent of n_e for an ionized atom and depends only on the geometry and electron temperature (Burgess and Cooper 1965 c).

If the plasma had been treated as optically thin the result

$$I_t = S_\nu(\tau_0/\phi_0)$$

would have been obtained for the total intensity.

Thus, for the actual emitted total intensity to be within 10% of this optically thin value, it is required that

$$\left| \frac{I_t - S_\nu(\tau_0/\phi_0)}{S_\nu(\tau_0/\phi_0)} \right| \leq 0.1$$

or from (13.14)

$$\frac{\tau_0}{2} \frac{\int \phi_\nu^2 d\nu}{\phi_0} \leq 0.1. \quad (13.16)$$

This gives the following limits on τ_0 for 10% change in total intensity:

$$\begin{aligned}\tau_0 \text{ (Doppler)} &\leq 0.28 \\ \tau_0 \text{ (dispersion)} &\leq 0.40.\end{aligned}$$

Similarly, the criteria that the apparent half half-width should not increase by more than 10% due to absorption can easily be shown to be

$$\tau_0 \text{ (Doppler)} \lesssim 0.55$$

and

$$\tau_0 \text{ (dispersion)} \lesssim 0.4.$$

Finally, if at any frequency it is required that the intensity should not differ from the value obtained from the optically thin approximation by more than 10%, it is necessary that

$$\left| \frac{I(\nu, 0) - S_\nu \tau_\nu}{S_\nu \tau_\nu} \right| \leq 0.1 \quad (13.17)$$

which, expanding equation (13.11), gives

$$\tau_\nu(D) \leq 0.2. \quad (13.18)$$

The following processes which contribute to the optical depth will be considered (after Wilson 1962): (a) absorption of line radiation; (b) absorption of recombination radiation; (c) absorption of free-free radiation and (d) scattering of photons by free electrons.

A homogeneous plasma of depth D is considered and the criterion $\tau_\nu(D) \leq 0.2$ is used, so that the intensity does not depart from its optically thin value by more than 10%.

(a) For line radiation resonance line absorption is most serious, and the depth at the line maximum has to be considered. Thus, using (13.6a)

$$\tau_0(D) = \frac{h\nu}{4\pi} B(1, 2) n(1) \left\{ 1 - \frac{g(1)n(2)}{g(2)n(1)} \right\} \phi_0 D \leq 0.2.$$

If the population in the upper state is ignored and the result expressed in terms of the absorption oscillator strength f_{12} (equation (10.6))

$$n(1) D f_{12} (\pi e^2 / mc) \phi_0 \leq 0.2.$$

Approximating the population density in the ground state by the number density n_Z of the absorbing ion or atom, for Doppler broadening of frequency half half-width w_D (in c/s), we find the criterion is

$$D n_Z \lesssim 16 w_D / f_{12} \text{ cm}^{-2}. \quad (13.19)$$

(b) For photoionization the optical depth in terms of the photoionization cross section is (neglecting stimulated recombinations)

$$\tau_\nu(D) = n(q) \sigma_{qv}(\nu) D.$$

This optical depth is maximum for transitions from the ground state to the absorption edge, i.e. $h\nu = E_{Z-1}(\infty)$. Using the hydrogenic cross section (equation (12.9)) with $h\nu = Z^2 E_H$ and $g_{fb} = 1$ this results in

$$D n_Z \lesssim 2.6 \times 10^{16} Z^2. \quad (13.20)$$

This result has been generalized by Wilson (1962) using Elwert's (1952) cross sections for non-hydrogenic species.

(c) The free-free absorption coefficient is (Spitzer 1956)

$$\frac{4}{3} \left(\frac{2\pi}{3kT_e} \right)^{1/2} \frac{n_e n_Z Z^2 e^6}{hcm^{3/2} \nu^3}.$$

Thus the requirement is that

$$Dn_e^2 \lesssim 8 \times 10^{35} (kT_e)^{1/2} (h\nu)^3 \bar{Z}^{-1} \text{ cm}^{-5} \quad (13.21)$$

where kT_e and $h\nu$ are in eV and \bar{Z} is the average charge of ions in the plasma.

This is best evaluated for the region of maximum bremsstrahlung emission, i.e. for $h\nu = 2kT_e$.

(d) The cross section of an electron for scattering a photon is the well-known Thompson cross section ($= (8\pi/3)(e^2/mc^2)^2 = 6.7 \times 10^{-25} \text{ cm}^2$). Thus

$$Dn_e \lesssim 3 \times 10^{23} \text{ cm}^{-2}. \quad (13.22)$$

For the intensity at any frequency not to differ from the optically thin value by more than 10%, examination of the above criteria ((13.19)–(13.22)), indicates that, for laboratory plasmas, (c) and (d) are unimportant, but (a) and (b) may be so. Often (a) is particularly severe.

To obtain the above results the source function S_ν has been considered as independent of frequency. Strictly, these criteria are applicable only to L.T.E. situations. However, Hearn (1964 b) indicates that for non-L.T.E. plasmas the above criteria on optical depth may, in general, be relaxed. Thus, if anything, the criteria are too severe.

McCumber and Platzman (1963) have argued that if radiation is reflected back into the plasma, under certain conditions, stimulated emission will become important. This is certainly true since laser oscillations occur for transitions in many ionized gases (see Bridges and Chester 1965). For a high temperature plasma in which the coronal approximation holds this is unlikely to be important since radiative decay already dominates over collisional de-excitation, and the total radiation loss rate is determined by the rate of excitation by collisions. Thus stimulated emission does increase the probability of radiative decay, but not the loss rate (see § 18).

In the laboratory it is necessary to be able to interpret the observed radiation in terms of the emission coefficient within the plasma, but equation (13.10) shows that even in the optically thin case the observed intensity is the integral of the emission coefficient along the line of sight. A solution exists for an optically thin cylindrical column for which n_e and T_e are functions of r only. Then (figure 11)

$$I(y) = 2 \int_0^{(r_0^2 - y^2)^{1/2}} \epsilon(r) dx = 2 \int_y^{r_0} \frac{r \epsilon(r) dr}{(r^2 - y^2)^{1/2}}$$

from which $\epsilon(r)$ is found by Abel inversion

$$\epsilon(r) = -\frac{1}{\pi} \int_r^{r_0} \frac{\{dI(y)/dy\} dy}{(y^2 - r^2)^{1/2}}. \quad (13.23)$$

Various numerical procedures (for example, Bochasten 1961), analogue computers (Yokley and Shumaker 1963, Becker and Drawin 1964) and automatic processing

systems (Paquette and Wiese 1964) are available for performing this inversion. The method has been extended to optically thick plasmas by Griem (1964) and Elder *et al.* (1965).

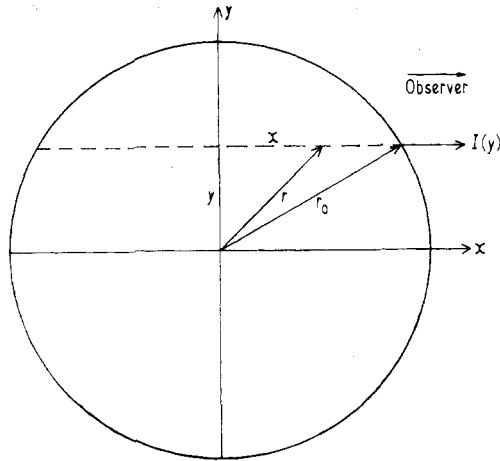


Figure 11. Cylindrical plasma column; the emission coefficient $\epsilon(r)$ is a function of radius:

$$I(y) = 2 \int_y^{r_0} \frac{\epsilon(r) r dr}{(r^2 - y^2)^{1/2}} \quad \text{and} \quad \epsilon(r) = -\frac{1}{\pi} \int_r^{r_0} \frac{\{dI(y)/dy\} dy}{(y^2 - r^2)^{1/2}}.$$

14. Plasma parameters†

The discussion in this section concerns the application of the details of the radiation to the investigation of conditions in a plasma.

Experimental plasmas fall into two types from the spectroscopic viewpoint. Firstly, there are those plasmas whose primary purpose is to act as a controlled source of radiation for the measurement of atomic parameters (such as oscillator strengths and linewidths). Secondly, there are the plasmas existing in controlled thermonuclear fusion devices.

Much of the theory discussed in this report is tentative in nature since approximations of one sort or the other are involved. Thus it is essential to check the theories with the use of light sources whose properties are accurately known, in order to be able to use the results with confidence. In general, this means a plasma in L.T.E. since only then do the population densities of the quantum states become independent of detailed rate coefficients. Thus the temperature and electron number density must be measured by methods depending on L.T.E. (such as line ratio methods for temperature, § 15.3) and independent of L.T.E. (such as the continuum step method, § 15.1). Only if these results agree for a given light source under time-varying conditions can L.T.E. be safely assumed. Arcs and shock tubes usually fall within the L.T.E. region, but not always (Eckerle and McWhirter 1966).

For a review on arcs, see Finkelnburg and Maecker (1956) and Lochte-Holtgreven (1958), and for conventional and electromagnetic shock-tubes, see Kolb

† For further reference see Huddleston and Leonard 1965, chaps 5–10

and Griem (1962) and Fowler (1962). The requirement for L.T.E. usually means that it is difficult to obtain high stages of ionization and hence it is difficult to obtain parameters for highly ionized atoms.

Since most of the plasmas of interest in controlled thermonuclear research are not in L.T.E., methods which do not depend explicitly on thermodynamic equilibrium will be stressed. Temperatures are often in excess of 100 eV, and in this region the Maxwellian distribution of the free electrons plays an essential role. At such temperatures the strongest emission is in the soft x-ray and vacuum ultra-violet regions of the spectrum.

It should be said here that, often, even semi-qualitative analysis can only be carried out for hydrogen-like and helium-like ions; the hydrogen-like and helium-like spectra of all elements between oxygen ($Z = 8$) and bromine ($Z = 35$) lie between $\lambda = 1 \text{ \AA}$ and 20 \AA .

The controlled thermonuclear research plasmas are often extremely transient in nature, so that adequate time resolution is necessary. Photoelectric recording is used whenever possible, and often instruments are specially designed (examples of such instruments are a time-resolved normal-incidence vacuum ultra-violet spectrograph (Gabriel and Waller 1963, Gabriel *et al.* 1962), a scanning Fabry-Pérot interferometer for line profile studies (Cooper and Greig 1963), and devices for measuring line shifts (Zaidel *et al.* 1961, Hirschberg 1965, Burgess and Cooper 1965 b).

Many of the methods to be discussed are limited to hydrogen-like systems, since only in this case are the calculations likely to be accurate. However, traces of impurities, small enough not to cause any appreciable error in, say, the continuum radiation, can, with care, be used to extend measurements to more complicated radiating systems.

Although this review is concerned with emission spectroscopy, it must be mentioned here that radiation can be used as a plasma probe. A few examples are briefly discussed below.

(1) The incoherent scattering of intense monochromatic light (from a laser!) can give information about n_e and T_e and also about the ion temperature of fully ionized hydrogen (a parameter which cannot be determined by other spectroscopic methods). In principle this method gives the plasma parameter at a point (the small region from which scattering occurs) instead of an average along the line of sight. This method is experimentally difficult (see, for example, Fiocco and Thompson 1963, Fünfer *et al.* 1963, Schwarz 1963, Davies and Ramsden 1964, Ascoli-Bartoli *et al.* 1964, De Silva *et al.* 1964, Kunze *et al.* 1964 a, b). For a theoretical treatment reference may be made to Salpeter (1960) or Rosenbluth and Rostoker (1962).

Various other scattering experiments have been proposed but these will not be discussed here (see, for example, Kroll *et al.* 1964, Salat and Schlüter 1965, Salat 1965).

(2) Line reversal techniques (Garton and Rajaratnam 1957, Gaydon and Hurlé 1963) permit the determination of the source function S_ν in a homogeneous plasma (cf. § 13). From this the ratio of population densities in the upper and lower states of an optically thick line and hence the effective 'excitation' temperature can be derived. By applying this method to autoionization levels (which are strongly

linked to the continuum) a sensitive test of L.T.E. should be possible (W. R. S. Garton, private communication).

(3) Refractive index measurements are important for number density determinations and oscillator strength measurements (for a summary see Griem 1964). In particular n_e is determined from the refractive index of free electrons ($\approx 1 - 2\pi n_e e^2/m\omega^2$ at frequency ω). Various interferometric techniques are available (see Alpher and White 1959, and 1964 General Electric Research Lab. Rep. No. 64-RL-3627C), and one of the most convenient is that using a He-Ne gas laser (Ashby and Jephcott 1963). For n_e determinations this is often the best and most straightforward method.

(4) Measurement of the Faraday rotation of light (usually from a gas laser) enables magnetic fields in the plasma to be determined (see Dougal *et al.* 1964, Falconer *et al.* 1965).

15. Temperature measurements

Often the methods to be discussed involve some knowledge of n_e , so that it is necessary to solve for n_e and T_e in a self-consistent manner.

15.1. Relative continuum intensities

For frequencies ν , such that $h\nu \gg kT_e$ (generally in the vacuum ultra-violet or soft x-ray region), both bremsstrahlung and recombination radiation fall off as $\exp(-h\nu/kT_e)$ provided the variation of the Gaunt factor is small (Stratton 1962). This is independent of L.T.E. in that it only depends on the free electron velocity distribution being Maxwellian. In principle a measurement of the continuum slope is required. Although this is certainly true for a pure hydrogen plasma, interpretation can become much more difficult when impurities (not necessarily hydrogenic) are present, since rapid variation of Gaunt factors are possible especially close to threshold. A crystal spectrograph has been used (Bearden *et al.* 1961, Sawyer *et al.* 1963), but the spectrum was considerably confused by large amounts of line radiation from impurities in the discharge. A grazing-incidence spectrograph could also be used, but intensity calibration in the vacuum ultra-violet is difficult (Griffin and McWhirter 1961, Hinnov and Hofmann 1963).

Alternatively the x-ray flux transmitted through various absorber foils may be used to determine the frequency distribution of the x-rays (Jahoda *et al.* 1960). Owing to the possible contribution from impurity line radiation in high temperature discharges, this method should be used with care. However, N. J. Peacock (private communication) has shown that, by suitable choice of absorbers, the transmission ratio (and hence the measured T_e) can remain almost constant in spite of the apparent absolute intensity of the continuum varying considerably owing to the presence of impurities.†

Equation (12.19) for hydrogenic continuum radiation shows that the ratio of continuum intensities on either side of a series limit is only a function of the electron

† A. H. Gabriel (private communication) has pointed out that the rapid decrease of intensity to short wavelengths beyond the bremsstrahlung maximum (at $h\nu = 2kT_e$) sometimes enables the maximum, and hence T_e , to be found relatively accurately from photographically recorded grazing-incidence spectra.

temperature (McWhirter 1963)—bremsstrahlung on one side and bremsstrahlung and recombination on the other (see also Griem 1964). It is usual to use the discontinuity across the Balmer series limit at $\lambda = 3646 \text{ \AA}$. To apply this result with confidence the system must be purely hydrogenic, so that contributions to the continuum from other species can be neglected (e.g. if ionized helium is used the temperature must be large enough to ignore neutral helium). Because of the smooth transition between lines and continuum there is no actual sharp discontinuity in the intensity. Thus one must scan the spectrum over and in between the higher series members and extrapolate to the series limit. Alternatively the absolute continuum

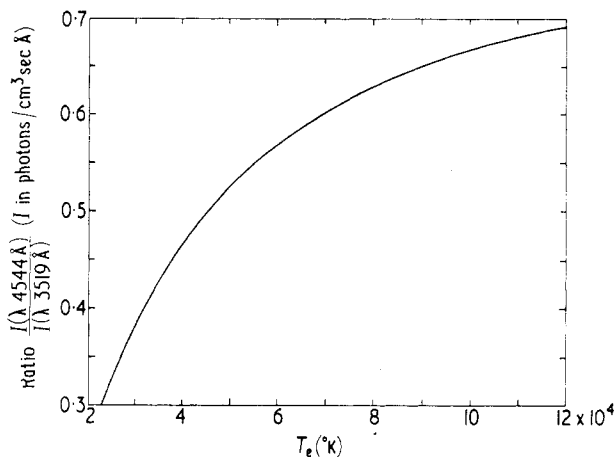


Figure 12. Intensity ratio across the Balmer discontinuity: $I(\lambda 4544 \text{ \AA})/I(\lambda 3519 \text{ \AA})$ against electron temperature. (After Eckerle and McWhirter 1966).

intensity has to be measured in two wavelength bands sufficiently distant from the series limit for the line radiation to be negligible. Figure 12 shows the ratio of intensities for 3.3 \AA bandwidths at $\lambda = 3519 \text{ \AA}$ and $\lambda = 4544 \text{ \AA}$ across the Balmer limit as a function of T_e (after Eckerle and McWhirter 1966).

The actual wavelength bands are often a question of convenience; for instance, Cooper and Kunkel (1965) use intervals at $\lambda = 3225 \text{ \AA}$ and $\lambda = 5320 \text{ \AA}$.

15.2. Relative line to continuum intensities

This method, like the intensity ratio across the series limit, is restricted to pure gases, such as hydrogen or helium, where calculations of the continuum are precise.

The total line intensity for number density $n_{Z-1}(p)$ in the upper state (and q the principal quantum number of the lower) is given by equation (10.10) for path length D in the optically thin case:

$$I_t = \frac{h\nu}{4\pi} A(p, q) n_{Z-1}(p) D. \quad (15.1)$$

If the upper state is in equilibrium with electrons and bare ions (hydrogenic system), Saha's equation can be written as

$$n_{Z-1}(p) = \frac{g_{Z-1}(p)}{2g_Z(1)} n_e n_Z(1) \left(\frac{h^2}{2\pi m k T} \right)^{3/2} \times \exp \left\{ \frac{E_{Z-1}(\infty) - E_{Z-1}(p) - \Delta E_{Z-1}(\infty)}{k T_e} \right\}. \quad (15.2)$$

For a hydrogenic system $n_Z(1) = n_Z$.

In terms of the absorption oscillator strength f_{qp} (equation (10.6))

$$I_t = \frac{h\nu n_e n_Z}{8\pi g_Z(1)} \left(\frac{h^2}{2\pi m k T} \right)^{3/2} g_{Z-1}(q) \frac{8\pi^2 e^2 \nu^2}{m c^3} f_{qp} \times \exp \left\{ \frac{E_{Z-1}(\infty) - E_{Z-1}(p) - \Delta E_{Z-1}(\infty)}{k T_e} \right\}. \quad (15.3)$$

For a wavelength interval $\Delta\lambda = \lambda^2 \Delta\nu/c$ centred at line, the intensity of the continuum is, from equation (12.19),

$$I^{B+R}(\Delta\lambda) = \frac{P^{B+R}(\lambda D) \Delta}{4\pi} = \frac{8e^4 h Z}{3^{3/2} \pi^{1/2} m^2 c^3} \left[g_{ff} \exp \left\{ \frac{Z^2 E_H}{k T_e (q^* + 1)^2} \right\} + \frac{2Z^2 E_H}{k T_e} \sum_{q \geq (Z^2 E_H / hc)^{1/2}}^{q^*} \frac{g_{fb}}{q^3} \exp \left\{ \frac{Z^2 E_H}{q^2 k T_e} \right\} \right] \times n_e n_Z \left(\frac{Z^2 E_H}{k T_e} \right)^{1/2} \exp \left\{ -\frac{hc}{\lambda k T_e} - \frac{\Delta E_{Z-1}(\infty)}{k T_e} \right\} \frac{\Delta \lambda c D}{\lambda^2}. \quad (15.4)$$

Dividing (15.3) by (15.4), for $Z = 1$, we find

$$\frac{I_t}{I^{B+R}(\Delta\lambda)} = \frac{3^{3/2} \pi^3 \left(\frac{h^3 c}{8\pi^3 m e^4} \right)^2 f_{qp} g_{Z-1}(q) \exp \left\{ \frac{E_{Z-1}(\infty) - E_{Z-1}(q)}{k T_e} \right\}}{2\lambda \Delta\lambda g_Z(1) \left[\frac{g_{ff}}{2} \left(\frac{k T_e}{E_H} \right) \exp \left\{ \frac{E_H}{(q^* + 1)^2 k T_e} \right\} + \sum_q^{q^*} \left(\frac{g_{fb}}{q^3} \right) \exp \left\{ \frac{E_H}{q^2 k T_e} \right\} \right]} \quad (15.5)$$

since $h\nu = E_{Z-1}(p) - E_{Z-1}(q)$.

Note that the high density corrections (terms with $\Delta E_{Z-1}(\infty)$) cancel out. This ratio is plotted in figure 13 (after Griem 1964) for several lines of the hydrogen Balmer series for 100 Å of continuum centred at the line. It is quite a steep function of T_e for temperatures up to about 60 000 °K. Below about 10 000 °K corrections have to be made for the H⁻ continuum. Further graphs are given by Griem for neutral and ionized helium. The intensity ratios in figure 13 refer to continuum bands centred at the lines. The results are directly applicable only if the spectrum is scanned over the whole line profile and if the underlying continuum is determined by extrapolation on the line wings. If adjacent continuum bands are used the above results have to be corrected: for example, Cooper and Kunkel (1965) have used the total intensity of Hβ ($\lambda = 4861$ Å) against 1 Å continuum bands at $\lambda = 5320$ Å and $\lambda = 3225$ Å.

For hydrogen the theoretical errors should be quite small. The method will be applicable when the upper state of the line is in equilibrium with ions and electrons

(i.e. the criterion of equation (9.2) must be applied ($p = 4$ for $H\beta$)). This does not mean complete L.T.E. The method may often be used up to about 60 000 °K in hydrogen. The ionized helium line to continuum intensity ratios may be used in a pure helium plasma from about 75 000 °K to 500 000 °K, when contributions from the neutral helium continuum are negligible. Berg and Tondello (1964, Institute for Plasma Phys., Jülich, Germany, Rep. Jül-182) have extended the helium results to lower temperatures by taking into account the neutral helium continuum

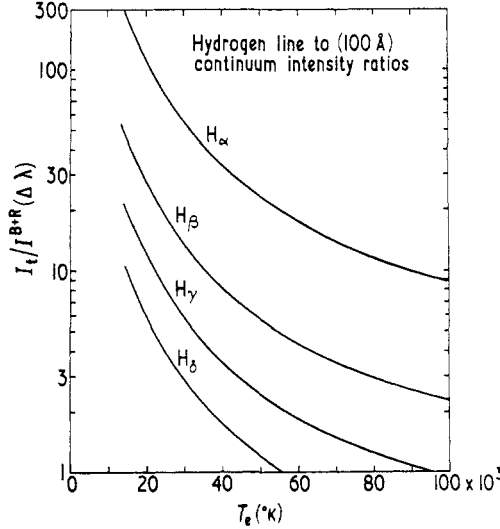


Figure 13. Ratio of the total line intensity (I_t) and continuum intensity ($I^{B+R}(\Delta\lambda)$) in 100 Å bands centred at the lines as a function of temperature for hydrogen lines. (After Griem 1964.)

emission. If accurate values were known for oscillator strengths and continuum emission coefficients (via quantum defect calculations, perhaps), this method could be applied equally well to other species.

15.3. Relative intensities of lines

For an optically thin plasma the ratio of total intensities for transitions from states p to q and p' to q' is given by

$$\frac{I_t}{I'_t} = \frac{n(p) A(p, q) \nu}{n(p') A(p', q') \nu'} \quad (15.6)$$

The ratio of the population densities in the upper states depends critically on whether the plasma is in L.T.E. or not.

For lines belonging to the same ionization stage

$$\frac{n(p)}{n(p')} = \frac{g(p)}{g(p')} \exp \left[-\frac{E(p) - E(p')}{kT_e} \right] \quad (15.7)$$

and this will be applicable when L.T.E. extends down to the lower of p and p' . However, owing to uncertainties in the transition probabilities (often $\sim 20\%$),

errors in intensity measurements, and the fact that $E(p) - E(p')$ is generally small with respect to kT_e , make this a rather insensitive and inaccurate method.

The effect of the energy separation of the lines being small with respect to kT_e can be eliminated by taking lines from consecutive ionization stages of the same element. Then, for L.T.E.

$$\frac{n_{Z-1}(p)}{n_Z(p')} = \frac{n_e g_{Z-1}(p)}{2g_Z(p')} \left(\frac{h^2}{2\pi m k T_e} \right)^{3/2} \times \exp \left\{ \frac{[\{E_{Z-1}(\infty) - \Delta E_{Z-1}(\infty)\} + \{E_Z(p') - E_{Z-1}(p)\}]}{kT_e} \right\} \quad (15.8)$$

where now $E_Z(p')$ is measured with respect to the ground state of the ion S_Z . But now a knowledge of electron density is necessary.

For the ratio to be given by equations (15.6) and (15.8) L.T.E. must be a good approximation, since it has been assumed in (15.8) that the level p' is in Maxwell-Boltzmann equilibrium with respect to the ground state of S_Z . For most plasmas at high temperatures this is not the case. Calculations of the ionization relaxation times show that these plasmas are not in a steady state so that successive ionization stages are not in equilibrium with each other. Thus intensity ratios for lines of different ionization stages should be used with care; Griem (1964) gives intensity ratios for lines of different ionization stages under various types of equilibrium.

The method due to Heroux (1963, 1964), for use when the coronal approximation (§ 6) is valid, gets round many of the above difficulties.

Although the time for the ground state of an ion to come into equilibrium is often long (equivalent to the ionization time for the particular species), the relaxation time for the upper levels is very fast (typically, about $1/A(p) \approx 10^{-8}$ sec). In general, therefore, the ground state is not in equilibrium, but its population density changes comparatively slowly and the population densities of the excited levels follow almost instantaneously.

Then, for coronal equilibrium, equation (6.1) is applicable, i.e.

$$\frac{n_Z(p)}{n_Z} = \frac{n_Z(p)}{n_Z(1)} = \frac{n_e K(1, p)}{A(p)} \quad (15.9)$$

where, as before, $A(p)$ is the total Einstein probability for spontaneous radiative decay from state p and $K(1, p)$ is the collisional excitation rate coefficient for excitation from the ground state. Thus for one and the same ion

$$\frac{n_Z(p')}{n_Z(p)} = \frac{K(1, p')}{A(p')} \frac{A(p)}{K(1, p)}. \quad (15.10)$$

This ratio depends only on a function of T_e , and does not depend on either the time or space variation of n_Z .

Care has to be taken to determine that there are no metastable states likely to affect the chosen levels significantly. Metastable states may become highly populated owing to both electron excitations and radiative decays, of which they are the lower state. Excitation to the level p could therefore also occur from the metastable levels, so that (15.10) would no longer represent the system. Metastable processes make invalid earlier helium singlet-to-triplet ratio methods (Cunningham 1955,

U.S.A.E.C. Rep. WASH-289, see also Thonemann 1961), although recent calculations by Drawin (1964 b) take them into account.

Heroux (1963, 1964) eliminates the problem of metastables by choosing low-lying levels in lithium-like ions. The intensity ratio for the $2S-2P_{3/2}$ and $2S-3P_{1/2,3/2}$ transitions are shown as a function of electron temperature for the ions C IV, N V, O VI, Ne VIII, Si XII and Ar XVI in figure 14. These curves differ from the original ones of Heroux by an appreciable amount, having been recalculated by R. W. P. McWhirter (private communication, after Burke and Tait) using more recent values of the excitation cross sections (see also e.g. Bely 1962, 1963).

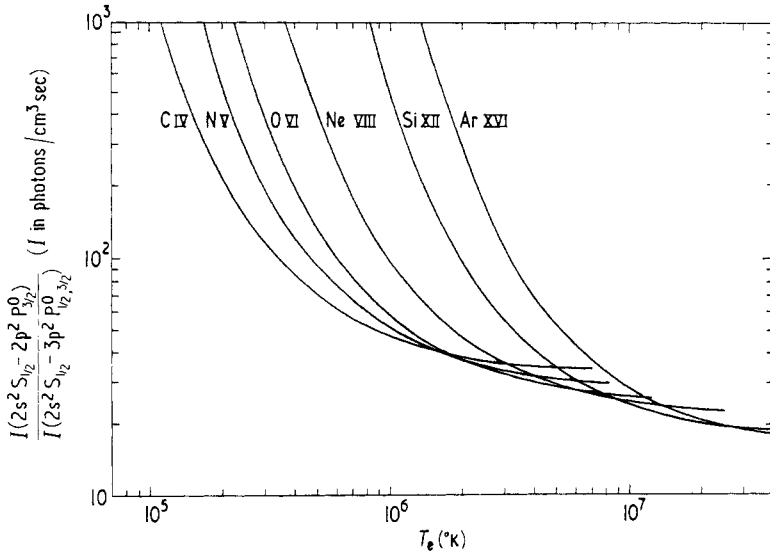


Figure 14. Intensity ratio of the transitions $2s\ 2S_{1/2}-2p\ 2P_{3/2}^0$ and $2s\ 2S_{1/2}-3p\ 2P_{1/2,3/2}^0$ against electron temperature for lithium-like ions.

To apply the method the coronal approximation must be valid (see § 9). In principle it is an excellent method; the overall accuracy, being determined by errors in the cross sections and in calibration in the vacuum ultra-violet, is probably about 10%.

15.4. Ionization times

In a transient plasma the times of appearance of spectral lines from various ionization stages of an element are relatively easy to measure. These times of appearance can only be related to the electron temperature by solution of the time-dependent rate equations. Estimates of electron temperature have been made in this manner (e.g. Goldman and Kilb 1964, Burton and Wilson 1961). Major inaccuracies occur through only approximate knowledge of many of the cross sections involved.

15.5. Shift-to-width ratio of Stark-broadened isolated lines

For many transitions with non-degenerate upper levels the Stark broadening due to ions is negligible (i.e. α in equations (11.40) and (11.41) of § 11.3.4 is small).

Thus the ratio of line shift d to half half-width w is due primarily to electron impact broadening and is then only a function of the electron temperature T_e (D. D. Burgess 1964, Burgess and Cooper 1965 a). This value of d/w depends only on the free electron velocity distribution and is thus independent of assumptions concerning L.T.E. This ratio is shown in figure 15 as a function of temperature, for transitions arising from multiplets in various elements. A quite usable temperature variation is often obtained for temperatures up to 60 000 °K.

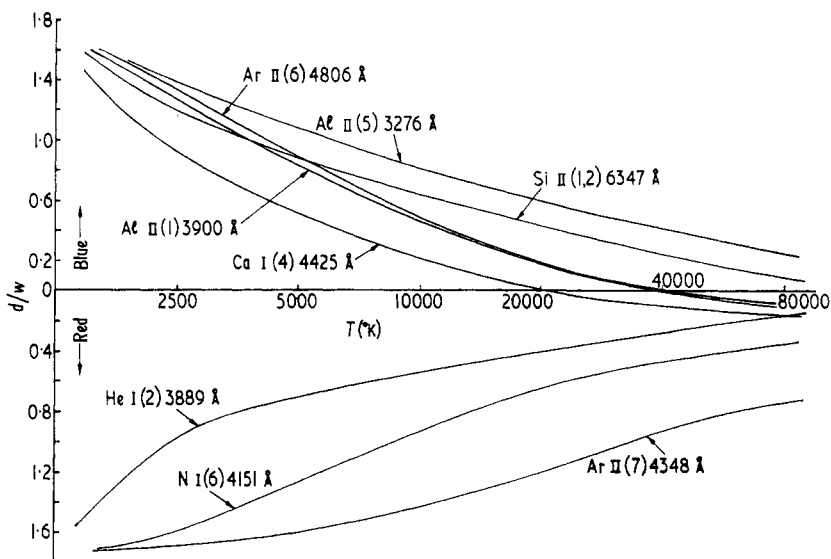


Figure 15. Shift-to-width ratio due to electron impacts for some common elements: from the tables of Griem (1964). Each curve refers to a given multiplet of the element (multiplet number in brackets), and one wavelength of the multiplet is quoted.

Although the high and low temperature limits of d/w are likely to be fairly accurate (as explained in § 11.3.4), in the intermediate region the theoretical uncertainty can be quite large. All the same, once this method has been calibrated under conditions of L.T.E. or at least where T_e is otherwise known, it will be useful for temperature measurements in non-L.T.E. situations. For the method to apply, Stark broadening due to the electrons must dominate Doppler and other broadening mechanisms. Corrections for finite α are easy to apply, owing to its slow ($n_e^{-1/4}$) variation with electron density.

Apparatus exists (D. D. Burgess 1965, Ph.D. Thesis, University of London, Burgess and Cooper 1965 b) which permits the measurement of d/w down to 0.1 with 10% accuracy. Since a single line is used absolute intensity calibration is unnecessary, which is a substantial advantage.

15.6. Doppler profiles

In the case of a highly ionized species the resonance lines are in general always dominated by the Doppler effect (see § 11.5). However, this is not always due to thermal motion of the emitting species, but can be caused by macroscopic, usually

unresolved, motion of turbulent elements. It is therefore necessary to measure profiles of lines of ions of different mass M and charge Z and to check if the individual profiles are Gaussian. If all profiles yield the same temperature one can assume that the turbulent motion is negligible. Should the mean square velocities be equal to each other then macroscopic motion overshadows thermal motion. Measurements for controlled thermonuclear research plasmas (Hirschberg and Palladino 1962, Jones and Wilson 1962, Wilson 1962, Sawyer *et al.* 1963, Hirschberg 1964) indicate that the average ion energy was some function of both Z and M .

15.7. Miscellaneous methods

The list of methods of measurement of temperature given in the preceding paragraphs is not exhaustive.

Other possible methods are listed as follows:

(1) In the infra-red, strong absorption may occur and the plasma radiates as a black body, from which a temperature may be derived (see Kimmitt and Niblett 1963, Harding and Roberts 1962, and § 16.1).

(2) When the optical depth at the centre of a line is very large, saturation occurs and a black-body temperature may again be derived (Wiese *et al.* 1963).

(3) The total intensity of lines from singly ionized species is under some conditions a rapidly varying function of T_e (as well as a function of n_e), and this may be used to measure T_e (Day and Griem 1965, Day 1965, Ph.D. Thesis, University of Maryland).

(4) Under certain conditions the peak intensity of Stark-broadened lines from singly ionized species may be a function of the electron temperature only (Burgess and Cooper 1965 c).

(5) In a very high temperature plasma Doppler broadening may dominate Stark broadening even for high members of a series. The merging of the lines (as in the Inglis-Teller limit—§§ 11.3.4 and 16.3) thus enables the ion temperature to be determined (see Stratton (1962), who gives also regions where this will be valid).

16. Density measurements

All the methods to be discussed, except those involving the Stark effect, depend on absolute intensity measurements and a knowledge (to some extent) of the electron temperature, so the overall accuracy is not likely to be high (20% may be regarded as quite good). It is worth emphasizing that, as discussed briefly in § 14, one of the most reliable methods for determination of the density of free electrons is via the refractive index.

16.1. Absolute continuum intensities

At low frequencies the continuum spectrum becomes constant with frequency since, in the formula (12.19), $(q^* + 1)^2 = Z^2 E_H/h\nu$. This is known as visible bremsstrahlung. Thus

$$P^{B+R}(\nu) d\nu = \frac{32\pi^{1/2} e^4 h Z^2}{3^{3/2} m^2 c^3} g_{ff} n_Z n_e \left(\frac{E_H}{kT_e} \right)^{1/2} d\nu. \quad (16.1)$$

Then for a length D of plasma (assumed uniform), consisting of one electron and bare ions, the continuum intensity is

$$I^{B+R}(\nu) d\nu = \frac{16}{3} \left(\frac{\pi}{6m^3} \right)^{1/2} \frac{e^6}{c^3} (kT_e)^{-1/2} g_{ff} \left(\sum_{Z=1}^Z n_e n_Z Z^2 \right) D d\nu. \quad (16.2)$$

For an almost pure hydrogen plasma this becomes

$$I^{B+R}(\nu) d\nu = \frac{16}{3} \left(\frac{\pi}{6m^3} \right)^{1/2} \frac{e^6}{c^3} (kT_e)^{-1/2} g_{ff} n_e^2 \left(1 + \sum_{Z \geq 2} \frac{n_Z}{n_e} Z^2 \right) D d\nu. \quad (16.3)$$

The summed term in parentheses represents the contribution of impurities. Karzas and Latter's (1961) values of Gaunt factors for hydrogen should be employed.

Although $I^{B+R}(\nu)$ depends only weakly on T_e , large errors may be incurred as a result of inhomogeneities. The observed $I^{B+R}(\nu)$ is proportional to the integral of $n_e^2/T_e^{1/2}$ along the line of sight and this is weighted towards regions of low T_e , whereas n_e is usually of most interest where T_e is highest. To measure the continuum intensity it is first necessary to ensure that line radiation does not contribute significantly. Absolute intensity measurements can often be made with an accuracy to better than 20%, which corresponds to an uncertainty of 10% in n_e for a hydrogen plasma under favourable conditions. (For an example of the use of this method, see Eberhagen and Keilhacker (1964).)

Harding and Roberts (1962) discuss the continuum measurements in the infra-red region. Here absorption becomes important and D in equation (16.3) should be replaced by

$$\frac{1 - \exp \{ -\chi_f(\nu) D \}}{\chi_f(\nu) D} \quad (16.4)$$

where $\chi_f(\nu)$ is the free-free absorption coefficient. For low frequencies (including the effects of stimulated emissions) this may be written as (Allen 1963)

$$\chi_f(\nu) = \frac{8}{3} \left(\frac{\pi}{6m^3} \right)^{1/2} \frac{e^6}{c} g_{ff} \left(\sum_{Z=1}^Z n_e n_Z Z^2 \right) \frac{(kT_e)^{-3/2}}{\nu^2}. \quad (16.5)$$

Thus, if $(\chi_f(\nu) D)$ is large, $I_{(\nu)}^{B+R}$ tends to $2\nu^2 kT_e/c^2$, which is the black-body value. Harding and Roberts (1962) point out that by suitable reduction of data in the infra-red region both n_e and T_e can in principle be determined.

However, as pointed out in §12, at low frequencies the spectrum becomes complicated. This is due, firstly, to possible effects of cyclotron radiation and, secondly, to collective effects appreciably modifying the spectrum in the region close to the plasma frequency. The rapid fall-off of emission close to the plasma frequency $\omega_p (= (4\pi n_e e^2/m)^{1/2})$ has been used by Kimmitt and Niblett (1963) to estimate the electron number density.

For completely ionized hydrogen plasmas containing no impurities, $n_e = n_Z$ by quasi-neutrality. Separate measurements of ion densities in controlled thermonuclear research plasmas are only required if impurity ions are present. In a pure hydrogen plasma the absolute intensity of the x-ray continuum ($h\nu > kT_e$) could be used to obtain electron (ion) densities employing temperatures deduced from other measurements. When impurities do not contribute significantly the resulting n_e , within experimental errors, will be the same as that obtained from visible bremsstrahlung measurements. Should the results disagree, the amount of contamination

may be estimated from the discrepancy. A procedure is outlined by Griem (1962 d), but only very crude estimates of the impurity concentration can be made in this way.

The above discussion has been limited to hydrogen and hydrogenic systems; however, in principle the method would apply equally to other species, provided accurate data for the emission coefficient (or trustworthy calculations) were available.

16.2. Absolute line intensities

The total line intensity of radiation emitted per unit solid angle in a transition from level p to level q in a uniform optically thin plasma of depth D is

$$I_t = \frac{h\nu}{4\pi} A(p, q) n_{Z-1}(p) D \quad (16.6)$$

where $n_{Z-1}(p)$ is the population density of the upper state. If the transition probability (or oscillator strength) is known this method enables $n_{Z-1}(p)$ to be determined. In measuring line intensities corrections must be made for the underlying continuum and the effects of overlapping line wings (and the effect of exclusion of part of the line wings if a monochromator is used). The expression above—equation (16.6)—depends on optical thinness and so self-absorption should be guarded against (see § 13). Although at high densities perturbations of the wave functions from those corresponding to an isolated atom are sufficient to cause normally forbidden transitions to become allowed, the effect on $A(p, q)$ of an allowed transition is negligible (Griem 1962 b).

In L.T.E. $n_{Z-1}(p)$ can be related by Maxwell-Boltzmann statistics to the total number density n_{Z-1} , but the final value depends on knowing the electron temperature.

Alternatively, $n_{Z-1}(p)$ at or near L.T.E. may be related to the population density of the ground state of the next ionization stage, as in equation (15.2). Only in the hydrogenic case when $n_e = n_Z = n_Z(1)$ does this reduce to a simpler case, and even then to determine n_e , T_e must be known.

In the coronal case equation (6.1) is applicable, i.e.

$$\frac{n_{Z-1}(p)}{n_{Z-1}} = \frac{n_e K(1, p)}{A(p)}. \quad (16.7)$$

But, owing to the facts that the rate coefficient $K(1, p)$ is generally a steep function of T_e and that often the absolute magnitude of the cross section is poorly known, this will give only a crude estimate of n_{Z-1} .

16.3. Stark broadening

When the Stark effect dominates Doppler and other broadening mechanisms, the profile is determined by the number (and, to a smaller extent, temperature) of perturbers in the region of the emitting atom. For quasi-static broadening the width of the line is proportional to $n_e^{2/3}$ and for impact broadening it is proportional to n_e (except possibly for a slow logarithmic variation). No assumptions are made in the theory concerning the distribution of atoms amongst the various quantum states, so that measurements will be independent of L.T.E.

In the relatively low temperature region, Stark broadening, especially of the hydrogen lines, is particularly large and hence easy to measure. However, as indicated in §11.5, Doppler broadening tends to dominate for multiply ionized species at high temperatures. Also effects of continuum radiation, of overlap with neighbouring lines and of possible self-absorption have to be considered.

It is generally sufficient to measure only half-widths, although the best possible results will be obtained by comparing the experimental profile with that theoretically predicted. Shifts could also give good indication of perturber densities, but, as already indicated in §11.3.4 the theory is particularly unreliable, and it is difficult to measure shifts which are only a few per cent of the linewidth.

The theory for widths of the hydrogenic lines is the most accurate, and best for $H\beta$ where the overall error is about 5%. For hydrogenic systems a relatively large portion of the broadening is due to quasi-static effects (proportional to $n_e^{2/3}$) and it is possible to write

$$n_e = C(n_e, T_e) \Delta\lambda_s^{3/2} \quad (16.8)$$

where $\Delta\lambda_s$ is the measured full half-width and $C(n_e, T_e)$ is weakly dependent on T_e and n_e . The table gives values of $C(n_e, T_e)$ for hydrogenic systems (after Griem 1964); a similar tabulation has been compiled by Hill (1964). The dependence on T_e is, in fact, extremely slight; for $H\beta$, for a given half-width, the values of n_e at 5000 °K and 20 000 °K differ by less than 4% from the value at 10 000 °K. The density may also be determined from the measured ratio of intensity in a small wavelength band at the line centre to the total line intensity (Griem *et al.* 1962 b). This method (with $H\beta$) has also been used by Irons and Millar (1965).

The widths of isolated lines (i.e. not degenerate in orbital quantum number) are only slow functions of electron temperature, and are given by the following formula (equation (11.40), see §11.3.4) for the total half half-width:

$$w_{\text{total}} \simeq \{1 + 1.75\alpha(1 - 0.75R)\} w \quad (16.9)$$

where w , the electron impact half half-width, scales as n_e , and α , the ion-broadening parameter, scales as $n_e^{1/4}$ (and for singly ionized emitters replace $0.75R$ by $1.2R$). This should be accurate to about 20%, provided the spacing of the nearest perturbing level from the upper level of the line is greater than the plasma frequency. For α small (as is often the case), w_{total} is almost exactly proportional to n_e and the line profile has dispersion shape. In the isolated line calculations for both neutral and singly ionized species, Griem (1964) used straight-line classical paths.

Very complete tables of w and α , as well as data concerning profiles for both hydrogenic and isolated lines, are given by Griem (1964).

In the calculations only singly ionized ions were considered, so that if multiple ionization is appreciable a correction to the ion broadening has to be applied. This amounts to approximately $Z^{1/3}$ for species exhibiting the linear Stark effect and approximately $Z^{2/3}$ for quadratic Stark effect, where Z is the average ionic charge. Since Stark broadening usually only dominates at low temperatures and for low ionization stages, this effect can often be neglected. For the neutral helium lines Lincke (1964, Ph.D. Thesis, University of Maryland) has proposed that an empirical correction of 10% be added to the electron density calculated by comparing experimental linewidths with theoretical estimates. Electrons of highly excited atoms,

which are 'almost free', will make some contribution to the broadening but even at very high densities this correction is negligible (Griem 1964, p. 306).

When Doppler broadening becomes important, the experimental half-width will have to be corrected. This is particularly easy for transitions from levels which are predominantly broadened by electron impacts (isolated lines), since their profiles are closely similar to the dispersion type and Voigt profile analysis can be

Coefficients $C(n_e, T_e)$ (in $\text{\AA}^{-3/2} \text{cm}^{-3}$) for electron density determinations from (full) half-widths of Stark broadened hydrogen and hydrogenic lines (after Griem 1964), i.e. $n_e = C(n_e, T_e) \Delta\lambda_s^{3/2}$

	T_e ($^{\circ}\text{K}$)	$n_e(\text{cm}^{-3})$					
		10^{14}	10^{15}	10^{16}	10^{17}	10^{18}	10^{19}
H α	10 000			$6.16 \cdot 10^{15}$	$3.61 \cdot 10^{15}$	$3.23 \cdot 10^{15}$	
	20 000			$7.13 \cdot 10^{15}$	$3.88 \cdot 10^{15}$	$2.79 \cdot 10^{15}$	
	40 000			$4.22 \cdot 10^{15}$	$6.01 \cdot 10^{15}$	$2.67 \cdot 10^{15}$	
H β	5000	$3.84 \cdot 10^{14}$	$3.68 \cdot 10^{14}$	$3.44 \cdot 10^{14}$			
	10 000	$3.80 \cdot 10^{14}$	$3.58 \cdot 10^{14}$	$3.30 \cdot 10^{14}$	$2.98 \cdot 10^{14}$		
	20 000	$3.72 \cdot 10^{14}$	$3.55 \cdot 10^{14}$	$3.21 \cdot 10^{14}$	$3.03 \cdot 10^{14}$		
	40 000	$3.76 \cdot 10^{14}$	$3.52 \cdot 10^{14}$	$3.30 \cdot 10^{14}$	$2.87 \cdot 10^{14}$		
H γ	10 000		$4.41 \cdot 10^{14}$	$2.90 \cdot 10^{14}$	$2.73 \cdot 10^{14}$		
	20 000		$3.68 \cdot 10^{14}$	$3.01 \cdot 10^{14}$	$2.81 \cdot 10^{14}$		
	40 000		$3.77 \cdot 10^{14}$	$3.46 \cdot 10^{14}$	$2.30 \cdot 10^{14}$		
H δ	10 000	$1.36 \cdot 10^{14}$	$1.18 \cdot 10^{14}$	$1.04 \cdot 10^{14}$			
	20 000	$1.35 \cdot 10^{14}$	$1.21 \cdot 10^{14}$	$9.79 \cdot 10^{13}$			
	40 000	$1.07 \cdot 10^{14}$	$1.22 \cdot 10^{14}$	$1.01 \cdot 10^{14}$			
He II 4686 \AA	5000		$1.58 \cdot 10^{16}$				
	10 000		$2.41 \cdot 10^{16}$	$1.09 \cdot 10^{16}$			
	20 000		$2.86 \cdot 10^{16}$	$2.30 \cdot 10^{16}$	$1.24 \cdot 10^{16}$		
	40 000		$4.34 \cdot 10^{16}$	$2.74 \cdot 10^{16}$	$1.37 \cdot 10^{16}$	$9.87 \cdot 10^{15}$	$6.24 \cdot 10^{15}$
	80 000				$1.65 \cdot 10^{16}$	$9.07 \cdot 10^{15}$	$6.74 \cdot 10^{15}$
He II 3203 \AA	10 000		$2.65 \cdot 10^{15}$				
	20 000		$2.56 \cdot 10^{15}$	$2.57 \cdot 10^{15}$	$2.65 \cdot 10^{15}$		
	40 000		$2.14 \cdot 10^{15}$	$2.36 \cdot 10^{15}$	$2.40 \cdot 10^{15}$		
	80 000			$2.34 \cdot 10^{15}$	$1.98 \cdot 10^{15}$	$1.93 \cdot 10^{15}$	
He I 3965 \AA	20 000				$9.99 \cdot 10^{14}$	} for $n_e = 3 \cdot 10^{17} \text{cm}^{-3}$	
He I 4471 \AA	20 000				$4.15 \cdot 10^{14}$		

applied (Allen 1963). For hydrogenic lines more involved folding procedures should be used (see Hansen 1964), but even here estimates using a Voigt analysis give surprisingly good results (Peacock *et al.* 1964). At high temperatures, when Doppler broadening dominates, estimates of n_e can probably be made by fitting the profile in the line wings. Although this is less reliable than the continuum intensity measurements, it may be a useful check when impurities cause ambiguities in the continuum analysis.

For high members of a series the broadening is almost always quasi-static (see § 11.3.4). The electron density may now be estimated, with the use of the Inglis-Teller relationship, from the principal quantum number p_m of the last discernible line. Thus

$$\log n_e = 23.26 - 7.5 \log p_m + 4.5 \log Z \quad (16.10)$$

where n_e is in cm^{-3} and $Z - 1$ is the net charge of the atom. This relationship should lead to the electron density within a factor of about 2 owing mainly to uncertainties in defining the last discernible line. Vidal (1964 and private communication) has improved the situation by considering how the ratio of the maximum intensity of a line to the minimum intensity between that line and the adjacent line varies as the series limit is approached. He considers that the spectrum may be represented by a superposition of quasi-static profiles corresponding to each principal quantum number. If this superposition procedure is accurate, the method should lead to determinations of the electron density to about 5 to 10%. However, there is some doubt as to the validity of this procedure. One would expect that, when considering the merging of broadened lines, perturbation matrix elements between states of different principal quantum numbers and also higher terms in the multipole interaction (due to large spatial extent of the wave functions) should be taken into account. None the less, Vidal obtains good agreement with his experimental results.

17. Magnetic field measurements

Magnetic fields are commonly used to contain controlled thermonuclear research plasmas. The fields may be quite high (several tens of kG) so that it is important to consider the Zeeman effect (see White 1934).

The splitting of energy levels in a magnetic field B is

$$\Delta E = (mg_L) \frac{eh}{4\pi mc} B \quad (17.1)$$

where (mg_L) is the magnetic quantum number times the Landé factor (not to be confused with the electron mass m in the denominator).

The actual broadening of the line profile due to the splitting of these energy levels (normally degenerate in magnetic quantum number) depends of course on the levels involved. But for an order-of-magnitude estimate (with $(mg_L) = 1$) the Zeeman splitting is

$$\Delta\lambda_{Ze} \simeq \frac{\lambda^2 e}{4\pi mc^2} B. \quad (17.2)$$

Along the field lines there are two components, circularly polarized in opposite directions, which lead to a total broadening of about $2\Delta\lambda_{Ze} \simeq (9.3 \times 10^{-11} \lambda^2 B) \text{ \AA}$ (where λ is in \AA and B in gauss). This should be compared with the Doppler (full) half-width

$$\Delta\lambda_D \simeq 7.1 \times 10^{-7} \left(\frac{T_i}{A}\right)^{1/2} \lambda \quad (17.3)$$

where T_i is in $^\circ\text{K}$ and A is the mass number.

At $10^6 \text{ }^\circ\text{K}$ and in a field of 30 kG, Doppler and Zeeman effects for oxygen ($A = 16$) are comparable for $\lambda \simeq 3000 \text{ \AA}$. Owing to the λ^2 variation of (17.2) the Zeeman

effect is not likely to be important in the soft x-ray region; however, in the visible region the above comparison should always be made.

The fact that, along the magnetic field, the two circularly polarized components shift in opposite directions with respect to the unperturbed wavelength has been employed to measure magnetic fields in plasmas. (See Jahoda *et al.* (1963) and Hubner (1964), who extend the technique used by Babcock (1953) for a solar magnetograph.)

As mentioned in §14, the Faraday rotation of light passing through a plasma can also be used to infer the average magnetic field along the line of sight.

18. Radiative energy losses

In a high temperature plasma the effects of radiative energy losses can be extremely important. This problem has been investigated by several authors, their attention being mainly directed to thermonuclear plasmas (Knorr 1958, Kogan 1959, Post 1961, Vasil'ev *et al.* 1962, Kolb 1963, Kolb and McWhirter 1964, Artsimovich 1964, Hinnov 1964, Griem 1964, etc.).

Solutions of the steady-state coronal equations have shown that, although light elements (such as hydrogen) are completely ionized at temperatures greater than a few eV, heavier ions are not fully stripped even at extremely high temperatures (figure 4).

Small impurities of high Z in a hydrogen plasma can greatly increase the radiation losses, even to the extent of rendering thermonuclear plasmas impossible on this ground alone. In this section is indicated the extent to which the losses due to impurities in a hydrogen plasma are important.

The bremsstrahlung power loss is given by equation (12.18), i.e.

$$P^B = 5 \times 10^{-31} n_Z n_e Z^2 T_e^{1/2} \text{ w cm}^{-3} \quad (T_e \text{ in kev}). \quad (18.1)$$

Although this bremsstrahlung power loss varies as Z^2 , it will be shown that line radiation is even more important.

For full thermodynamic equilibrium at a temperature T the radiation losses R_{BB} depend only on the surface area and temperature. Thus, by Stefan's law,

$$R_{BB} \simeq 10^{17} T^4 \text{ w cm}^{-2} \quad (T \text{ in kev}). \quad (18.2)$$

The thermal equilibrium (Planck) value is important, for the radiation losses must lie between a lower bound given by the bremsstrahlung losses (lowest of course for $Z = 1$) summed over the volume of the plasma, and an upper bound given by the Planck value, summed over the surface area of the plasma.

Also, in general, it is not possible for the plasma to radiate at a rate greater than the local spectral intensity of the Planck radiation law, which gives the radiation loss per unit frequency interval:

$$R_{BB}(\nu) = \left(\frac{2\pi h\nu^3}{c^2} \right) \left\{ \exp\left(\frac{h\nu}{kT}\right) - 1 \right\}^{-1} \text{ w cm}^{-2}. \quad (18.3)$$

This immediately indicates that at high temperatures the major radiation loss will be at short wavelengths.

To estimate these radiative losses, the coronal approximation is considered. Radiation occurs when electron collisions produce excitation of bound states of the

ion. Excitation is immediately followed by radiation, since, in the coronal approximation, the lifetime of the excited states is short compared with the time between excitations. The electron thus loses a definite amount of energy for each collision causing excitation, which is immediately lost from the optically thin plasma.

Thus the total power radiated per unit volume for an ion S_Z (number density n_Z) is

$$P_Z^L = \sum_p n_Z n_e K_Z(1, p) (h\nu_{1p}) \quad (18.4)$$

since $K_Z(1, p)$ is the excitation rate coefficient from the ground state to level p and $n_Z(1) \simeq n_Z$. The population densities n_Z have been determined from the steady-state ionization equations (equation (6.2)) for hydrogen-like and lithium-like species. The total power radiated per unit volume by line radiation (i.e. equation (18.4)) is then determined. For hydrogen-like ions the Lyman α ($2 \rightarrow 1$) transition accounts for the bulk of the radiation and, similarly, the $2p-2s$ transition is most important for lithium-like ions. The $2p-2s$ transition leads to particularly intense radiation, since the $2p$ level is rather low lying and easily excited.

The results for these dominant transitions are shown in figure 16 in terms of the power P_H^B radiated by hydrogenic bremsstrahlung ($P_H^B = 5 \times 10^{-31} n_e^2 T_e^{1/2}$, the lowest possible value) on an atom-for-atom basis. Thus to find the actual radiation loss it is necessary to multiply the value given in the curves by the *total* abundance fraction of the element in question (the degree of ionization at any given temperature having already been taken into account in the steady-state ionization equations). Therefore, if the total abundance of, for example, oxygen is 1%, the ratio given in the curves must be multiplied by 0.01. The high temperature limit in figure 16 is the pure bremsstrahlung for completely stripped ions which is Z^2 times the hydrogenic value. Since only the dominant transitions have been considered these results must be considered as an underestimate.

It can be seen that steady-state radiation losses, due to line radiation, can be expected to be large at low temperatures and to fall with increasing temperature. Various approximations for the cross sections may be made, but they all lead to high power losses due to the presence of high Z impurities (see Griem 1964). Methods of extending these results to radiation loss when radiative transfer effects become important have been considered by Cuperman *et al.* (1963).

Recombination radiation also leads to energy loss from the plasma. Recombination to the ground state (the dominant factor) gives (equation (12.15))

$$P_1^R = 1.3 \times 10^{-32} n_Z n_e Z^4 T_e^{-1/2} \text{ w cm}^{-3} \quad (T_e \text{ in kev}). \quad (18.5)$$

This may often increase the loss rate, but in general its contribution is much less than that due to line radiation.

The results that have been indicated so far are for steady-state plasmas; however, most experimental plasmas are transient, and ionization does not reach its steady-state value. To determine the radiation loss from transient plasmas it is necessary to determine the rate of approach of ionization equilibrium and to determine the radiation losses occurring during this time. Generally speaking, during the approach to equilibrium, the line radiation from impurity ions partially stripped of their electrons will be greater than in the steady state. During transient build-up of a plasma many stages of ionization will be passed through as the steady final state is approached.

Between each successive ionization event many collisional excitation events may occur, each of which results in a loss of energy. Thus to ionize a high Z atom up to a highly ionized state will require an inevitable 'fee' in line radiation losses. This 'fee' may be much larger than the sum of the ionization energies.

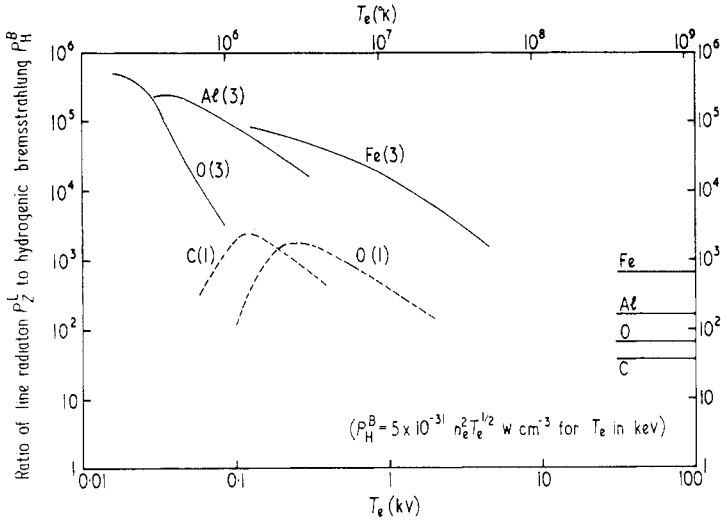


Figure 16. Steady-state radiation loss: the curves show the ratio of the energy lost by line radiation, P_Z^L , to the energy lost by hydrogenic bremsstrahlung, P_H^B , for the Lyman- α and 2S-2P transitions of various one- and three-electron ions respectively. The lines at high temperature represent the bremsstrahlung radiation produced by completely stripped ions. To obtain the actual radiation loss it is necessary to multiply by the total abundance fraction of the element. (After Post 1961.)

The complete solution of this problem requires the solution of the time-dependent rate equations describing the ionization. This has been done numerically by McWhirter and Hearn (1963) for hydrogen-like ions, and even in this case the energy lost by the electrons per ionization can be many times the ionization energy (see figure 17).

A particularly simple approach is that of Post (1961). In the initial stages of ionization recombination is unimportant and the rate equations take on the following simple form (in the coronal approximation):

$$\frac{dn_Z}{dt} = n_{Z-1} n_e K_{Z-1}(1, c') - n_Z n_e K_Z(1, c') \quad \text{for } Z \gg 1 \tag{18.6}$$

and

$$\frac{dn_0}{dt} = -n_0 n_e K_0(1, c') \quad \text{for } Z = 0. \tag{18.7}$$

From these equations (18.6) and (18.7) a characteristic time τ_Z for ionization of S_Z (to S_{Z+1}) is given by

$$\tau_Z \approx \frac{1}{n_e K_Z(1, c')}. \tag{18.8}$$

But $K_{Z-1}(1, c')$ varies roughly as

$$[T_e^{1/2}\{E_{Z-1}(\infty)\}^{-2} \exp\{-E_{Z-1}(\infty)/kT_e\}]$$

for $E_{Z-1}(\infty) > kT_e$ (Allen 1963). Thus, since the ionization energy $E_{Z-1}(\infty)$ increases approximately as Z^2 , the characteristic time τ_Z to ionize a highly charged species obviously becomes long compared with the time $\tau_{Z=0}$ to ionize the neutral species.

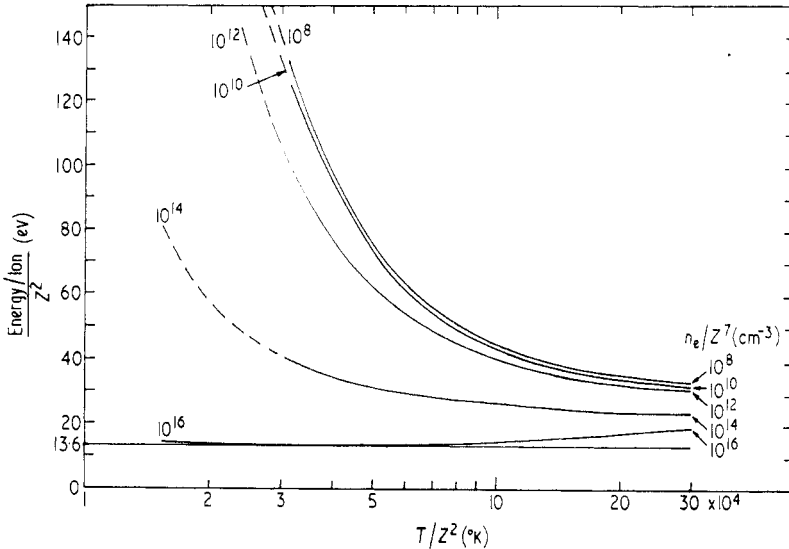


Figure 17. Optically thin hydrogenic ion plasma: energy absorbed from the free electrons per ionization. (After McWhirter and Hearn 1963.)

The above set of equations is similar to those describing radioactive decay and can easily be solved when the $K_Z(1, c')$ coefficients (for all Z) are constant. The result then corresponds to the ionization of a group of test particles of a high Z impurity immersed in a plasma of constant electron temperature (since the $K_Z(1, c')$ are a function of T_e).

Post (1961) gives a specific example of the transient ionization of oxygen immersed in a plasma. He shows that the time to ionize to highly ionized states may be easily up to 1000 times as large as that for the first ionization of the neutral atom (e.g. the time to ionize O VI in a 50 eV plasma ($190 \mu\text{sec}$ for $n_e = 10^{14} \text{ cm}^{-3}$) is 500 times that for the neutral atom).

Now the total energy released as line radiation during transient ionization will be the integral of P_Z^L over time, summed over all stages of ionization and excitation. However, to find the total 'fee' for ionization, the additional losses occurring when recombination becomes important are separated out. Thus the integral of P_Z^L is carried out for all time, but only up to the final ionization stages reached (i.e. only for those Z (Z' say) for which the steady-state number densities ($t = \infty$) are negligible). The solution of the ionization equations (6.2) show that, in a steady state, all stages of ionization, except those adjacent to the dominant ionization

state, have negligible populations. Thus, the fee for ionization Q^L is

$$\begin{aligned} Q^L &= \sum_{Z=0}^{Z'} \int_0^\infty P_Z^L dt \\ &= \sum_{Z=0}^{Z'} \int_0^\infty \sum_p n_Z n_e (h\nu_{1p})_Z K_Z(1, p) dt. \end{aligned} \quad (18.9)$$

For ions immersed in a plasma of constant T_e the $K_Z(1, p)$ are also constant. Now, equation (18.6) may be integrated directly for all $Z \leq Z'$, since $n_Z(t = \infty) = 0$ and $n_Z(t = 0) = 0$ ($Z \neq 0$), i.e.

$$\int_0^\infty n_Z n_e K_Z(1, c') dt = \int_0^\infty n_{Z-1} n_e K_{Z-1}(1, c') dt \quad \text{for } Z \gg 1$$

and

$$\int_0^\infty n_0 n_e K_0(1, c') dt = n_0(0) \quad (18.10)$$

where $n_0(0)$ is the initial number density of atoms in the neutral state. Thus (18.9) becomes, for constant T_e ,

$$\begin{aligned} Q^L &= \sum_{Z=0}^{Z'} \sum_p K_Z(1, p) \frac{n_0(0)}{K_Z(1, c')} (h\nu_{1p})_Z \\ &= \sum_{Z=0}^{Z'} \frac{1}{n_e K_Z(1, c')} \sum_p n_0(0) n_e K_Z(1, p) (h\nu_{1p})_Z \\ &= \sum_{Z=0}^{Z'} \tau_Z P_Z^L(n_0(0)) \end{aligned} \quad (18.11)$$

where $P_Z^L(n_0(0))$ represents the power radiated in line radiation for the entire population of impurity ions in the state of charge Z .

Equation (18.11) shows that, during transient ionization, each successive stage of ionization radiates as if it possessed the entire population of impurity ions for one time constant τ_Z , after which the population jumps discontinuously to the next higher state of ionization, and so on.

It is clear that the most important contributions come from the higher ionization stages since they exist longer. For example, for oxygen in a 50 eV plasma the 'fee' for ionization through the O VI ionization stage is about 8 keV per atom, compared with the sum of the ionization energies of about 0.43 keV (Post 1961). At higher temperatures and for higher Z impurities the fee would be even larger. This type of analysis gives a simple way of estimating transient energy losses and demonstrates their importance.

When a magnetic field is present, as it is in all thermonuclear devices, cyclotron radiation has to be considered. Since this occurs at relatively low frequencies, self-absorption is important. (For a treatment of this problem, see Trubnikov (1958), Drummond and Rosenbluth (1961, 1963), Rose and Clark (1961) and Trubnikov (1961).)

It is found that many thermonuclear discharges are radiation-cooled owing to line radiation from high Z impurities (e.g. Hinnov 1964). The importance of purity in such devices has been stressed by various authors. In particular, the work

of Kolb and McWhirter (1964), in which they couple the rate equations for populations of the quantum states with the magnetohydrodynamic equations, shows that impurities of only a few per cent (C, N, O and Ne were considered) can have a drastic effect on the electron temperature.

Thus for thermonuclear machines the purity of the discharge is as much of a problem as stability. Each high Z atom which comes off the wall into the discharge collects its 'fee' in energy loss.

19. Conclusions

Some of the more recent progress in plasma spectroscopy has been reviewed in this article.

It has been seen that the radiation from the plasma is characterized not only by the properties of the isolated radiating species, but also by the properties of the plasma in the immediate environment of the radiator. This dependence on the plasma properties is a consequence of the fact that ions and electrons interact with themselves and other species via the long-range Coulomb potential.

Electrons completely dominate collisional excitation and de-excitation processes in plasmas which are more than a few per cent ionized, and the solution of the rate equations describing the detailed population and de-population processes of quantum states in a plasma (in the collisional-radiative decay model) has led to a more complete understanding of both L.T.E. and non-L.T.E. situations. Even in L.T.E. (when the plasma is collision-dominated) there have been improvements in the theory concerning the lowering of the ionization potential and in the treatment of internal partition functions (which diverge for an isolated atom).

Great improvements, too, have been made in the understanding of the details of the radiation. In particular, line broadening theory, especially that part concerned with impact broadening by electrons, now enables fairly accurate calculations to be made of the profiles of Stark broadened lines. Detailed and fairly accurate calculations of oscillator strengths and ionization cross sections (and ultimately recombination radiation) have been made for many species using, for instance, Hartree-Fock wave functions or the Coulombic approximation of the quantum defect and Bates-Damgaard procedures. Calculations of radiative transfer in non-L.T.E. situations have also been performed.

However, there is still plenty of scope for yet further advance, both experimentally and theoretically. Experimentally, highly ionized species are important, yet there is a lack of a really satisfactory light source, whose properties are accurately known, to measure their properties.

Most of the quantitative theory is only available for hydrogen and hydrogenic species, since only for these are the wave functions really accurately known, and so there is a need for detailed measurements to be made on other species.

Apart from improvement to calculations of matrix elements and wave functions of non-hydrogenic species (and hence further improvement in oscillator strengths, ionization cross sections, etc.) there are many situations which need further investigation (both for hydrogenic and non-hydrogenic species). Many of these topics have been discussed in the text, but, for convenience, some of them will be mentioned again here.

Although advances have been made in the theory of partition functions and of the lowering of the ionization potential, further understanding will probably come through a physical model describing the time dependence of the fluctuating micro-field (§5). Convincing experimental evidence for the lowering of the ionization potential is also needed.

The influence in the collisional-radiative decay model for non-hydrogenic species of metastable levels and dielectronic recombination (§8) will have to be examined, and at the same time it is hoped that more required cross sections and rate coefficients will be forthcoming.

There are many problems still outstanding in the details of Stark line broadening theory, for although linewidths are fairly accurate, the situation with line shifts and the detailed shape of line wings is not so good (§11.3.4), especially for ionic lines and non-hydrogenic species. The importance of the quadrupole interaction and higher order terms in the perturbation expansions is still unclear, both in the impact and quasi-static approximations (§§11.3.1 and 11.3.4), as is the existence of a plasma polarization shift (§11.4). The present treatment of 'strong collisions' (§11.3.3) yields fairly accurate linewidths, but, for isolated lines, the error in the shift may become very large. No really satisfactory broadening theory exists either in the regions of merging of lines (the Inglis-Teller limit—§§11.3.4 and 16.3) or in the regions where the main approximations (classical path, impact and quasi-static) break down.

The overall effect of autoionization on the continuum emission of non-hydrogenic species is not completely understood, and still further improvements should be possible in the region of the spectrum close to the plasma frequency, where collective effects become important.

Although there has been a substantial change in our knowledge of plasma spectroscopy in the last few years (for instance, since the review by Lochte-Holtgreven 1958), there still remain several areas in which detailed theoretical treatment and accurate experimentation are required.

Acknowledgments

The help of Dr. D. D. Burgess and Dr. A. Folkierski at all stages of the preparation of this article is gratefully acknowledged. This research was supported in part by the Advanced Research Projects Agency (Project DEFENDER) and was monitored by the U.S. Army Office, Durham, under Contract DA-31-124-ARO-D-139.

Nomenclature

Some modifications of standard nomenclature have had to be made to prevent disparity of meaning of symbols in different parts of the text. It is hoped that this does not lead to confusion.

	A	Mass number
	$A(p, q)$ and $A(2, 1)$	Spontaneous transition probability from level p to level q
	$A(p) \left(= \sum_{q \succ p} A(p, q) \right)$	Total spontaneous transition probability from level p

$A(d'', p)$	Spontaneous transition probability from doubly excited level d'' to level p
$A_a(d'')$	Autoionization transition probability of doubly excited level d''
$A(t)$	Amplitude of classical oscillator
B	Magnetic field
$B(p, q)$ and $B(2, 1)$	Induced-emission probability coefficient
$B(q, p)$ and $B(1, 2)$	Absorption probability coefficient
$B_Z(T_e)$	Excitational part of partition function of S_Z at T_e
$B_\nu(T_e)$	Planck (black-body) function at T_e
c	Velocity of light (3×10^{10} cm sec ⁻¹)
c'	Denotes state of the continuum
C^μ	Stark coefficient
C_2	Stark coefficient for linear Stark effect
C_4	Stark coefficient for quadratic Stark effect
$C(n_e, T_e)$	Coefficients for electron density determination from Stark linewidths
d	Shift of energy level from unperturbed value (occasionally refers to a d electron)
\mathbf{d}	Dipole moment of a radiating species
d''	Denotes doubly excited state
D	Depth of plasma along line of sight
e	Electron charge (4.8×10^{-10} e.s.u.)
\mathbf{E} and E	Electric field
E_0	Mean electric field at a radiating species ($= e/\rho_m^2$).
$E_Z(p)$ and $E(p)$	Energy of level p of S_Z
$E_Z(\infty)$	Ionization energy of S_Z
$E_{a''}$	Energy of doubly excited state d'' of S_{Z-1} , above the first ionization potential of S_{Z-1}
$E_H (= 2\pi^2 e^4 m/h^2)$	Ionization energy of hydrogen
f_{qp} or f_{12}	Absorption oscillator strength from lower level q to upper level p
$f(t)$	Dipole moment of classical oscillator
$f^*(t)$	Complex conjugate of $f(t)$
$f(v)$	Electron velocity distribution
F	Helmholtz free energy
F_0	Helmholtz free energy of plasma, for no interaction between the plasma particles
F_c	Helmholtz free energy representing Coulomb interactions between the plasma particles
$F(\omega)$	Fourier component of $f(t)$
$g_{Z-1}(p)$ and $g(p)$	Statistical weight of level p of S_{Z-1}
$g(d'')$	Statistical weight of doubly excited level d'' of S_{Z-1}
g_{bb}	Bound-bound Gaunt factor
g_{fb}	Free-bound Gaunt factor
g_{ff}	Free-free Gaunt factor
g_L	Landé factor

$G_{vi}(r)$	Normalized continuum radial wave functions multiplied by r
h	Planck constant (6.63×10^{-27} erg sec)
\hbar	$= h/2\pi$
$I(\omega)$ and $I(\nu, x)$	Intensity of radiation at frequency ν or ω
$I^{B+R}(\Delta\lambda)$	Intensity of bremsstrahlung and recombination radiation in wavelength interval $\Delta\lambda$
I_t	Total line intensity
$I(p) = E_{Z-1}(\infty) - E_{Z-1}(p)$	Ionization energy of level p
j	$= \sqrt{-1}$
$j_R(x, \alpha); j(x, \alpha)$ and $j(x, \alpha, \sigma)$	Reduced Stark profiles for isolated lines
j_ν	Normalized profile for spontaneous emission
J	Total angular momentum quantum number
$J(\nu, x) (= \varepsilon(\nu))$	Emission coefficient
k	Boltzmann constant (1.38×10^{-16} erg deg K^{-1})
$K_{Z-1}(p, c')$ or $K(p, c')$	Rate coefficient for collisional ionization from level p of S_{Z-1} to all possible levels c' of the continuum
$K(c', p)$	Rate coefficient for three-body recombination from the continuum to level p
$K(p, q)$	Rate coefficient for collisional de-excitation from upper level p to lower level q
$K(q, p)$	Rate coefficient for collisional excitation from lower level q to upper level p
$K(p) = K(p, c') + \sum_{q \neq p} K(p, q)$	Rate coefficient for collisional processes from level p to all other levels
l	Orbital angular momentum quantum number
$l_>$	The larger of l' and l''
L	Total orbital angular momentum quantum number
L_1	Total orbital angular momentum quantum number for parent configuration of excited state of S_{Z-1}
m	Mass of electron (9.1×10^{-28} g)
(mg_L)	Magnetic quantum number times Landé factor
M	Mass of atom or ion
n_e	Electron number density
n_Z	Number density of ions of charge Z (i.e. of S_Z)
n_{e0} and n_{i0}	Equilibrium number density of electrons and ions respectively
$n_Z(p)$ and $n(p)$	Number density of level p of S_Z
$n_E(p)$	Number density of level p in Saha equilibrium
n	Number density of perturbers (ions or electrons)
$n_0(0)$	Initial number density of neutral atoms
N_e	Total number of electrons
N_Z	Total number of ions of charge Z (i.e. of S_Z)
p and p'	Denotes a singly excited quantum state (level) of principal quantum number p (or p') (occasionally refers to a p electron)
p_t	Principal quantum number of the 'thermal limit'

p_u and p_l	Principal quantum number of upper and lower level respectively
p_{\max}	Principal quantum number of reduced ionization limit
p_m	Principal quantum number at which merging of levels occurs (Ingliš-Teller limit)
P	Pressure
P_Z^L	Total power radiated per unit volume in line radiation from S_Z
$P_q^R(\nu)$	Power radiated per unit volume and frequency interval by recombination to level q
$P^R(\nu)$	Total power radiated per unit volume and frequency interval by recombination
P_1^R	Total power radiated per unit volume by recombination to the ground state
$P^{B+R}(\nu)$	Total power radiated per unit volume and frequency interval by bremsstrahlung and recombination radiation
$P^B(\nu)$	Total power radiated per unit volume per unit frequency interval by bremsstrahlung only
P_B	Total power radiated per unit volume by bremsstrahlung only
P_H^B	Total power radiated per unit volume by hydrogenic bremsstrahlung
$P(r)$	Probability of finding the nearest ion at distance r from a radiating species
$P(E)$	Probability of a radiating species being subjected to a field E
q	Denotes a singly excited quantum state (level) of principal quantum number q
Q	Total partition function of complete system of particles
Q_e	Total partition function for electrons only
Q_Z	Total partition function of S_Z
Q^L	'Fee' for ionization due to line radiation
r	Radius
$\langle r \rangle$	Radial matrix element (expectation value of radius)
$R = \rho_m / \rho_D$	Debye shielding parameter
$R_{pl}(r)$	Normalized radial wave function multiplied by r
$R_{BB}(\nu)$	Power radiated by a black body per unit area and per unit frequency interval
R_{BB}	Total power radiated per unit area by a black body
s	Time, used in autocorrelation function (occasionally refers to s electron)
S	Total spin quantum number
S_1	Total spin quantum number for parent configuration of an excited state of S_{Z-1}

	S	S matrix (scattering matrix)
	S_Z	Denotes a species (ion or atom) of charge Z
	$S_Z(p)$	Denotes the singly excited level of principal quantum number p of S_Z
	S_Z^{**}	Denotes doubly excited state of S_Z
	S^{CR}	Collisional-radiative ionization coefficient
	S_t	Collisional excitation rate from the ground state to levels p_t above the thermal limit
$S_\nu(x) = J(\nu, x)/\chi(\nu, x)$		Source function
	t	Time
	t_{ee}	Electron-electron relaxation time
	T	Temperature (1 eV = 11 600 °K)
	T_e	Electron temperature
	T_i	Ion temperature
	u_q	$= Z^2 E_H/q^2 kT_e$
$U(U_e \text{ and } U_Z)$		Individual partition function (for an electron or ion respectively)
	v	Velocity of free electron
	\bar{v}	Mean velocity of a perturber ($= (\pi kT/2m)^{1/2}$)
	V	Volume
	$V(r)$	Potential as a function of r
	$V(t)$	Interaction potential as a function of t
	$\tilde{V}(t)$	Time-dependent perturbation
	w	Half half-width (in frequency units) due to electron impacts
	w_D	Half half-width in frequency units due to Doppler broadening
	w_N	Half half-width in frequency units due to natural broadening
	w_S	Half half-width in frequency units due to Stark broadening
	$W_H(\beta)$	Holtmark ion field strength distribution function
	x	Coordinate or reduced frequency ($= (\omega - \omega_0 - d)/w$)
	\mathbf{x}	Atomic coordinate, such that $\langle p e\mathbf{x} q \rangle$ is the dipole matrix element between states $ p\rangle$ and $ q\rangle$
	X	$= n_e/n_Z$
	Z	Charge of an ion ($Z = 0$ for neutral atom)
	\bar{Z}	Average charge of ions in the plasma
$\alpha = (2\pi C_4/w\rho_m^4)^{3/4}$		Quasi-static ion broadening parameter
	α^{CR}	Collisional-radiative recombination coefficient
	α^D	Dielectronic recombination coefficient
	α_t	Radiative decay rate coefficient from levels p_t above the thermal limit
	β	$= E/E_0$
	β^2	$= 2kT_i\omega_0^2/Mc^2$
	$\beta(p)$	Radiative recombination rate coefficient from the continuum to level p

ΔE	Change in energy
$\Delta_Z E(\infty)$	Lowering of the ionization potential in species S_Z
Δs	Interval of time considered in impact approximation
$\Delta \lambda$	Change in wavelength or wavelength interval
$\Delta \lambda_D$	Doppler (full) half-width (\AA)
$\Delta \lambda_S$	Stark (full) half-width (\AA)
$\Delta \lambda_{Ze}$	Zeeman splitting of level (\AA)
$\Delta \nu$ and $\Delta \omega$	Change in frequency
$\epsilon(\omega)$ and $\epsilon(\nu) (= J(\nu, x))$	Emission coefficient—power radiated per unit volume and frequency interval
$\epsilon(r)$	Emission coefficient as a function of r
ϵ_t	Total power radiated per unit volume for a particular transition
$\eta(t)$	Sum of phase shifts of classical oscillator in time t
η' and $\eta'(\rho)$	Additional phase shift in time interval Δs
η_0	Phase shift for which collisions are effective in the Weisskopf picture ($\eta_0 \simeq 1$)
λ	Wavelength
$\Lambda (= (3/2e^3)(k^3 T_e^3/\pi n_e)^{1/2})$	$\ln \Lambda$ is a slowly varying function of n_e and T_e of the order of 10
μ	Coefficient describing Stark broadening: $\mu = 2$ for linear Stark effect, and $\mu = 4$ for quadratic Stark effect
ν	Frequency
ν_{pq}	Frequency of line radiation between levels p and q
ν_{vp}	Frequency of recombination from continuum (electron of velocity v) to level p
ρ	Impact parameter
ρ_{\max} and ρ_{\min}	Maximum and minimum impact parameters respectively
$\rho_m (= (4\pi n/3)^{-1/3})$	Average distance between perturbers
$\rho(r)$	Change density as function of r
$\rho(p) (= n_{Z-1}(p)/n_E(p))$	Ratio of number density of level p to its thermal equilibrium value
ρ_D	Debye length $\left(= kT_e / \left\{ 4\pi e^2 \left(n_e + \sum_{Z=1}^Z Z^2 n_Z \right) \right\} \right)^{1/2}$
$\rho_L (\simeq \bar{v}/\Delta \omega)$	Impact parameter for Lewis cut-off
ρ_W	Weisskopf radius
$\sigma (= w/\rho_m \bar{v})$	Parameter in time-dependent ion broadening
σ^2	Square of radial matrix element
σ_i and σ_r	Optical cross sections
$\sigma_{qp}(\nu)$	Absorption cross section for transition from lower level q to upper level p
$\sigma_{qv}(\nu)$	Photoionization cross section from level q to the continuum
σ_{vq}	Recombination cross section for an electron with velocity v to level q

$\tau_c (= \rho/\bar{v})$	Duration of a collision
$\tau_Z (= 1/n_e K_Z(1, c'))$	Characteristic time for ionization of S_Z
τ_v	Optical depth
τ_0	Optical depth at line maximum
T_Z	Translational part of individual partition function of S_Z
$\phi(\lambda), \phi(\nu)$ and $\phi(\omega)$	Normalized line profiles ($\int \phi(\nu) d\nu = \int \phi(\omega) d\omega = 1$)
ϕ_ν	Normalized profile for absorption
ϕ_ν'	Normalized profile for induced emission
ϕ_0	Value of $\phi(\nu)$ at line maximum
$\phi(s) = \Phi(s) \exp(-j\omega_0 s)$	
$\Phi(s)$	Autocorrelation function
$\chi(\nu, x)$	Absorption coefficient
$\chi_f(\nu)$	Mean free-free absorption coefficient
ω	Angular frequency
ω_0	Unperturbed angular frequency
$\omega_p (= (4\pi n_e e^2/m)^{1/2})$	Plasma frequency
$\langle \rangle_{av}$	Denotes time average

References

- ALEXANDER, E., FELDMAN, U., and FRAENKEL, B. S., 1965, *Phys. Letters*, **14**, 40.
 ALLEN, C. W., 1963, *Astrophysical Quantities*, 2nd edn (London: University of London).
 ALPHER, R. A., and WHITE, D. R., 1959, *Phys. Fluids*, **2**, 162.
 AMBARTSUMYAN, V. A., 1958, *Theoretical Astrophysics* (Oxford: Pergamon Press).
 ANDERSON, A. D., and GRIEM, H. R., 1963, *Proc. 6th Conf. Ionisation Phenomena in Gases*, Paris, Vol. 3, Ed. P. Hubert (Orsay: Faculté des Sciences), p. 293.
 ANDERSON, P. W., 1949, *Phys. Rev.*, **76**, 647.
 ——— 1952, *Phys. Rev.*, **86**, 809.
 ANDERSON, P. W., and TALMAN, J. D., 1955, *Proc. Conf. on the Broadening of Spectral Lines*, Univ. of Pittsburgh, Pa., Bell Lab. Monograph No. 3117 (New York: Bell Telephone Laboratories).
 ARMSTRONG, B. H., 1964 a, *J. Quant. Spectrosc. Radiative Transfer*, **4**, 491.
 ——— 1964 b, *J. Quant. Spectrosc. Radiative Transfer*, **4**, 207.
 ARTSIMOVICH, L. A., 1964, *Controlled Thermonuclear Reactions* (Edinburgh: Oliver and Boyd), pp. 52–56.
 ASCOLI-BARTOLI, U., KATZENSTEIN, J., and LOVISETTO, L., 1964, *Nature, Lond.*, **204**, 672.
 ASHBY, D. E. T. F., and JEPHCOTT, D. F., 1963, *Appl. Phys. Letters*, **3**, 13.
 ATHAY, R. G., and THOMAS, R. N., 1961, *Physics of the Solar Chromosphere* (New York: Interscience).
 BABCOCK, H. W., 1953, *Astrophys. J.*, **118**, 387.
 BARANGER, M., 1958 a, *Phys. Rev.*, **111**, 494.
 ——— 1958 b, *Phys. Rev.*, **112**, 855.
 ——— 1962, *Atomic and Molecular Processes*, Ed. D. R. Bates (New York: Academic Press), chap. 13.
 BATES, D. R., 1946, *Mon. Not. R. Astr. Soc.*, **106**, 432.
 ——— 1962, *Planet Space Sci.*, **9**, 77.
 BATES, D. R., and DALGARNO, A., 1962, *Atomic and Molecular Processes*, Ed. D. R. Bates (New York: Academic Press), chap. 7.
 BATES, D. R., and DAMGAARD, A., 1949, *Phil. Trans. R. Soc. A*, **242**, 101.
 BATES, D. R., and KINGSTON, A. E., 1961, *Nature, Lond.*, **189**, 652.
 ——— 1963, *Planet. Space Sci.*, **11**, 1.
 ——— 1964 a, *Proc. Roy. Soc. A*, **279**, 10.
 ——— 1964 b, *Proc. Roy. Soc. A*, **279**, 32.

- BATES, D. R., KINGSTON, A. E., and McWHIRTER, R. W. P., 1962 a, *Proc. Roy. Soc. A*, **267**, 297.
 — 1962 b, *Proc. Roy. Soc. A*, **270**, 155.
- BEARDEN, A. J., RIBE, F. L., SAWYER, G. A., and STRATTON, T. F., 1961, *Phys. Rev. Letters*, **6**, 257.
- BECKER, L., and DRAWIN, H. W., 1964, *Z. Instrumentenkde*, **72**, 251.
- BELY, O., 1962, *C.R. Acad. Sci., Paris*, **254**, 3075.
 — 1963, *Ann. Phys., Paris*, **8**, 303.
- BERG, H. F., ALI, A. W., LINCKE, R., and GRIEM, H. R., 1962, *Phys. Rev.*, **125**, 199.
- BERG, H. F., ECKERLE, K. L., BURRIS, R. W., and WIESE, W. L., 1964, *Astrophys. J.*, **139**, 751.
- BETHE, H. A., and SALPETER, E. E., 1957, *Quantum Mechanics of One and Two Electron Atoms* (New York: Academic Press).
- BIBERMAN, L. M., NORMAN, G. E., and ULYANOV, K. N., 1961, *Optika Spectrosk.*, **10**, 297.
- BIRMINGHAM, T., DAWSON, J., and OBERMAN, C., 1965, *Phys. Fluids*, **8**, 297.
- BOCHASTEN, K., 1961, *J. Opt. Soc. Amer.*, **51**, 943.
- BOCHASTEN, K., HALLIN, R., and HUGHES, T. P., 1963, *Proc. Phys. Soc.*, **81**, 522.
- BOGEN, P., HINTZ, E., and SCHLÜTER, J., 1964, *Phys. Fluids*, **7**, 616.
- BOLDT, G., and COOPER, W. S., 1964, *Z. Naturf.*, **19a**, 968.
- BRÉCHOT, S., and VAN REGEMORTER, H., 1964 a, *Annl. Astrophys.*, **27**, 432.
 — 1964 b, *Annl. Astrophys.*, **27**, 739.
- BRIDGES, W. B., and CHESTER, A. N., 1965, *Appl. Optics*, **4**, 573.
- BURGESS, A., 1964, *Astrophys. J.*, **139**, 776.
 — 1965, *Astrophys. J.*, **141**, 1588.
- BURGESS, A., and SEATON, M. J., 1960, *Mon. Not. R. Astr. Soc.*, **120**, 121.
 — 1964, *Mon. Not. R. Astr. Soc.*, **127**, 355.
- BURGESS, D. D., 1964, *Phys. Letters*, **10**, 286.
- BURGESS, D. D., and COOPER, J., 1965 a, *Proc. Phys. Soc.*, **86**, 1333.
 — 1965 b, *J. Sci. Instrum.*, **42**, 829.
 — 1965 c, *Proc. Phys. Soc.*, **85**, 1261.
- BURTON, W. M., and WILSON, R., 1961, *Proc. Phys. Soc.*, **78**, 1416.
- BYRON, S., STABLER, R. C., and BORTZ, P. I., 1962, *Phys. Rev. Letters*, **8**, 376.
- CHANDRASEKHAR, S., 1950, *Radiative Transfer* (New York: Dover).
- CONDON, E. U., and SHORTLEY, G. H., 1935, *Theory of Atomic Spectra* (London: Cambridge University Press).
- COOPER, J., and GREIG, J. R., 1963, *J. Sci. Instrum.*, **40**, 433.
- COOPER, J. W., 1962, *Phys. Rev.*, **128**, 681.
- COOPER, W. S. III, and KUNKEL, W. B., 1965, *Phys. Fluids*, **8**, 482.
- COWAN, R. D., and DIEKE, G. H., 1948, *Rev. Mod. Phys.*, **20**, 418.
- CUPERMAN, S., ENGELMANN, F., and OXENIUS, J., 1963, *Phys. Fluids*, **6**, 108.
 — 1964, *Phys. Fluids*, **7**, 428.
- D'ANGELO, N., 1961, *Phys. Rev.*, **121**, 505.
- DAVIES, W. E. R., and RAMSDEN, S. A., 1964, *Phys. Letters*, **8**, 179.
- DAVIS, J. T., and VAUGHAN, J. M., 1963, *Astrophys. J.*, **137**, 1302.
- DAWSON, J., and OBERMAN, C., 1962, *Phys. Fluids*, **5**, 517.
 — 1963, *Phys. Fluids*, **6**, 394.
- DAY, R. A., and GRIEM, H. R., 1965, *Phys. Rev.*, **140**, A1129.
- DE SILVA, A. W., EVANS, D. E., and FORREST, M. J., 1964, *Nature, Lond.*, **203**, 1321.
- DEWITT, H., and NAKAYAMA, T., 1964, *J. Quant. Spectrosc. Radiative Transfer*, **4**, 623.
- DIRAC, P. A. M., 1958, *Quantum Mechanics* (London: Oxford University Press).
- DITCHBURN, R. W., and ÖPIK, U., 1962, *Atomic and Molecular Processes*, Ed. D. R. Bates (New York: Academic Press), chap. 3.
- DOUGAL, A. A., CRAIG, J. P., and GRIBBLE, R. F., 1964, *Phys. Rev. Letters*, **13**, 156.
- DRAWIN, H. W., 1964 a, *Ann. Phys., Lpz.*, **14**, 262.
 — 1964 b, *Z. Naturf.*, **19a**, 1452.
 — 1965, *Z. Phys.*, **186**, 99.
- DRAWIN, H. W., and FELENBOK, P., 1965, *Data for Plasmas in Local Thermodynamic Equilibrium* (Paris: Gauthier-Villars).

- DRAWIN, H. W., FUMELLI, M., and WESTE, G., 1965, *Z. Naturf.*, **20a**, 184.
- DRELLISHAK, K. S., KNOPP, C. F., and CAMEL, A. B., 1963, *Phys. Fluids*, **6**, 1280.
- DRUMMOND, W. E., and ROSENBLUTH, M. N., 1961, *Phys. Fluids*, **4**, 277.
- 1963, *Phys. Fluids*, **6**, 276.
- DUCLOS, B. P., and CAMEL, A. B., 1961, *Z. Naturf.*, **16a**, 711.
- EBERHAGEN, A., and KEILHACKER, M., 1964, *Proc. 6th Conf. Ionisation Phenomena in Gases, Paris*, Vol. 2, Ed. P. Hubert (Orsay: Faculté des Sciences), p. 577.
- ECKER, G., and KROLL, W., 1963, *Phys. Fluids*, **6**, 62.
- 1965, *Phys. Fluids*, **8**, 354.
- ECKER, G., and WEIZEL, W., 1956, *Ann. Phys., Lpz.*, **17**, 126.
- ECKERLE, K. L., and McWHIRTER, R. W. P., 1966, *Phys. Fluids*, in the press.
- EDLÉN, B., 1964, *Handb. d. Phys.*, **27** (Berlin: Springer-Verlag).
- EDMONDS, A. R., 1957, *Angular Momentum in Quantum Mechanics* (Princeton: Princeton University Press).
- ELDER, P., JERRICK, T., and BIRKELAND, J. W., 1965, *Appl. Optics.*, **4**, 589.
- ELTON, R. C., and GRIEM, H. R., 1964, *Phys. Rev.*, **135**, 1550.
- ELTON, R. C., *et al.*, 1964, *Astrophys. J.*, **140**, 389.
- ELWERT, G., 1948, *Z. Naturf.*, **3a**, 477.
- 1952, *Z. Naturf.*, **7a**, 432.
- FALCONER, I. S., BENESCH, R., and RAMSDEN, S. A., 1965, *Phys. Letters*, **14**, 38.
- FANO, U., 1961, *Phys. Rev.*, **124**, 1866.
- FANO, U., and COOPER, J. W., 1965, *Phys. Rev.*, **137**, A1364.
- FAWCETT, B. C., and GABRIEL, A. H., 1965, *Astrophys. J.*, **141**, 343.
- FAWCETT, B. C., *et al.*, 1963, *Nature, Lond.*, **200**, 1303.
- FAWCETT, B. C., GABRIEL, A. H., JONES, B. B., and PEACOCK, N. J., 1964, *Proc. Phys. Soc.*, **84**, 257.
- FAWCETT, B. C., JONES, B. B., and WILSON, R., 1961, *Proc. Phys. Soc.*, **78**, 1223.
- FERGUSON, E., and SCHLÜTER, H., 1963, *Ann. Phys., N.Y.*, **22**, 351.
- FINKELNBURG, W., and MAECKER, H., 1956, *Handb. d. Phys.*, **22**, 254 (Berlin: Springer-Verlag).
- FINKELNBURG, W., and PETERS, TH., 1957, *Handb. d. Phys.*, **28**, 79 (Berlin: Springer-Verlag).
- FIOTTO, G., and THOMPSON, E., 1963, *Phys. Rev. Letters*, **10**, 89.
- FOLEY, H. M., 1946, *Phys. Rev.*, **69**, 616.
- FOSTER, E. W., 1964, *Rep. Progr. Phys.*, **27**, 469 (London: Institute of Physics and Physical Society).
- FOWLER, R., and GUGGENHEIM, E. A., 1952, *Statistical Thermodynamics* (London: Cambridge University Press).
- FOWLER, R. G., 1962, *Electrically Energised Shock Tubes* (Norman, Oklahoma: University of Oklahoma Research Institute).
- FREEMAN, J. J., 1958, *Principles of Noise* (New York: John Wiley).
- FÜNFER, E., KRÖNAST, B., and KUNZE, H. J., 1963, *Phys. Letters*, **5**, 125.
- GABRIEL, A. H., FAWCETT, B. C., and JORDAN, C., 1965, *Nature, Lond.*, **206**, 390.
- GABRIEL, A. H., NIBLETT, G. B. F., and PEACOCK, N. J., 1962, *J. Quant. Spectrosc. Radiative Transfer*, **2**, 491.
- GABRIEL, A. H., and WALLER, W. A., 1963, *J. Sci. Instrum.*, **40**, 10.
- GARSTANG, R. H., 1954, *Mon. Not. R. Astr. Soc.*, **114**, 118.
- 1962, *Atomic and Molecular Processes*, Ed. D. R. Bates (New York: Academic Press), chap. 1.
- GARTON, W. R. S., and RAJARATNAM, A., 1957, *Proc. Phys. Soc.*, **70**, 815.
- GAUNT, J. A., 1929, *Phil. Trans. R. Soc. A*, **229**, 163.
- GAYDON, A. G., and HURLE, I., 1963, *The Shock Tube in High Temperature Chemical Physics* (London: Chapman and Hall).
- GELTMAN, S., 1962, *Astrophys. J.*, **136**, 935.
- 1965, *Astrophys. J.*, **141**, 376.
- GLENNON, B. M., and WIESE, W. L., 1962 and 1963, *Bibliography on Atomic Transition Probabilities, Nat. Bur. Stand. Monograph 50 (Suppl. 1963)* (Washington: U.S. Gov. Printing Office).

- GOLDMAN, L. M., and KILB, R. W. C., 1964, *J. Nucl. Energy C*, **6**, 217.
- GOLDMAN, R., and OSTER, L., 1964, *Phys. Rev.*, **136**, A606.
- GREEN, L. C., RUSH, P. P., and CHANDLER, C. D., 1957, *Astrophys. J. (Suppl. No. 26)*.
- GRIEM, H. R., 1962 a, *Proc. 5th Conf. Ionisation Phenomena in Gases, Munich*, 1961, Vol. 2, Ed. H. Maecker (Amsterdam: North-Holland), p. 1857.
- 1962 b, *Phys. Rev.*, **128**, 997.
- 1962 c, *Phys. Rev.*, **128**, 515.
- 1962 d, *Temperature: Its Measurement and Control in Science and Industry*, Vol. 3, Pt. 1, Ed. C. M. Herzfeld (New York: Reinhold), p. 615.
- 1962 e, *Astrophys. J.*, **136**, 422.
- 1963, *Phys. Rev.*, **131**, 1170.
- 1964, *Plasma Spectroscopy* (New York: McGraw Hill).
- 1965, *Phys. Rev.*, **140**, 1140.
- GRIEM, H. R., BARANGER, M., KOLB, A. C., and OERTEL, G., 1962 a, *Phys. Rev.*, **125**, 177.
- GRIEM, H. R., KOLB, A. C., LUPTON, W. R., and PHILLIPS, D. T., 1962 b, *Nucl. Fusion (Suppl.)*, **2**, 543.
- GRIEM, H. R., KOLB, A. C., and SHEN, K. Y., 1959, *Phys. Rev.*, **116**, 4.
- 1962 c, *Astrophys. J.*, **135**, 272.
- GRIEM, H. R., and SHEN, C. S., 1962, *Phys. Rev.*, **125**, 196.
- GRIEM, H. R., and SHEN, K. Y., 1961, *Phys. Rev.*, **122**, 1490.
- GRIFFIN, W. G., and McWHIRTER, R. W. P., 1961, *Proc. Conf. on Optical Instruments and Techniques* (London: Chapman and Hall), p. 14.
- HAM, F. S., 1955, *Solid State Physics*, Vol. 1, Eds F. Seitz and D. Turnbull (New York: Academic Press), p. 127.
- HANSEN, C. F., 1964, *J. Opt. Soc. Amer.*, **54**, 1198.
- HARDING, G. N., and ROBERTS, V., 1962, *Nucl. Fusion (Suppl.)*, **3**, 883.
- HARRIS, G. M., 1964, *Phys. Rev.*, **133**, A427.
- HARTREE, D. R., 1957, *The Calculation of Atomic Structures* (New York: John Wiley).
- HEARN, A. G., 1963, *Proc. Phys. Soc.*, **81**, 648.
- 1964 a, *Proc. Phys. Soc.*, **84**, 11.
- 1964 b, *Proc. 6th Conf. Ionisation Phenomena in Gases, Paris*, Vol. 3, Ed. P. Hubert (Orsay: Faculté des Sciences), p. 289.
- HEITLER, W., 1954, *The Quantum Theory of Radiation* (London: Oxford University Press).
- HEROUX, L., 1963, *Nature, Lond.*, **198**, 1291.
- 1964, *Proc. Phys. Soc.*, **83**, 121.
- HILL, R. A., 1964, *J. Quant. Spectrosc. Radiative Transfer*, **4**, 857.
- HINNOV, E., 1964, *Phys. Fluids*, **7**, 130.
- HINNOV, E., and HIRSCHBERG, J. G., 1962, *Phys. Rev.*, **125**, 795.
- HINNOV, E., and HOFMANN, F. W., 1963, *J. Opt. Soc. Amer.*, **53**, 1259.
- HINTEREGGER, H. E., HALL, L. A., and SCHWEIZER, W., 1964, *Astrophys. J.*, **140**, 319.
- HIRSCHBERG, J. G., 1964, *Phys. Fluids*, **7**, 543.
- 1965, *Appl. Optics*, **4**, 243.
- HIRSCHBERG, J. G., and PALLADINO, R. W., 1962, *Phys. Fluids*, **5**, 48.
- HOBBS, G. D., McWHIRTER, R. W. P., GRIFFIN, W. G., and JONES, T. J. L., 1962, *Proc. 5th Conf. Ionisation Phenomena in Gases, Munich*, Vol. 2, Ed. H. Maecker (Amsterdam: North-Holland), p. 1965.
- HOLTSMARK, J., 1919, *Ann. Phys., Lpz.*, **58**, 577.
- HOUSE, L. L., 1964, *Ann. Astrophys.*, **27**, 763.
- HOUSE, L. L., DEUTSCHMANN, W. A., and SAWYER, G. A., 1964, *Astrophys. J.*, **140**, 319.
- HOUSE, L. L., and SAWYER, G. A., 1964, *Astrophys. J.*, **139**, 775.
- HUBNER, K., 1964, *Z. Naturf.*, **19a**, 1111.
- HUDDLESTONE, R. H., and LEONARD, S. L. (Eds), 1965, *Plasma Diagnostic Techniques* (New York: Academic Press).
- HUMMER, D. G., 1962, *Mon. Not. R. Astr. Soc.*, **125**, 21.
- INGLIS, D. R., and TELLER, E., 1939, *Astrophys. J.*, **90**, 439.
- IRONS, F. E., and MILLAR, D. D., 1964, *Aust. J. Phys.*, **18**, 23.

- JAHODA, F. C., *et al.*, 1960, *Phys. Rev.*, **119**, 843.
- JAHODA, F. C., RIBE, F. L., and SAWYER, G. A., 1963, *Phys. Rev.*, **131**, 24.
- JAHODA, F. C., RIBE, F. L., SAWYER, G. A., and MCWHIRTER, R. W. P., 1964, *Proc. 6th Conf. Ionisation Phenomena in Gases, Paris*, Vol. 3, Ed. P. Hubert (Orsay: Faculté des Sciences), p. 347.
- JONES, B. B., and WILSON, R., 1962, *Nucl. Fusion (Suppl.)* **3**, 889.
- JUNG, M., 1963, *Z. Astrophys.*, **58**, 93.
- KARZAS, W. J., and LATTER, R., 1961, *Astrophys. J. (Suppl.)*, **6**, 167.
- KELLY, P. S., 1964 a, *J. Quant. Spectrosc. Radiative Transfer*, **4**, 117.
- 1964 b, *Astrophys. J.*, **140**, 1247.
- KHINTCHINE, A., 1934, *Math. Ann.*, **109**, 604.
- KIMMITT, M. F., and NIBLETT, G. B. F., 1963, *Proc. Phys. Soc.*, **82**, 938.
- KNORR, G., 1958, *Z. Naturf.*, **13a**, 941.
- KOGAN, V. I., 1959, *Soviet Physics—Doklady*, **4**, 1057.
- KOGAN, V. I., and MIGDAL, A. B., 1961, *Plasma Physics and the Problem of Controlled Thermonuclear Reactions*, Vol. II (Oxford: Pergamon Press), p. 205.
- KOLB, A. C., 1963, *J. Quant. Spectrosc. Radiative Transfer*, **3**, 365.
- KOLB, A. C., and GRIEM, H. R., 1958, *Phys. Rev.*, **111**, 514.
- 1962, *Atomic and Molecular Processes*, Ed. D. R. Bates (New York: Academic Press), chap. 5.
- KOLB, A. C., and MCWHIRTER, R. W. P., 1964, *Phys. Fluids*, **7**, 519.
- KOOPMAN, D. W., 1964, *J. Opt. Soc. Amer.*, **54**, 1354.
- KRAMERS, H. A., 1923, *Phil. Mag.*, **46**, 836.
- KROLL, N. M., RON, A., and ROSTOKER, N., 1964, *Phys. Rev. Letters*, **13**, 83.
- KUDRIN, L. P., and SHOLIN, G. V., 1963 a, *Soviet Physics—Doklady*, **7**, 1015.
- 1963 b, *Optika Spectrosc.*, **14**, 322.
- KUDRIN, L. P., and TARASOV, Y. A., 1963, *Soviet Physics—JETP*, **16**, 1062.
- KUNZE, H. J., EBERHAGEN, A., and FÜNFER, E., 1964 a, *Phys. Letters*, **13**, 38.
- KUNZE, H. J., FÜNFER, E., KRÖNAST, B., and KEGEL, W. H., 1964 b, *Phys. Letters*, **11**, 42.
- LAYZER, D., 1959, *Ann. Phys.*, N.Y., **8**, 271.
- LENZ, W., 1933, *Z. Phys.*, **80**, 423.
- LEWIS, M., 1961, *Phys. Rev.*, **121**, 501.
- LINDHOLM, E., 1941, *Ark. Mat. Astron. Fys.*, **28B**, No. 3.
- LINHART, J. G., 1960, *Plasma Physics* (Amsterdam: North-Holland).
- LOCHTE-HOLTGREVEN, W., 1958, *Rep. Progr. Phys.*, **21**, 312 (London: Institute of Physics and Physical Society).
- LORENTZ, H. A., 1906, *Proc. Sect. Sci. K. Ned. Akad. Wet.*, **8**, 591.
- MAECKER, H., and PETERS, T., 1954, *Z. Phys.*, **139**, 448.
- MAKIN, B., and KECK, J. C., 1963, *Phys. Rev. Letters*, **11**, 281.
- MARGENAU, H., and LEWIS, M., 1959, *Rev. Mod. Phys.*, **31**, 569.
- MASTRUP, F., and WIESE, W., 1958, *Z. Astrophys.*, **44**, 259.
- MAZING, M. A., 1961, *Trudy Fiz. Inst. P.N. Lebedeva*, **15**, 55 (New York: Trans. Consultants Bureau, 1962).
- MCCHESNEY, M., 1964, *Canad. J. Phys.*, **42**, 2473.
- MCCHESNEY, M., and JONES, N. R., 1964, *Proc. Phys. Soc.*, **84**, 983.
- McCUMBER, D. E., and PLATZMAN, P. M., 1963, *Phys. Fluids*, **6**, 1446.
- MCWHIRTER, R. W. P., 1961, *Nature, Lond.*, **190**, 902.
- 1963, *Bull. Amer. Phys. Soc.*, **8**, 164.
- MCWHIRTER, R. W. P., and HEARN, A. G., 1963, *Proc. Phys. Soc.*, **82**, 641.
- MENZEL, D. H., and PEKERIS, C. L., 1936, *Mon. Not. R. Astr. Soc.*, **96**, 77.
- MILNE, E. A., 1921, *Mon. Not. R. Astr. Soc.*, **81**, 361.
- MOORE, C. E., 1949, 1952, 1958, *Atomic Energy Level Tables, Nat. Bureau Stand. Circ. 467*, Vols. I, II and III (Washington: U.S. Gov. Printing Office).
- MOTLEY, R. W., and KUCKES, A. F., 1962, *Proc. 5th Conf. Ionisation Phenomena in Gases, Munich*, Vol. 1, Ed. H. Maecker (Amsterdam: North-Holland), p. 651.
- MOZER, B., and BARANGER, M., 1960, *Phys. Rev.*, **118**, 626.

- MÜLLER, K. G., 1965, *J. Quant. Spectrosc. Radiative Transfer*, **5**, 403.
- NGUYEN-HOE, DRAWIN, H. W., and HERMAN, L., 1964, *J. Quant. Spectrosc. Radiative Transfer*, **4**, 847.
- NICHOLLS, R. W., and STEWART, A. L., 1962, *Atomic and Molecular Processes*, Ed. D. R. Bates (New York: Academic Press), chap. 2.
- OERTEL, G. K., and GRIEM, H. R., 1965, *Phys. Fluids*, **8**, 186.
- OLSEN, H. N., 1961, *Phys. Rev.*, **124**, 1703.
- 1963, *J. Quant. Spectrosc. Radiative Transfer*, **3**, 59.
- OSTER, L., 1961, *Rev. Mod. Phys.*, **33**, 525.
- 1964, *Phys. Fluids*, **7**, 263.
- OSTERBROCK, D. E., 1962, *Astrophys. J.*, **135**, 195.
- OXENIUS, J., 1966, *Astrophys. J.*, in the press.
- PAQUETTE, D. R., and WIESE, W. L., 1964, *Appl. Optics*, **3**, 291.
- PEACOCK, N. J., 1964, *Proc. Phys. Soc.*, **84**, 803.
- PEACOCK, N. J., COOPER, J., and GREIG, J. R., 1964, *Proc. Phys. Soc.*, **83**, 803.
- PFENNIG, H., STEELE, R., and TREFFTZ, E., 1965, *J. Quant. Spectrosc. Radiative Transfer*, **5**, 335.
- POST, R. F., 1961, *J. Nucl. Energy, C*, **3**, 273.
- RACAH, G., 1942, *Phys. Rev.*, **62**, 438.
- 1943, *Phys. Rev.*, **63**, 367.
- 1949, *Phys. Rev.*, **76**, 1352.
- VAN REGEMORTER, H., 1964, *C.R. Acad. Sci., Paris*, **259**, 3979.
- ROHRlich, F., 1959, *Astrophys. J.*, **129**, 441.
- ROSE, D. J., and CLARK, M., 1961, *Plasmas and Controlled Fusion* (New York: John Wiley), chap. 11.
- ROSENBLUTH, M. N., and ROSTOKER, N., 1962, *Phys. Fluids*, **5**, 776.
- SALAT, A., 1965, *Phys. Letters*, **15**, 139.
- SALAT, A., and SCHLÜTER, A., 1965, *Phys. Letters*, **14**, 106.
- SALPETER, E. E., 1960, *Phys. Rev.*, **120**, 1528.
- SALPETER, E. E., and ZAIDI, M. H., 1962, *Phys. Rev.*, **125**, 248.
- SAWYER, G. A., *et al.*, 1963, *Phys. Rev.*, **131**, 1891.
- SCHLÜTER, D., 1962, *Z. Astrophys.*, **56**, 43.
- 1965, *J. Quant. Spectrosc. Radiative Transfer*, **5**, 87.
- SCHWARZ, S. E., 1963, *Proc. Instn. Elect. Electron. Engrs*, **51**, 1362.
- SEATON, M. J., 1958, *Mon. Not. R. Astr. Soc.*, **118**, 504.
- 1964, *Planet. Space Sci.*, **12**, 55.
- SMITH, C. R., 1964, *Phys. Rev.*, **134**, A1235.
- SOBEL'MAN, I. I., 1957, *Fortschr. Phys.*, **5**, 175.
- SPITZER, L., 1940, *Phys. Rev.*, **58**, 348.
- 1956, *Physics of Fully Ionised Gases* (New York: Interscience).
- STAMPA, A., 1963, *Z. Astrophys.*, **58**, 82.
- STONE, P. M., 1962, *Phys. Rev.*, **127**, 1151.
- STONE, P. M., and AGNEW, L., 1962, *Phys. Rev.*, **127**, 1157.
- STRATTON, T. F., 1962, *Temperature, Its Measurement and Control in Science and Industry*, Vol. 3, Pt. 1, Ed. C. M. Herzfeld (New York: Reinhold), p. 663.
- THONEMANN, P. C., 1961, *Optical Spectrometric Measurements of High Temperature*, Ed. W. Dickerman (Chicago: University of Chicago Press).
- TOUSEY, R., 1964, *Q. J. R. Astr. Soc.*, **5**, 123.
- TRAVING, G., 1960, *Über die Theorie der Druckverbreiterung von Spektrallinien* (Karlsruhe: G. Braun).
- TREFFTZ, E., *et al.*, 1957, *Z. Astrophys.*, **44**, 1.
- TRUBNIKOV, B. A., 1958, *Soviet Physics-Doklady.*, **3**, 136.
- 1961, *Phys. Fluids*, **4**, 195.
- UNDERHILL, A. B., and WADDELL, J. A., 1959, *Nat. Bur. Stand. Circ. 603* (Washington: U.S. Gov. Printing Office).
- UNSÖLD, A., 1948, *Z. Astrophys.*, **24**, 235.
- 1955, *Physik der Sternatmosphären*, 2nd edn (Berlin: Springer-Verlag).

- VAINSHTEIN, L. A., and SOBEL'MAN, I. I., 1959, *Optika Spectrosk.*, **6**, 440.
- VARSAVSKY, M., 1961, *Astrophys. J. (Suppl.)*, **6**, 75.
- VASIL'EV, A. P., DOLGOV-SAVEL'EV, G. G., and KOGAN, V. I., 1962, *Nucl. Fusion (Suppl.)*, **2**, 655.
- VIDAL, C. R., 1964, *Z. Naturf.*, **19a**, 947.
- WEISSKOPF, V. F., 1963, *Z. Phys.*, **75**, 287.
- WHITE, H. E., 1934, *Introduction to Atomic Spectra* (New York: McGraw Hill).
- WIENER, N., 1930, *Acta Math., Stockh.*, **55**, 117.
- WIESE, W. L., and MURPHY, P. W., 1963, *Phys. Rev.*, **131**, 2108.
- WIESE, W. L., PAQUETTE, D. R., and SOLARSKI, J. E., 1963, *Phys. Rev.*, **129**, 1225.
- WILSON, R., 1962, *J. Quant. Spectrosc. Radiative Transfer*, **2**, 477.
- WOOLLEY, R. v. d. R., and ALLEN, C. W., 1948, *Mon. Not. R. Astron. Soc.*, **108**, 292.
- YOKLEY, C. R., and SHUMAKER, J. B., 1963, *Rev. Sci. Instrum.*, **34**, 551.
- ZAIDEL, A. N., MALYSHEV, G. M., BERZIN, A. B., and RAZOBARIN, G. T., 1961, *Soviet Physics-Tech. Phys.*, **5**, 1360.
- ZANSTRA, H., 1949, *Bull. Astr. Inst. Neth.*, **11**, 1.
- ZIRIN, H., 1964, *Astrophys. J.*, **140**, 1332.